

PRACA DOKTORSKA

A-21-7

H-66

Jerzy Karpiuk

Photophysical and photochemical processes in lactones of some rhodamines

H - N.

Praca doktorska wykonana pod kierunkiem
prof. dr Zbigniewa R. Grabowskiego w
Zakładzie Fotochemii i Spektroskopii Instytutu
Chemii Fizycznej Polskiej Akademii Nauk

Warszawa 1996

Biblioteka Instytutu Chemii Fizycznej PAN

B.319/1996



00000000278409



B. 319/96

Pragnę złożyć głębokie podziękowanie Panu Prof. dr Zbigniewowi R. Grabowskiemu za zaproponowanie tematu tej pracy, wiele cennych uwag i pomysłów wniesionych podczas jej wykonywania, stałą gotowość do dyskusji i przede wszystkim za ogromną cierpliwość okazaną w trakcie wykonywania tej pracy.

Ponadto, pragnę podziękować:

Panu doc. dr Janowi Jasnemu za wszechstronną pomoc w zakresie optycznych technik pomiarowych, a w szczególności za skonstruowanie spektrofotometru TAN 2,

Panu prof. dr Fransowi De Schryverowi z Wydziału Chemii Uniwersytetu w Leuven, Belgia, za umożliwienie wykonania pomiarów krzywych zaniku fluorescencji, oraz

wszystkim pracownikom Zakładu Fotochemii i Spektroskopii Instytutu Chemii Fizycznej PAN, którzy pomagali mi przy wykonywaniu tej pracy.

*Mai i Dawidowi oraz
mojej Mamie, której praca ta
sprawiłaby przyjemność*

Streszczenie

W ramach niniejszej pracy zbadano procesy fotofizyczne i fotochemiczne zachodzące w laktonowych formach wybranych rodamin w niepolarnych i polarnych rozpuszczalnikach aprotycznych. Stwierdzono, że procesem inicjującym relaksację wzbudzonej cząsteczki laktonu jest reakcja przeniesienia elektronu z części ksantenowej na ftalid, a struktura spiranowa laktonów o prostopadłym ułożeniu układów π -elektronowych w szczególnym stopniu nadaje się do stabilizacji rozseparowanych ładunków. We wszystkich badanych laktonach stwierdzono powstawanie stanu wzbudzonego z przeniesieniem ładunku, $^1L_{CT}$, i stanu wzbudzonego formy zwitterjonowej 1Z_1 , powstającego po rozerwaniu wiązania C-O w pierścieniu laktonowym. Przeprowadzono badania mechanizmu tego procesu oraz tworzenia i dezaktywacji stanów przejściowych występujących po wzbudzeniu cząsteczki laktonu. Oba stany wzbudzone są produktami relaksacji wzbudzonej pary jonorodników tworzących się po wzbudzeniu na skutek reakcji przeniesienia elektronu: stan $^1L_{CT}$ po relaksacji oscylacyjnej, a stan 1Z_1 po reakcji powrotnego przeniesienia elektronu. W odróżnieniu od dotychczas opublikowanych wyników stwierdzono, że obie formy powstają zawsze, natomiast w warunkach, gdy się nie obserwuje jednej z nich (1Z_1) - podlega ona szybkiemu zanikowi bezpromienistemu. Niezależność wydajności obsadzenia stanu 1Z_1 od rozpuszczalnika sugeruje wewnątrzcząsteczkowy mechanizm jej powstawania. Wykryto występowanie stanu tripletowego formy **Z** oraz stanu tripletowego laktonu z przeniesionym ładunkiem. Zbadano reakcję wewnątrzcząsteczkowego wygaszania formy **Z** i w konkluzji zaproponowano, że jej mechanizm polega na termicznie aktywowanym przejściu do wyższego stanu tripletowego. Stwierdzono, że polarność rozpuszczalnika odgrywa kluczową rolę w mechanizmie dezaktywacji stanów wzbudzonych $^1L_{CT}$ i 1Z_1 poprzez wpływ na energię stanów uczestniczących w procesie i modyfikowanie bariery energetycznej reakcji wygaszania.

Abstract

In this thesis photophysical and photochemical processes occurring in lactone forms of selected rhodamines have been investigated in nonpolar and polar aprotic solvents. It has been found that spiro-structure of lactones with orthogonal π -electron systems seems to be especially favourable for stabilisation of charge separation. In all lactones studied, occurrence of the reaction leading to generation of the excited charge-transfer state, $^1L_{CT}$, and the excited state of the zwitterion form 1Z_1 , formed after the cleavage of the C-O bond in the lactone ring has been found. The mechanism of this process as well as the formation and deactivation of intermediates occurring upon excitation of the lactone molecule have been investigated. Both excited states are products of relaxation of an excited ion radical pair that is produced upon excitation due to an electron transfer reaction: the $^1L_{CT}$ state after vibrational excitation and the 1Z_1 state after the back electron transfer reaction. In contrary to the results published hitherto, it has been found that both forms are produced always, and under conditions where one of them (1Z_1) is not observed - it undergoes a fast radiationless deactivation. The independence of the quantum efficiency of population of **Z** form of the solvent suggests an intramolecular mechanism of its generation. Occurrence of the triplet state of the **Z** form and the charge-transfer triplet state of the lactone have been found. The reaction of intramolecular quenching of the **Z** form has been investigated and in conclusion it has been proposed that its mechanism consists of a thermally activated transition to a higher triplet state. Solvent polarity was found to play a crucial role in the mechanism of $^1L_{CT}$ and 1Z_1 excited state deactivation by influencing the energy levels of the states participating in the process and modifying the energy barrier height of the quenching reaction.

Contents

CHAPTER 1

PHOTOPHYSICS OF RHODAMINES - A REVIEW OF THE STATE OF ART 1

1.1. Introduction	1
1.1.1. Definition of the compounds studied	1
1.1.2. The scope of the thesis.....	1
1.1.3. Compounds used in this work.	3
1.2. Review of the equilibria between different molecular forms of rhodamines in the ground state	4
1.3. Photophysics of the zwitterion and cation forms of rhodamines	9
1.3.1. Singlet states.....	9
1.3.2. Intersystem crossing and triplet states of rhodamines	11
1.4. Thermally activated deactivation of excited ionic forms - a review of the mechanisms postulated in the literature	13
1.5 Photophysics of the lactone form of rhodamines	17
1.5.1 Existing foundations for this thesis	17
1.5.2 The objectives of this thesis	20
References and notes.....	21

CHAPTER 2

EXPERIMENTAL METHODS AND INSTRUMENTATION..... 24

2.1. Introduction	24
2.2. Materials used in the investigations	24
2.2.1. Lactones.....	24
2.2.2. Solvents	25
2.3. Absorption and emission spectra.....	27
2.4. Measurements of fluorescence decays	27
2.4.1. Sampling technique	27
2.4.2. Single photon timing technique.....	29
2.4.3. Time-resolved fluorescence spectra	29
2.5. Transient absorption measurements	29
2.6. Temperature measurements.....	32
References and notes.....	32

CHAPTER 3

PHOTOPHYSICS OF THE LACTONE FORMS OF RHODAMINES 33

3.1. Absorption spectra.....	33
3.1.1. Ground-state equilibria.....	33
3.1.2. Absorption spectra of the lactone forms.....	36
3.2. Fluorescence spectra at room temperature	39
3.3. Fluorescence decays at room temperature.....	44

3.3.1. LRB	45
3.3.2. LR101	48
3.3.3. Efficiency of population of the zwitterion.....	50
3.3.4. Time-resolved fluorescence spectra	52
References and notes.....	54
CHAPTER 4	
TEMPERATURE STUDIES.....	55
4.1. Introduction	55
4.2. Fluorescence spectra as a function of temperature.....	55
4.3. Luminescence in glass.....	64
4.4. Temperature studies of the decay kinetics.....	67
References and notes.....	71
CHAPTER 5	
TRANSIENT ABSORPTION MEASUREMENTS.....	73
5.1. Introduction	73
5.2. Review of the literature	73
5.2.1. $S_1 \rightarrow S_n$ transient absorption	73
5.2.2. $T_1 \rightarrow T_n$ transient absorption.....	75
5.3. Transient absorption study of LRB - spectra and kinetic curves.....	77
5.3.1. Low polar solvents	77
5.3.2. Polar aprotic solvents	79
5.3.3. Solvent effect on kinetics of the excited state process	83
5.4. The excited state process - conclusions from transient absorption study.....	86
References and notes.....	89
CHAPTER 6	
DISCUSSION OF RESULTS.....	91
6.1. Ground state equilibria	91
6.2. Primary excited state process	91
6.3. Diagram of energy levels	93
6.4. Transitions between excited states - excited state equilibria?	96
6.5. Intramolecular quenching of the singlet excited state of zwitterion.....	99
6.5.1. Structure of the amino group.....	99
6.5.2. Solvent polarity effect and temperature effect.....	100
6.5.3. Ring closure.....	107
6.6. Intersystem crossing process in the zwitterion form	107
References and notes.....	109
CHAPTER 7	
CONCLUSIONS	111

CHAPTER 1

PHOTOPHYSICS OF RHODAMINES - A REVIEW OF THE STATE OF ART

1.1. Introduction

1.1.1. Definition of the compounds studied

Rhodamines represent a class of xanthene dyes known for a long time and during recent two decades widely used as laser dyes¹. The simplest of the rhodamine dyes (known as rho-

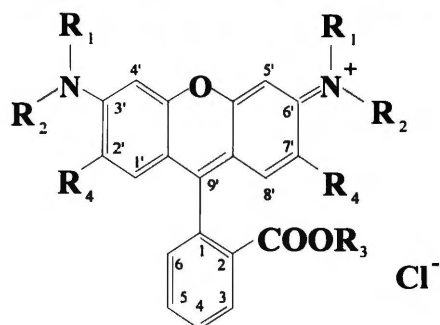


Fig. 1.1: General skeletal structure of rhodamine dye in a form of a chloride salt.

damine 110; R₁, R₂, R₃, R₄ = H, Fig. 1.1) was mentioned for the first time in a German patent of 1887, and then a more detailed description of this dye was given by Piutti and Picolli², and subsequently by Meyer and Sundmacher³ in late nineties of 19th century. The dye very well known today as rhodamine B (R₁, R₂ = C₂H₅, R₃, R₄ = H), was described for the first time by Noelting and Dziewoński in 1905⁴. That paper contained also a discussion of basic properties of other rhodamines investigated in this thesis (i.a.

diethylrhodamine **DR10**, (R₁ = C₂H₅, R₂, R₃, R₄ = H) and tetramethylrhodamine, below referred to as **RMET** (R₁, R₂, = CH₃, R₃, R₄ = H). Rhodamine 101, a dye with alkyl substituents at amino groups rigidly fixed to the xanthene skeleton (julolidine-type substituents at amino nitrogen, see Fig. 1.2), was, on the other hand, synthesised on the basis of some conceptual considerations concerning the influence of the substituents at amino nitrogen atoms (see below) on the radiationless deactivation of singlet excited states of the rhodamines⁵.

At present, the term *rhodamines* covers a broad range of compounds, the chemical formula of which can be generally described as 3',6'-(dialkylamino)-xanthene substituted in 9' (central) position with a phenyl-2-carboxylic acid group or its ester derivative (Fig. 1.1). As in the following almost exclusively rhodamines with xanthene system substituted with phenyl-2-carboxylic acid will be considered, the term **rhodamine** will in this work generally refer only to this sub-category of dyes. The esterified rhodamines cannot occur in the lactone form, and as such are not the main subject of interest for this study. They are used, however, at certain places as model compounds.

1.1.2. The scope of the thesis.

The photophysics and photochemistry of the lactone forms of the rhodamines involve three of the dominating problems in current organic physical chemistry, namely (i) the *solvent effect* on the photophysical processes of a molecule in the excited state, (ii) the *hypersurface crossing* while passing from one electronic state to another, and (iii) the photoinduced

electron transfer reaction in the excited state. The electron transfer from the xanthene part of the molecule to the phthalide one, which seems to be an initialising step in the photophysics of this molecule⁶, results in a **charge transfer excited state** or produces the **excited zwitterionic form** of the molecule after bond cleavage between the C and O atoms and opening of the lactonic ring, passing in this way onto the potential energy hypersurface of the excited state of the zwitterion. To our knowledge this represents the one of very few known adiabatic photoreactions of a bond cleavage that occur with preservation of the excitation.

Closely related to these questions is a problem more particularly connected with the class of rhodamine dyes, namely the radiationless deactivation pathway observed for zwitterion and cation forms of these dyes. As this will be discussed in detail later on in this chapter, here only a broad outline will be given. This phenomenon was studied by several research groups. The conclusions drawn from their investigations suggested that conformational changes of the amino groups in the excited state are responsible for the non-radiative decay. Drexhage⁷ postulated that torsional motion of the diethylamino group in rhodamine B is involved in the non-radiative process. The synthesis of rhodamine 101 having amino groups rigidly linked to the xanthene skeleton, its very high luminescence quantum yield, and - in particular - the independence of this quantum yield of temperature - seemed to be a very strong evidence confirming this model of the nature of the non-radiative decay. Vogel *et al.*⁸ investigated several rhodamines with different substitution patterns at the amino nitrogens and postulated a presence of a non-emissive TICT state being accessible from the S₁ state after crossing an activation barrier in the torsional motion. This explanation found support in other studies⁹⁻¹¹. The increase of temperature would in this model accelerate the crossing of the barrier between the S₁ excited state of the zwitterion and the TICT state, which should be accompanied by twisting of the dialkylamino groups. This temperature dependence has also been reported to be linked to the degree of alkylation of the amino groups. One of the main structural arguments which supported the TICT hypothesis for rhodamine dyes was the lack of temperature dependence of the fluorescence quantum yields and lifetimes for ethyl ester of rhodamine 101. According to the TICT model, the rigidly fixed amino group cannot yield the TICT states, the twisting motion being impossible. The question is also of great importance for the photophysics of lactones in view of the observed intramolecular quenching of the zwitterions generated in the excited state reaction⁶.

Rhodamines occur in different molecular forms. Equilibria between such forms of rhodamine B in the ground state have been known for a long time¹². The existence of the dye in a definite molecular form depends primarily on solvent polarity and proticity. The zwitterion is favoured by polar protic solvents whereas the lactone dominates in low polar and polar aprotic media. Cations occur under acidic conditions. Recent studies on the ground state equilibria between the lactone and the zwitterion form of rhodamine B suggested that even in ethanol at room temperature, although the equilibrium is strongly shifted towards the zwitterion, there is a considerable amount of molecules being in lactone form¹³. This fact additionally enhances the importance of studying the photophysical behaviour of this form of

the dye. Furthermore, possible excited state equilibria would significantly influence lasing properties of these dyes.

The lactone molecule - due to interruption of π conjugation in the xanthene moiety - represents from the point of view of optical transitions a completely different system compared with the zwitterion. Depending on the polarity of the solvent, the rhodamine B lactone was found to display either a single luminescence band at shorter wavelengths or a dual luminescence, one band of which (at longer wavelengths) has been ascribed to originate from the electronically excited zwitterionic form produced by the ring opening process¹⁴.

Studies on the lactones have furthermore an additional advantage that no protons or counterions are present in solution. These species influence significantly ground state equilibria and may also affect the excited state processes.

This study has been undertaken in order to investigate the processes taking place in the excited states of lactone forms of rhodamines, to identify the intermediates occurring in course of the excited state reaction and, in particular, to clarify the role that the solvent plays in the photophysics of these molecules. A more detailed specification of the goals of this thesis is given in section 1.5.2.

1.1.3. Compounds used in this work.

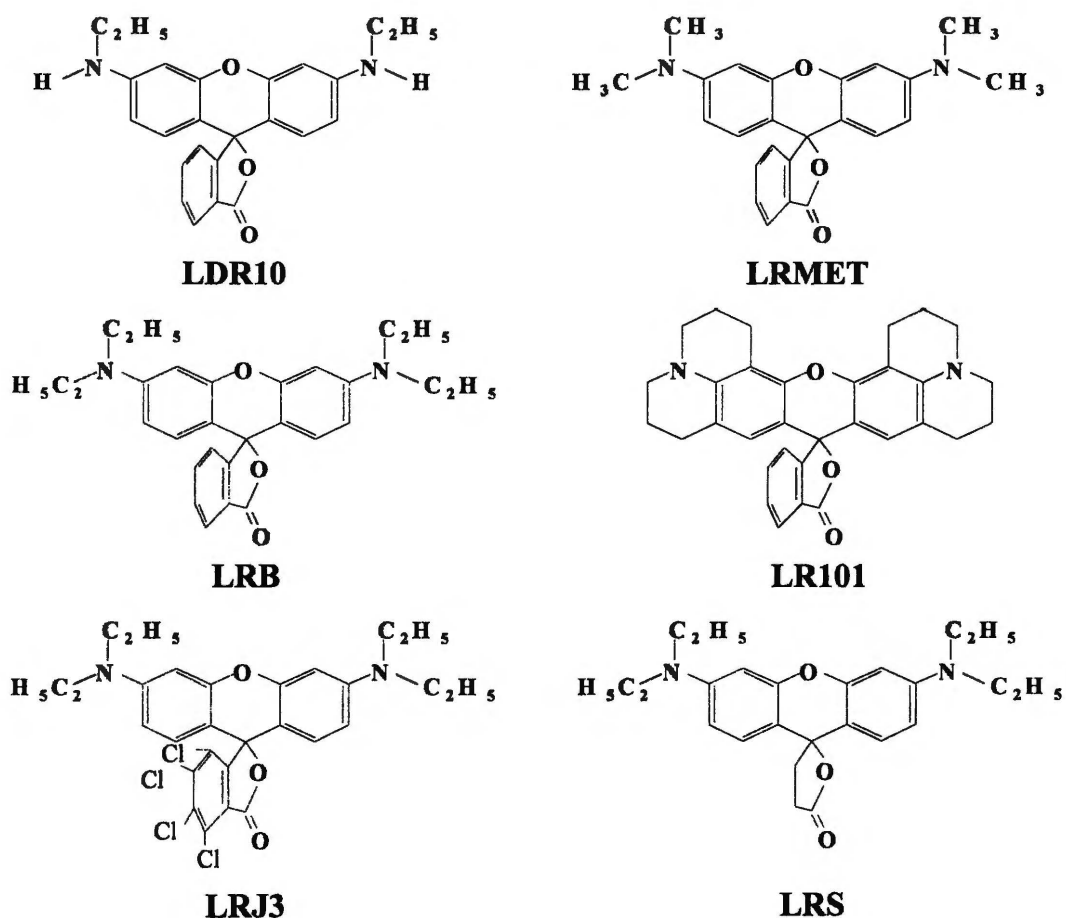


Fig. 1.2: Structures of the lactone forms of rhodamines investigated within this study.

In the study we have included six rhodamine lactones, the structural formulae of which are shown in Fig. 1.2, and particular attention was paid to the LDR10, LRMET, LRB and LR101. The remaining two lactones were used occasionally and for comparison only. All of the lactones have been synthesised for the purpose of this thesis starting from corresponding rhodamine salts (mostly chlorides). The spectroscopy and the photophysics of these dyes was investigated by means of both stationary and time-resolved techniques.

In the literature existing hitherto, a few streams of investigations on the ground and excited state equilibria exhibited by rhodamines and on the photophysics of these dyes can be distinguished. The studies carried out so far that are of interest for the purposes of this thesis may be grouped into the following categories:

- ground state equilibria of various forms of rhodamines,
- photophysics of zwitterion and cation forms of rhodamines,
- thermally activated deactivation of excited ionic forms,
- intersystem crossing in rhodamines,
- excited state equilibria and the photophysics of the lactone form.

Because this study covers, at least in part, all the problems mentioned above, a summary of the literature dealing with these issues is given below.

1.2. Review of the equilibria between different molecular forms of rhodamines in the ground state

The equilibria between different molecular forms of rhodamines are a key factor in understanding the photophysics of these dyes, hence, before attempting to discuss photophysical properties of lactones a survey covering this issue must be given. As the study of ground state equilibria for different rhodamines was not a goal of this work, I confined myself to an overview of these equilibria mainly for rhodamine B (**RB**), rhodamine 101 (**R101**), and for lactam analogues of RB, with subsequent addition (in Chapter 3) of our own results for R101.

The occurrence of rhodamines in different molecular forms has been known for a long time. Apart from the well known quinoid (ionic) forms that give intense colour solutions, colourless rhodamine solutions in ether or in benzene were mentioned already in first papers dealing with rhodamines²⁻³. Noelting and Dziewoński⁴ in their study of rhodamine B have proposed that the lactone form of the molecule is responsible for the lack of absorption in the visible. This was confirmed by Deutsch¹² who found that rhodamine esters (alkyl = R₃, Fig. 1.1) do not yield colourless solutions because the formation of the lactonic structure is not possible in that case. He has also shown that rhodamine B occurs at interfaces in two forms (lactone and zwitterion) being in equilibrium. Ramette and Sandell¹⁵ made a quantitative study on equilibria of different forms of rhodamine B at room temperature showing their absorption spectra and identifying conditions of their occurrence. They found that the colourless lactone form (LRB) existing e.g. in benzene or in diethyl ether undergoes ring opening and separation of charges in protic solvents to form an intensely coloured violet

zwitterion (RB^+ , in the following termed **Z** form) with the maximum of absorption band in the visible at $\lambda_{\text{abs}} = 553 \text{ nm}$ ¹⁶ (in water). On lowering pH to about 3, **Z** adds a proton to the carboxyl group and converts into cation (RBH^+ , $\lambda_{\text{abs}} = 556 \text{ nm}$, in the following termed **C** form). Further increase in acidity of the solution resulted in adding another proton to the cation (probably at one of the amino nitrogens) and formation of a dication RBH_2^{++} ($\lambda_{\text{abs}} = 494 \text{ nm}$). In concentrated sulphuric acid, the dication takes on a third proton and forms trication RBH_3^{+++} ($\lambda_{\text{abs}} = 366 \text{ nm}$). From this variety of molecular forms we will confine ourselves to the lactone (**L**), the zwitterion (**Z**) and the cation (**C**) as only these forms are involved in the excited state equilibria studied in this work. These forms of rhodamine B are depicted in Fig. 1.3:

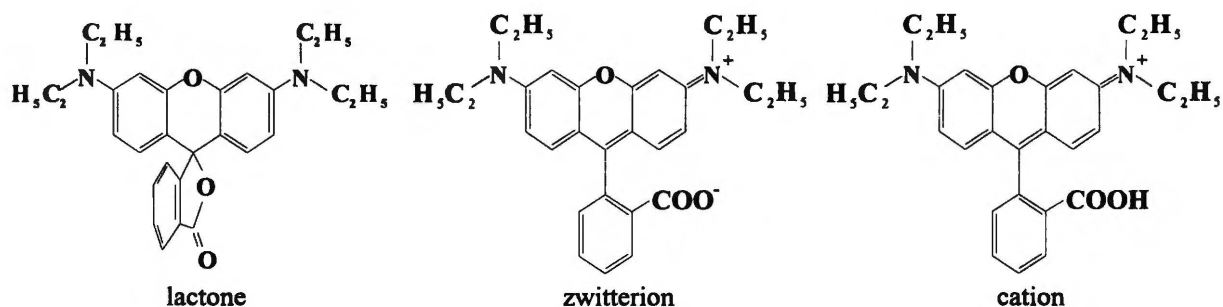


Fig. 1.3: Molecular forms of rhodamine B.

In a series of papers devoted to the synthesis and properties of various rhodamines, Ioffe and Otten¹⁷⁻²⁰ have discussed the conditions of existence and the properties of the lactone forms of rhodamines. Their experiments have shown that the lactone form of rhodamine 110 is formed on heating the free dye (probably the zwitterion) in some low polar solvents, where the solution became colourless, but on cooling coloured zwitterion was formed again¹⁷. They have experimentally verified that the colourless form of rhodamine B has indeed a structure resembling that of 3,6-diaminofluorane (lactonic structure)¹⁷. Investigating the solvent polarity effect on the lactone-zwitterion ($\text{L} \rightleftharpoons \text{Z}$) equilibria in dioxane-water binary mixtures for rhodamine 110 and for rhodol, they have found that an increase of medium polarity results in a gradual "polarisation" of the colourless lactonic structure and in subsequent transformation into the coloured form¹⁹. Our results suggest that the conclusions by Ioffe and Otten may be doubtful to a certain extent because of the influence the water contained in dioxane-water binary mixtures may have on the position of equilibrium (cf. Chapter 3).

Furthermore, Ioffe and Otten have concluded that opening of the lactone ring, which transforms the colourless form into the dye, depends on the nature of the substituents in positions 3 and 6 of the xanthene subsystem. Among the substituents studied, amino group was the substituent favouring to a highest degree the opening of the lactone ring (compared, for instance, with fluoresceine containing O and OH substituents), which can be explained by participation of the non-bonding electron pair of the nitrogen atom in that process. The motion of this electron pair towards the aromatic system causes a shift of electron density along the

coupling chain, which subsequently weakens the covalent bond between the carbon atom of the xanthene system and oxygen atom of the lactone cycle. The influence of polar solvents leads to a cleavage of the bond followed by creation of the zwitterion according to the scheme:

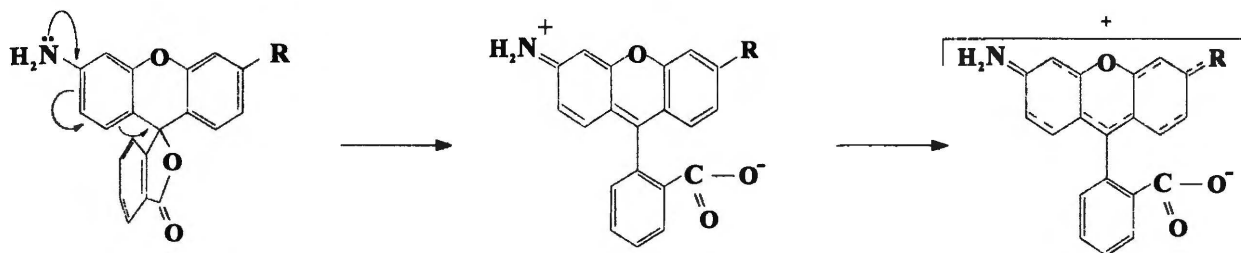


Fig. 1.4: Creation of the zwitterion in rhodamine 110 ($R = NH_2$) and in rhodol ($R = OH$)¹⁹.

The positive charge generated on the transformation is delocalised over the entire xanthene system along the π -electron chain between the two nitrogen atoms, the oxygen atom and the central carbon atom. This type of charge redistribution can also accompany the excited state reaction in rhodamine lactones.

Various ionic forms of rhodamine B under different pH conditions have been studied by Gutsze and Waleryś²¹. They have found that RB in aqueous solution occurs in a form of a coloured cation that is stable and may exist in slightly basic solutions. According to their paper, an increase in basicity leads to a generation of the zwitterion (at $pH \approx 9$). In strongly acidic media the cation undergoes hydration: the proton is associated with the nitrogen atom and the OH^- group is located at the central carbon atom, which leads to disappearance of the colour. At very high proton concentrations (1 - 10 n H_2SO_4) the RB molecule is transformed (in a reversible process) in species with the absorption spectrum resembling that of fluoresceine. Similar effect of colour disappearance was found after adding a base to the dye solution. Above certain pH level (corresponding to 1 n NaOH), the absorption of the solution in the visible strongly decreases without any shift of the position of the maximum and disappears completely at 10 n NaOH). This is explained by addition the OH^- group to the central carbon atom and creation of the colourless anion (leuco form). The authors conclude that saturation of the central carbo-cation atom by the OH^- group or by the lactone bond leads to similar changes in the xanthene skeleton and thus to similar changes in electron energy distribution in this part of the molecule.

In early seventies, Selwyn and Steinfeld²² have studied absorption spectra of RB solutions in ethanol with small amounts of HCl and NaOH added to the sample and postulated that spectral shifts observed under these various conditions are to be ascribed to formation of RB dimers. Ferguson and Mau²³⁻²⁴, on the other hand, have proposed an acid-base ($C \rightleftharpoons Z$) equilibrium as the reason for these shifts, attributing respective absorption and fluorescence spectra to the acid and to the base (zwitterion) form of the dye. Applying the technique of depolarisation kinetics to determine rotational diffusion time constants for the species involved in the equilibrium process, Sadkowski and Fleming²⁵ have found that these times are

identical for both species. Based on this finding it has been postulated that the species involved are the cation and the zwitterion form of the dye.

$L \rightleftharpoons Z$ equilibria of rhodamine B in mixtures of aprotic solvents with alcohols have been investigated by Poleuktov *et al.*²⁶, who have found that conversion of the lactone molecule into the zwitterion was accomplished by formation of solvates in which one molecule of the dye co-ordinates 1 to 3 alcohol molecules. Rosenthal *et al.*²⁷ have re-examined the conditions and factors which control the existence of a particular isomer of RB in solution. They dissolved rhodamine B in a form of its hydrochloride salt and in the lactone form in various aprotic solvents, and studied the $L \rightleftharpoons Z$ equilibria at various temperatures. They have concluded, firstly, that the aprotic nature of the solvent and not its polarity is the decisive factor determining the position of lactone-zwitterion equilibrium. Secondly, they have found a significant temperature effect on the position of the equilibrium. Cooling down the solution resulted in dramatic increase of absorbance of the solution measured at 550 nm. In addition, in non polar and aprotic solvent (methylcyclohexane-isohehexane mixture) formation of dimers of rhodamine B with lowering the temperature has been observed. At the same time, it has been found that the change in $L \rightleftharpoons Z$ equilibrium constant was dependent on the form of rhodamine B being dissolved, i.e. depended on whether the lactone or the hydrochloride salt of RB was dissolved. However, it has subsequently been noted that some of the variations observed must be attributed to participation of the intensely coloured cation form of RB²⁸. The findings concerning the lactone-zwitterion equilibria reported by Rosenthal *et al.* have been reinterpreted in a series of papers by Hinckley *et al.*^{13, 29-30}. Using rhodamine B in two forms (the hydrochloride salt and the lactone) these authors have examined electronic absorption spectra of RB in an extensive series of protic and aprotic solvents and have taken into account three molecular forms of RB that exist in solution, i.e. the lactone, the zwitterion and the cation. They have concluded that the Z form of RB is absent in aprotic solvents and present in equilibrium with the L form in protic solvents. The position of the $L \rightleftharpoons Z$ equilibrium was found to depend on solvent-dye hydrogen bonding that favours the zwitterion. The cation form of RB was found to appear in both protic and aprotic media under acidic conditions. The authors concluded that the hydrogen bonding is necessary but not sufficient condition for stabilisation of the Z form. In addition, the solvent must be capable of stabilising the dipole of the Z form via its dielectric and polarisability properties. Furthermore, they suggested that dramatic differences in the $L \rightleftharpoons Z$ equilibrium constant obtained by starting with either the RB-HCl or RB-lactone forms, especially in aprotic solvents²⁷, are clearly due to interference from the C form, as use of the RB-HCl salt implies equimolar presence of HCl with the dye. At higher concentrations of the RB-HCl salt, the equilibrium favours the cation, an effect that can mimic or occur in addition to dimer formation²³.

The electrostatic factors affecting the position of the $L \rightleftharpoons Z$ equilibrium of rhodamine B in the ground state have been very recently investigated by Sueishi *et al.*³¹ who studied solvent and pressure effect on the equilibrium in a series of primary alcohols. Their findings

show that the position of the $L \rightleftharpoons Z$ equilibrium in these solvents can be explained in terms of electrostatic interaction between the solute and the solvent dipoles, although hydrogen bonding is necessary for formation of the Z form. These authors have confirmed the observation made by Hinckley *et al.*¹³ that the equilibrium constant ($K = [Z]/[L]$) increases with increasing the dielectric constant and that this parameter can be used as a measure of solvent polarity. They have also found that the equilibrium constant increases with increasing pressure and that the estimated reaction volumes, ΔV_0 , for the $L \rightleftharpoons Z$ reaction are in the range from -4 to -13 $\text{cm}^3\cdot\text{mol}^{-1}$ and their absolute values increase with decreasing the dielectric constant of the alcohol. Dividing ΔV_0 into three components: the solvational part, the part being a sum consisting of the difference in volume between the Z and the L form without electrostriction and the volume change arising from the hydrogen bond formation in the Z form, and assuming the dipole moment of the L form to be equal to 2.0 D, they were able to estimate the dipole moment of the Z form to 14.5 D. The reaction volumes decreased linearly with the q_p values of the solvent ($q_p = \partial[(\epsilon - 1)/(2\epsilon + 1)]/\partial p$) and the reaction volumes calculated for each solvent using $\mu_z = 14.5$ D well reproduced the observed ones. This value for the dipole moment deviates significantly from the value determined for rhodamine B by Desai and Pandhava (5.5 D in toluene)³². The difference is most probably due to a large contribution from the lactone molecules present in toluene solutions of RB.

Barigelletti³³ has reported the occurrence of the $L \rightleftharpoons Z$ equilibrium in the case of rhodamine 101 (R101, known also as rhodamine 640, structure of the lactone form see Fig. 1.2) in butyronitrile-propionitrile mixture. On the basis of temperature dependent absorption spectra in the visible he determined the free energy for this equilibrium. Our results obtained for this dye³⁴ indicate, however, that the dominant source of absorption in the visible in butyronitrile-propionitrile solution is the cation form of the molecule produced through protonation by protic impurities present in the solvent. At the same time, we do not exclude a possible equilibrium between the lactone and the zwitterion form in the ground state. Detailed discussion of this topic is given in section 3.1 of this thesis.

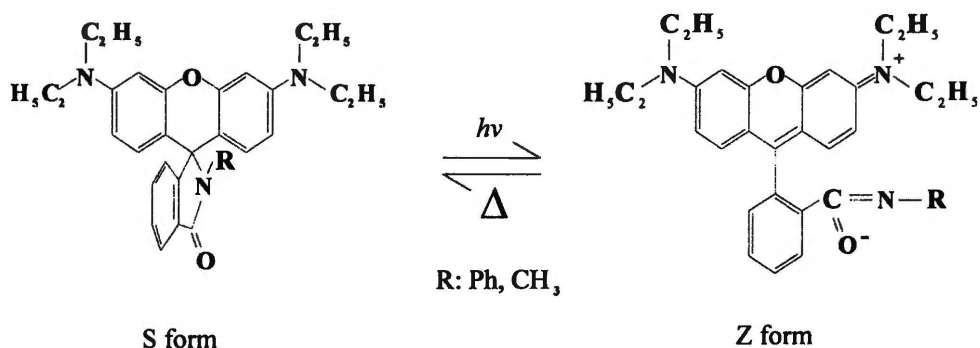


Fig. 1.5: $S \rightleftharpoons Z$ equilibrium in the rhodamine lactams³⁶.

The isomerisation involving the closed-ring and the open-ring form was also reported by Knauer and Gleiter³⁵ in the case of N-methyl-rhodamine-lactam, a compound which is a close structural analogue of rhodamine B. In their next paper, Gleiter and co-workers have

found³⁶ that the lactam is converted into a coloured zwitterionic structure by photoinduced bond fission, observing the rise of the absorption signal at 550 nm on a time scale of μs . In the dark, **Z** form reverts to the spiro (**S**) form (Fig. 1.5). The kinetics of the thermal fading reaction at 295 K was studied by time resolved absorption at 550 nm on a time scale of ms in dioxane and in mixtures dioxane-alcohol, and on a time scale of s in acetonitrile. From the deviation of the fading reaction from the first order kinetics the authors concluded that there are at least two coloured compounds; these are likely the rotamers of the zwitterionic form (Fig. 1.6).

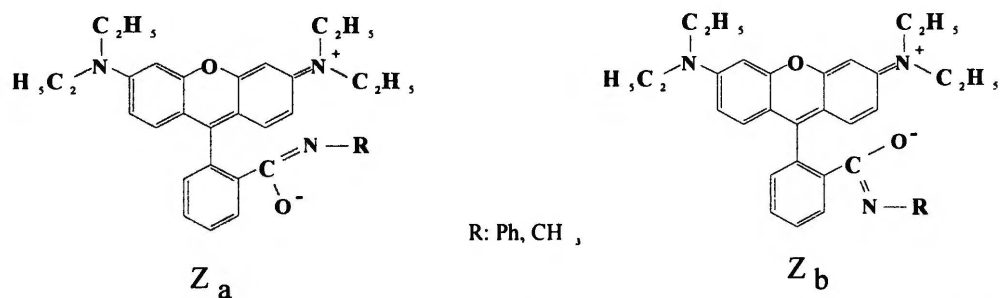


Fig. 1.6: Structures of two proposed isomers, involved in the photochromism of the rhodamine-lactams.

Sueishi *et al.*³⁷ have studied the solvent and pressure effects on thermal isomerisations of N-phenyl- and N-methyl-rhodamine-lactams from their zwitterionic to the spiro forms. From pressure dependence of the reaction rate they have estimated the activation volumes, ΔV^\ddagger for both molecules. They supported the hypothesis proposed by Gleiter and co-workers³⁶ that two rotamers of the coloured zwitterionic form are involved in the isomerisation, and discussed their role and the kinetic effects of solvent and pressure. In conclusion they stated that the thermal isomerisation proceeds *via* a dipolar transition state, and their results are consistent with a reaction mechanism involving heteropolar ring closure on activation.

1.3. Photophysics of the zwitterion and cation forms of rhodamines

1.3.1. Singlet states

Due to a widespread use, in particular as active media in laser applications, ionic forms of rhodamines are very well known^{1,7}. The photophysics of these species is determined by the xanthene part of their molecules which is in the plane perpendicular to that of the carboxylphenyl group, with the latter being of minor importance for the photophysics of the zwitterion and of the cation³⁸.

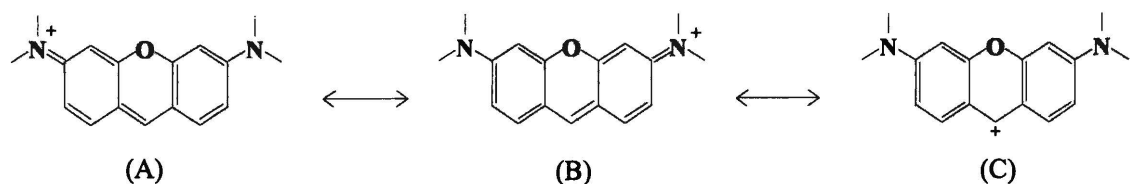


Fig. 1.7: Mesomeric forms of the xanthene group (not included have been the structures involving a less energetically favourable oxonium configuration).

Therefore, as (from the point of view of the photophysics of the lactone form) the photophysics of both these species does not differ much from each other, the **Z** and the **C** form are treated here as two representatives of the same xanthene chromophore. The π -electron distribution in the xanthene chromophore can be described approximately by three mesomeric resonance structures shown in Fig. 1.7. While none of these mesomeric structures alone depicts the real π -electron distribution in the chromophore, they all contribute according to their relative energies. Particular attention must be paid to structures A and B, as their contributions are most significant. For symmetry reasons these forms have the same weight, and hence in xanthene group there is no permanent dipole moment component parallel to the long axis of the molecule either in the ground or in the excited state. In the literature one can find at least two values of the ground state dipole moment (along the short axis of the xanthene group) of the zwitterion form of RB. As mentioned on page 8, the estimate by Sueishi *et al.*³¹ (14.5 D) is more probable.

The transition moment of the main absorption band that occurs between 450 nm and 600 nm (Fig. 1.8) is oriented parallel to the long axis of the xanthene group. Some of the transitions at shorter wavelengths are oriented perpendicular to the long axis³⁹. The position of the absorption maximum in the visible markedly depends on the substituents in 3'- and 6'-positions of the xanthene nucleus. The absorption maximum of the zwitterion in ethanol shifts from 517 nm for rhodamine 110 to 568 nm for rhodamine 101.

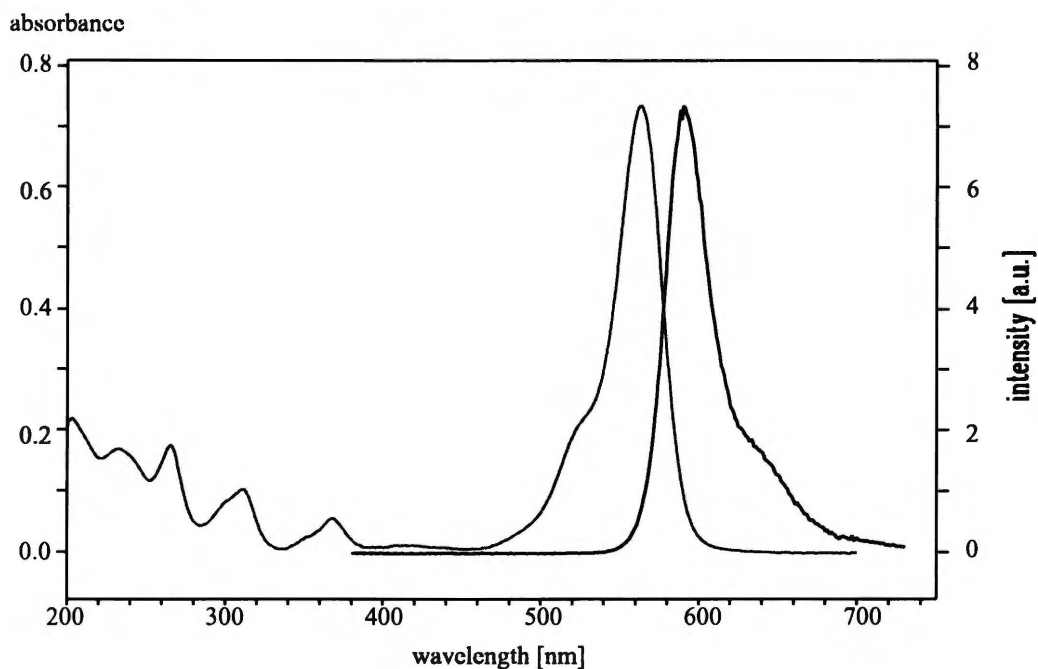


Fig. 1.8: Absorption and fluorescence spectrum of zwitterion form of R101 (in ethanol).

Simplified quantum mechanical treatment of the main absorption features of the xanthene group has been presented by Kuhn⁴⁰, Sens³⁸ and most recently by Bergamasco *et al.*⁴¹ (and by Artyukhov, see section 6.3). The authors of the latter paper⁴¹ have performed molecular orbital calculations on the basis of the Pariser-Parr-Pople (PPP) and extended Hückel molecular orbital method (EHMO). They found that a single configuration is adequate

and sufficient for the description of the S_0 and S_1 state in the planar forms of the xanthene. Investigating planar and 90° torsional angle conformations of the amino group they have found that negative charge is transferred upon excitation from the amino nitrogen to carbon atom in the 9'- position to about the same extent in both conformations. The corresponding change in the dipole moment is relatively small, since for the symmetry reasons only the charge transfer component parallel to the short molecular axis is important. This is also manifested by relative insensitivity of the position of fluorescence maximum to the solvent.

The interest in rhodamines during last 25 - 30 years was driven mainly by potential use of these substances as laser dyes or as luminescent probes, which was in turn connected with excellent luminescence properties of the ionic forms of these dyes. Because of very high fluorescence quantum yield (0.96)⁴² and the insensitivity of this yield to variations of the temperature, rhodamine 101 in ethanol has been even proposed as a standard for fluorescence measurements⁴³. The fluorescence spectra of zwitterion and cation forms of rhodamines closely resemble the mirror image of the long-wave absorption band (see Fig. 1.8). The fluorescence maximum is shifted by about 500 - 800 cm^{-1} in respect to the absorption maximum.

Fluorescence quantum yield of the zwitterion forms of rhodamines is markedly influenced by different structural factors and medium effects such as the nature of the solvent and the pH value. In particular, the rate constant of radiationless deactivation of the S_1 state of rhodamines was found to depend on the degree of alkylation of the amino groups, counter ions, solvent temperature, viscosity and polarity, specific solute-solvent interactions and the $S_0 - S_1$ energy gap. The distinct exception was R101 where almost no non-radiative process has been found until now. Increasing the solvent viscosity or lowering the temperature significantly slows down the rate of radiationless processes in other rhodamines. The solvent does not apparently have, however, any significant influence on the position of their fluorescence maximum. A more detailed description of the above mentioned factors is given below in section 1.4.

1.3.2. Intersystem crossing and triplet states of rhodamines

An astonishing feature of ionic forms of rhodamines is their low quantum yield of intersystem crossing. This peculiarity was also one of the reasons for applications in dye lasers. In rhodamines, the triplet state has sometimes been included in the radiationless process⁴⁴, other works, however, seem to contradict this, pointing to very low triplet yields. Triplet quantum yield measurements carried out both by means of flash photolysis⁴⁵⁻⁴⁶ and energy transfer method⁴⁷ gave low values of Φ_T (e.g. for RB ranging from 0.003 to 0.006 in protic solvents; ethanol or water were used) and indicated that the intersystem crossing seems to play a minor role in degradation of excitation energy in rhodamines. This was confirmed by a very high (close to 1.0) quantum yield of fluorescence for some rhodamines (e.g. R101 mentioned above). The dye RB was also reported to reach fluorescence quantum yield of approximately 1.0 (in absolute ethanol) at temperatures below 200 K⁴³. In fact, there are only

very few reports investigating the phosphorescence of rhodamines. A phosphorescence spectrum (not corrected for spectral response of the detection system) of rhodamine B in ethanol-water solution at 77 K was reported by Chambers and Kearns⁴⁸. The spectrum was measured in 1:1 ethanol-water mixture containing 10 M LiBr, so it is still not clear where the phosphorescence comes from, what is the nature and what are the properties of the emitting triplet state. In the following paper, the phosphorescence of rhodamine B was reported to be polarised out-of-plane⁴⁹. A more detailed data on phosphorescence of rhodamines in ethanol at 77 K has been reported by Nurmukhametov *et al.*⁴⁷. For a series of rhodamines (including RB, DR10 and R110) they published, *inter alia*, phosphorescence spectra together with fluorescence and phosphorescence quantum yields, triplet quantum yields and phosphorescence decay times (2.2 s and 1.6 s for DR10 and RB, respectively). The phosphorescence spectra exhibit a red shift in line with the degree of alkylation of amino groups of rhodamines (R110, DR10, RB have estimated energies of the lowest triplet state equal to 15930 cm⁻¹, 15350 cm⁻¹ and 14890 cm⁻¹, respectively). Phosphorescence quantum yields were found extremely low as compared with those of fluorescence (4.5·10⁻⁵ and 6·10⁻⁵ for RB and DR10, respectively). In presence of heavy atoms an increase in Φ_T accompanied by a decrease in both the fluorescence quantum yield and the yield of internal conversion was observed⁴⁶. External heavy atom effect was studied more thoroughly by Kezle *et al.*⁵⁰ who applied the flash photolysis method to investigate the changes in Φ_T at different concentrations of iodide or bromide salts in aqueous solutions. Concluding that - contrary to previous suggestions⁵¹ - fluorescence quenching in aqueous solutions of rhodamine dyes containing halogen salts is not only due to formation of non-luminescent ionic associates of dye molecules with halogen ions, they have confirmed the observation reported by Chibisov *et al.*⁴⁶. The presence of KI at concentration equal to 2.5·10⁻² M in water caused an increase in Φ_T by *ca.* 10 times for rhodamine B, which - compared with triplet quantum yields given above - is still rather a small growth in Φ_T . Apart from an enhanced spin orbit coupling resulting from proximity of a heavy atom, excitation energy was found to be a factor significantly influencing the intersystem crossing process in rhodamines. It has been shown⁵² that the ISC process proceeds also from higher excited singlet states which confirmed earlier suggestions⁵³ derived from transient absorption measurements⁵⁴. Investigating the elementary mechanism of intersystem crossing in rhodamines (including RB), Rylkov and Cheshev⁵⁵ have concluded that an effective ISC process from higher excited singlet states occurs in these dyes. Using the data on lifetimes of higher singlet states⁵⁶ and the quantum yields of S_n → T transitions, and assuming that internal conversion within the triplet manifold is much faster than the reverse ISC process (triplet-to-singlet) they estimated the rate constants for S_n → T intersystem crossing. The values obtained for rhodamines had been found by 3 - 5 orders of magnitude larger than the rates of S₁ → T₁ intersystem crossing.

1.4. Thermally activated deactivation of excited ionic forms - a review of the mechanisms postulated in the literature

Intramolecular rotational diffusion

The radiationless deactivation of zwitterion and cation forms of rhodamines has been investigated for a long time and attracted considerable attention, since this process competes with fluorescence emission of these dyes, affecting i.a. their lasing properties. The radiationless process exhibits marked temperature dependence. Various explanations of the process have been proposed in the literature. Considerable support has received the relation between the radiationless deactivation of the singlet excited state and the rotation of amino groups of the dye. It was originally formulated by Drexhage⁷, who postulated that torsional motion of the diethylamino group in rhodamine B is involved in the non-radiative process. The synthesis of rhodamine 101 having amino groups rigidly linked to the xanthene skeleton, its very high luminescence quantum yield, and - in particular - the independence of this quantum yield of the temperature - seemed to be very strong arguments confirming this suggestion to explain the nature of the non-radiative decay. The hypothesis was further supported by the observation that rhodamines in frozen or in very viscous solvents (e.g. glycerol) have a fluorescence quantum yield close to 1.0⁴². The intramolecular rotation process of the amino groups hindered by the solvent viscosity turned out, however, to be too simple model to explain the radiationless deactivation observed in rhodamines.

TICT model and dependence of non-radiative decay on solvent polarity

Investigating rhodamines and pyronines with various substitution pattern at the amino nitrogen atoms, Vogel *et al.*⁸ have noticed that based on the model derived from the loose bolt theory (describing the radiationless deactivation by intramolecular rotation) one would expect the rotation to slow down with increasing rotational volume, which is contrary to observation. They have further found that in n-butyl chloride, a solvent much less polar than DMSO or ethanol, all investigated rhodamines show long fluorescence lifetimes corresponding to high fluorescence quantum yield indicating that no intramolecular quenching takes place, which is also not expected if loose bolt theory is valid. Furthermore, the rate of internal conversion of RB does not correlate in a simple way with the solvent viscosity, since the rate constant for the zwitterion form of RB in ethanol at 293 K was found similar to that in glycerol and three times smaller than in water whereas ethanol has a viscosity almost 16 times smaller than that of glycerol and 1.2 times higher than that of water⁵⁷. Analogous radiationless process was observed by Vogel *et al.*⁵⁸ in pyronines and by Jones *et al.*⁵⁹ in structurally related coumarines. In water, the quenching was found in all coumarines, independently of their molecular structure (also in those conformationally rigid!). The observations made by Vogel *et al.* lead to the following conclusions: (i) the non-radiative deactivation of the excited singlet states appears to be a process connected with the rotation of dialkylamino groups, and (ii) this rotation is not purely diffusive but is stimulated by a driving force which depends on solvent polarity and viscosity as well as on the steric and electronic properties of the rotating groups.

Based on these findings they concluded that kinetic behaviour of rhodamine dyes can be explained by assuming an intramolecular rotational motion towards a low-lying non-emissive TICT-like (Twisted Intramolecular Charge Transfer) state with charge localisation. The formation of the TICT state involves an electron transfer from the amino group to the xanthene ring of the molecule accompanied by a rotation around the C-N bond⁶⁰. Thermally activated formation of the non-emissive TICT-like state leads to a corresponding decrease in the observed fluorescence quantum yield. The population probability of the TICT state from the S_1 state has to depend on the donor and acceptor properties as well as on the solvent polarity which would stabilise the highly polar structure of the TICT state in respect to the S_1 excited state. The emission from the TICT state, however, was not observed for any rhodamine or pyronine. Lack of the TICT emission was thought to be due to a forbidden radiative transition and/or an ultrafast rate constant of internal conversion to the S_0 state⁸.

The TICT hypothesis for rhodamines was also used by other authors to explain their observations. Casey and Quitevis studied fluorescence lifetimes of RB in a series of normal alcohols⁹ and concluded that their results are consistent with the model assuming the equilibrium of the planar and the twisted configuration of the diethylamino groups on the xanthene ring of rhodamine B, and internal conversion from the twisted configuration. Chang and Borst⁶¹ studied the effects of solvent polarity and solvent viscosity on the non-radiative rates of rhodamine B deactivation and found that variations in the non-radiative rates are mainly due to solvent polarity changes and the solvent viscosity has no significant effect on the non-radiative process. In the subsequent paper, Chang and Cheung¹¹ have considered the effect of solvent polarity in the Arrhenius-type equation by introducing a polarity dependence into the activation energy, and have taken into account the effect of solvent viscosity by including a fractional power viscosity factor in the pre exponential coefficient. In the empirical expression postulated in their paper they used E_T^N , a normalised solvent polarity parameter recommended by Reichardt *et al.*⁶², to describe the dependence of the barrier height on solvent polarity. They found that this empirical formula can describe satisfactorily the non-radiative process in RB in solvents used (water-alcohol mixtures, monoalcohols, ethylene glycol and glycerol). In addition, studying cationic form of RB in alcoholic solutions they found that the effect of solvent polarity is stronger for the zwitterionic form than for the cationic one. The effect of solvent viscosity was about the same for both forms.

TICT states have been proposed by Rettig and Klock as an explanation of the intramolecular non-radiative process in 7-aminocoumarines⁶³. This hypothesis has been recently verified and confirmed by Rechthaler and Köhler⁶⁴. The latter authors did not observe any luminescence from the TICT state and interpreted the quenching rate as the rate of the rotatory relaxation to the TICT state. Furthermore, they proposed fast back electron transfer *via* a low polarity triplet state of the perpendicular configuration as a reason of the rapid deactivation of the TICT state as well as the interplay of twist and pyramidal (umbrella like) motion of the amino group during rotation and dielectric solvent effects as an explanation of the solvent influence on the energetics of this deactivation pathway.

The TICT model explains the decrease in the rate constant of the non-radiative process in rhodamines with monoethylamino groups (i.e. rhodamine DR10 ($R_1 = C_2H_5$, $R_2, R_3, R_4 = H$), Fig. 1.1) in respect to those with diethylamino groups by considering the donor-acceptor capabilities of the moieties. The TICT state of rhodamines with monoethylated amino groups is not populated probably because the energy of the state is higher than that of the S_1 state. Strong structural argument in favour of the TICT model was the fact that no thermally activated non-radiative process was observed in rhodamines with amino groups rigidly linked to the xanthene moiety (e.g. rhodamine 101).

However, the TICT model cannot satisfactorily explain several experimental aspects, such as (i) the influence of the carboxylphenyl group (much lower rate of radiationless deactivation in rhodamines with COO^- group compared to those with $COOH$ or $COOEt$ group), (ii) non-formation of the TICT state in rhodamines with monoalkylated amino groups⁸ (which would suggest a different radiationless mechanism for these dyes with respect to rhodamines with dialkylamino groups) or (iii) the effects of specific rhodamine - solvent interactions^{57, 65}. Moreover, in their extensive study on rhodamine B, rhodamine 101 and pyronine B adsorbed on single crystals of aromatic hydrocarbons, Kemnitz *et al.*⁶⁶ provided with strong arguments against the TICT mechanism of radiationless deactivation although their work was published prior to the paper by Vogel *et al.*⁸. As their work will be discussed later on in this thesis (in section 6.6), we mention here only that they have observed, among others, non-exponential decay and a significant shortening of the decay time in rhodamine 101, which proved that a non-radiative process - analogous to that occurring in RB - does take place also in this molecule.

ULM model

In order to overcome the problems connected with the TICT model, López-Arbeloa *et al.*^{65, 67-68} have proposed an alternative and to a certain extent, complementary mechanism of non-radiative deactivation of rhodamines. In this model, the radiationless process is attributed to a structural change of the amino groups from a planar xanthene= $N^+<$ (with sp^2 hybridisation) to a pyramidal xanthene $^+< N$ (with sp^3 hybridisation). This structural transformation (resembling opening and closure of an umbrella, therefore Umbrella-Like Motion) involves a disruption of xanthene=amine double bond to the xanthene-amine single bond (enabling the amino group to rotate) and a displacement of the rhodamine positive charge from the nitrogen atom to the xanthene ring. The radiationless deactivation can be visualised as the change between the symmetrically and energetically equivalent structures (A) and (B) of Fig. 1.7, which could be stabilised by the solvent or by the intramolecular interactions. In the resonance structure (C), rotation of the amino group does not interrupt the π -electron system, and hence does not lead to internal conversion. In systems, where the structures (A) and (B) have higher statistical weights than the resonance structure (C), internal conversion is more probable because of a high electron density in the xanthene-amine bond. Stabilising the positive charge at either the 9-carbon atom or at the amino nitrogen prevents

the disruption of the π -electron system at the xanthene-amine bond and decreases the probability of internal conversion.

The ULM model explains the effect of amino group alkylation taking into account the fact that the inductive effect of the ethyl substituents generates a higher electronic density in the xanthene-amine bond increasing in this way the rate constant of radiationless deactivation, since the $sp^2 \rightarrow sp^3$ structural change becomes more feasible.

In ULM model, the solvent influences internal conversion in rhodamine dyes through specific solute-solvent interactions at the amino and at the carboxylphenyl (PhCOOR) group. In rhodamines, the PhCOOR group is essentially perpendicular to the xanthene system. In such a configuration, the negative field of the COOR group can stabilise the positive charge at the 9-carbon atom. Increase of the xanthene-COOR interaction increases the statistical weight of the resonance structure (C), whereas increasing the molecular interaction at the amino nitrogen atom increases the statistical weight of the resonance structures (A) and (B). Solvent coupling at the PhCOOR group reduces the xanthene-COOR interaction and thus destabilises the positive charge at the 9-carbon atom, whereas the solvent coupling at the amino group stabilises the positive charge on the amino nitrogen atom.

Casey and Quitevis have introduced a two-state model^{9, 69} (a variation of the TICT model) quantitatively relating the non-radiative rate constant, k_{nr} , to the solvent parameter $E_T(30)$. This model was used to explain the linear increase in $\ln k_{nr}$ with $E_T(30)$ and the linear increase in activation energy of the non-radiative transition with $E_T(30)$ for the cation form of rhodamine B in normal alcohols. In this model the temperature dependence of k_{nr} arises from the temperature dependence of equilibrium constant between the two states. The variation of k_{nr} in normal alcohols results from the polarity dependence of the Gibbs free energy difference, ΔG_0 , between the two states. In their next paper⁷⁰, the same authors have compared the rates of non-radiative process in the cation of rhodamine B in nitriles with those in alcohols and concluded that the dependence on solvent polarity is due to specific solute-solvent interactions at the amino group and at the PhCOOR group. In conclusion, they state that their results agree with the ULM model and contradict the TICT model.

Both the TICT and the ULM model trying to explain the mechanism of the non-radiative decay in rhodamines emphasise the structural aspects of the molecules involved and limit the role of the solvent to specific solute-solvent interactions and stabilisation of the interaction between the xanthene system and the PhCOOR group. In the following chapters of this thesis it will be shown that - at least for zwitterions generated from the lactones in the excited state ring opening reaction - this approach is not justified, and that the role of the solvent is much larger than it can be expected from the work described in this section.

1.5 Photophysics of the lactone form of rhodamines

1.5.1 Existing foundations for this thesis

Although the studies described briefly above cover the properties of the excited states of rhodamines and use spectroscopic methods, they were mostly focused on the ground state equilibria and properties, and on the non-radiative deactivation processes in the ionic forms. Another contributions to our knowledge on rhodamines came from dedicated studies on the lactone forms of rhodamines. The number of papers dealing with the photophysics of the lactone forms until now has been very limited. But the picture of the photophysics of lactones that can be drawn up on the basis of these studies turns out to be completely different from that existing for the ionic forms. Below a brief summary of the results obtained in photophysical studies of the lactone forms of rhodamines is given.

The first paper was that by Klein and Hafner¹⁴, who studied the lactone form of rhodamine B (LRB) in a series of aprotic solvents covering the polarity range from cyclohexane to acetonitrile. They have presented a detailed description of the photophysical parameters of the lactone form, giving the positions of the absorption and fluorescence maxima, as well as the fluorescence quantum yields and decay times. They have found that - unlike the absorption spectra - the fluorescence exhibits a very large solvent effect. On increasing the solvent polarity, the lactone fluorescence (**L**) could be shifted by up to 5000 cm⁻¹, while the quantum yield increased and then decreased. In solvents of medium polarity (e.g. CH₂Cl₂) they discovered a double fluorescence and ascribed the second band (**Z**) to come from the zwitterion generated in its excited state. In highly polar solvents (e.g. acetonitrile) the **L** band disappears almost completely, so that the dual fluorescence appearing upon excitation of the lactone form can only be observed in a narrow range of solvent polarity. The excitation spectra of both fluorescences were the same and agreed well with the absorption spectrum of the lactone. The ratio of the **L** and the **Z** fluorescence did not depend on the excitation wavelength. In order to elucidate the nature of the state emitting in less polar solvents they calculated natural lifetimes from the long-wave absorption band of LRB in various solvents using the Strickler-Berg equation⁷¹. The values of the natural lifetimes from the measured quantum yields and fluorescence decays turned out to be much greater than those calculated from the absorption and fluorescence spectra. Based on the measured fluorescence quantum yields of both luminescences they determined the fraction of the molecules relaxing to the **L** and the **Z** state and concluded that quantum efficiency of population depends on the solvent: in solvents up to $\Delta f \approx 0.2$ (where $\Delta f = (\epsilon - 1)/(2\epsilon + 1) - (n^2 - 1)/(2n^2 + 1)$, a solvent polarity function), the lactone excited state is populated with the constant efficiency of about $\eta_L = 0.05$, and 95% of the excited molecules are deactivated *via* other states (probably triplets). On increasing Δf , a sudden decrease in population of the excited states of the lactone was reported to take place and was accompanied by a corresponding increase in efficiency of population of the excited zwitterion form (reaching the value close to unity). Using the solvatochromic shifts as a function of solvent polarity they

estimated the dipole moment of the lactone excited state to 25 D. The authors concluded that the observed L fluorescence does not arise from the primarily excited state and that the calculated natural lifetimes may describe the emitting state. With the relaxation from the Franck-Condon state to the fluorescent state a process of non-radiative deactivation competes in less polar media, and in the media highly polar enough - the process of the ring opening with population of the excited zwitterion.

Following the paper by Klein and Hafner a paper by Grigorieva *et al.*⁷² appeared in a very short time. These two independent papers from two different research groups represent a very interesting example in the history of science, as both contributions contain studies of the same process investigated from two different points of view. Both articles described the photophysics of the lactone form of rhodamine B and reported solvent-dependent fluorescence spectra. Klein and Hafner emphasised the intramolecular electron transfer reaction in the excited state process, resulting in the emitting states of the lactone and the zwitterion form, while Grigorieva *et al.* proposed an adiabatic photodissociation of the heterocyclic ring in the excited state as the most important property of the photophysics of the dye.

In the latter paper the lactone form of RB was studied in chloroform, acetonitrile, DMF and in mixtures dioxane-water. In chloroform, the authors observed a double fluorescence with the maxima at 490 nm and 565 nm, which they ascribed similarly as Klein and Hafner¹⁴ (L and Z band, respectively). On increasing the concentration of the dissolved lactone they observed a proportional increase in fluorescence intensity of both bands. They have also determined quantum efficiency of population of the excited Z state ($\eta_Z = 0.13$) in chloroform. Studying the lactone form of rhodamine B in mixtures dioxane-water, they have observed a dramatic decrease in fluorescence intensity of the L form accompanied by an increase of the zwitterion fluorescence at no absorption from the ionic form in the visible. Only single fluorescence band was observed in acetonitrile and in DMF. The authors reported also on accumulation of the cation form during the irradiation in chloroform and in acetonitrile. In their second paper, measuring fluorescence build up and decay curves, Grigorieva *et al.*⁷³ found no delay in creation of the excited zwitterion as compared with the excited lactone (on a ns time scale). Analysing kinetics of possible excited state reactions, they concluded that the adiabatic photodissociation proceeds from a non-relaxed state of the lactone molecule. Furthermore, they postulated that the processes of creation of the fluorescent state and the dissociation of the lactone ring are not associated with the relaxation of intramolecular vibronic states, but with the relaxation of the solvent. Laser flash photolysis on a μs time scale in water containing dioxane did not reveal any creation of the zwitterion ground state, so the authors have narrowed down the time of the ground state reverse reaction of ring closure below 1 μs .

Grabowski *et al.*⁶⁰ postulated the CT state of LRB to be analogous to the TICT states, as stabilised by mutually perpendicular conformation of the xanthene and the phthalide part. Another explanation of the source of L fluorescence has been proposed by Ponomaryev *et al.*⁷⁴ who tried to investigate the nature of this emission with anomalous Stokes shift.

Comparing rhodamines with different substituents at amino nitrogen atom (i.e. $-\text{NH}_2$, $-\text{NHC}_2\text{H}_5$ and $-\text{N}(\text{C}_2\text{H}_5)_2$) and using analogy with 7-dialkyl substituted coumarines, they have excluded structures with intramolecular charge transfer as those being responsible for the L fluorescence. Their main argument was that in coumarines such structures are formed in polar solvents and in presence of alkyl substituents at amino nitrogen atom only⁵⁹, whereas in rhodamine lactones an anomalously shifted fluorescence may be observed in neutral low polar solvent in monoalkyl substituted molecules and even in rhodamine 110. In an attempt to explain the anomalous Stokes shift of the lactone fluorescence they postulated formation of a highly polar molecule with a carbinol structure (Fig. 1.9) as a result of the photoprocess taking place in the Franck-Condon state. However, they did not give any evidence for such a structure and support their hypothesis only by comparison with absorption and fluorescence spectra of carbinols of pyronine G and of ester derivative of rhodamine DR10. Time-resolved fluorescence spectra with ns time resolution show that the L fluorescence appears immediately (on the ns time scale) and that the spectrum does not change at longer delay times (up to 20 ns) which in their opinion proves the origin of the fluorescent structure from the Franck-Condon state reached upon excitation of the lactone molecule. Although fluorescence maximum of carbinol and that of corresponding rhodamine are very close, the hypothesis about carbinol structure does not explain, however, numerous experimental observations, such as, for instance, the dependence of the Stokes shift on solvent polarity or the dependence of position of maximum of L fluorescence on the substituent at amino nitrogen atom. Furthermore, it was reported that carbinol structures exist only in a strongly alkaline solutions¹⁷.

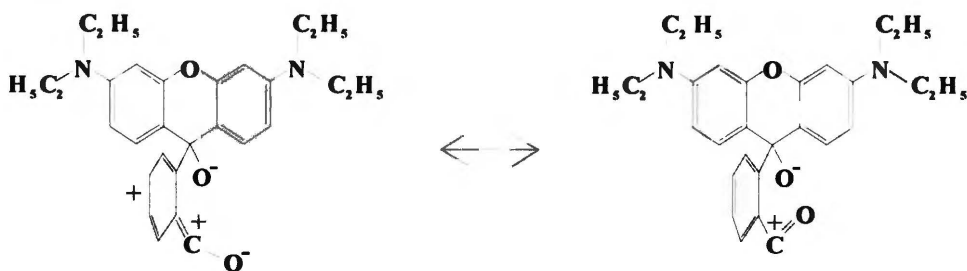


Fig. 1.9: Products of the excited state reaction according to Ponomaryev *et al.*⁷⁴

Dynamics of population of the zwitterion excited state in rhodamine B and in rhodamine S in DMF and in polymer matrices plastified with DMF was studied by Vlaskin *et al.*⁷⁵ by means of flash photolysis with picosecond time resolution. The authors reported transient absorption spectrum and the gain spectrum of LRB in DMF recorded 20 ps after the excitation pulse and they ascribed the band with maximum at 475 nm to the excited zwitterion form. It was shown by comparison of experimental results with model calculations taking into account the finite width of the laser pulses (6 ps) that the rise time of the zwitterion appearance is not longer than 1 ps. So high build up rate of the Z form and lack of any changes in the transient absorption and in the gain spectra with time was also observed on increasing solvent viscosity and in polymer matrices. This confirms that the dynamic process observed is not connected

with intermolecular interactions but is conditioned by the dissociation of the C-O bond and the redistribution of the electron density within the xanthene chromophore. Linear dependence of the fluorescence intensity on the intensity of the excitation pulse proved that the zwitterion is built up in a monophotonic mechanism of excitation.

1.5.2 The objectives of this thesis

As one may judge from the above overview, the studies on lactone forms of rhodamines have been rather scarce and the photophysics of these forms has not been investigated more thoroughly until now. In general, the five papers on photophysics of the lactone forms of rhodamines described above constituted the base and the starting point for the work performed within this study. The original goal of this thesis was to investigate the mechanism and the structure of products (possibly by identification of intermediates using time-resolved spectroscopic methods) of the excited state processes, which occur upon excitation of the lactone form of rhodamine B, to explain mutual relationship between the emitting states of two forms: **L** and **Z**, and to clarify the role the solvent plays in the photophysics of this molecule. Particular regard was to be devoted to the kinetics and solvent effect on ring opening reaction, resulting in formation of the excited zwitterion and to possible excited state $L \rightleftharpoons Z$ equilibrium. Special attention was to be drawn to verify whether a relationship of a parent-daughter type exists between these two species. Furthermore, it was intended to study the electron transfer reaction in the excited lactone molecule by studying the temperature effect on emission spectra as well as by modifying the electron donating capabilities of the xanthene part (supposed to be the donor) and the electron-accepting capabilities of the phthalide part (supposed to be the acceptor). This had led to the synthesis of lactones of other rhodamines (see section 1.1.3), which - in addition - allowed us to study the effect of the structure of xanthene part and the influence of the degree of alkylation of its amino substituents on the excited state processes.

At early stages of work it turned out, however, that the scope of this thesis had to be significantly modified and extended. That was due to results obtained in initial experiments, namely (i) the observation of a strong solvent effect on both the quantum yield and the lifetime of **Z** fluorescence, and (ii) the observation of a very intense phosphorescence from rigid lactone solutions at low temperature. On the other hand, some of the above mentioned processes, especially the ring opening reaction, occur much faster than the time resolution of the nanosecond and subnanosecond time resolved techniques available and could be studied within this thesis only indirectly. In the light of these facts, the main goal of this thesis became investigation of the intramolecular deactivation pathway of the **Z** form. The quenching of zwitterion fluorescence resembled very much the non-radiative process described for zwitterions directly excited from the ground state and an attempt was made to explain its mechanism in detail. A series of lactones synthesised for the purposes of this study turned out to be particularly suitable from the structural point of view for verification of quenching mechanisms postulated in the literature. Observation of a strong phosphorescence

stimulated to pose two fundamental questions: (i) what is the role of triplet states in photophysics of both the lactone and the zwitterion form of rhodamines with particular regard to their possible participation in non-radiative deactivation, and (ii) why the yield of triplet formation upon excitation of the L molecule exceeds by orders of magnitude that achieved upon direct excitation of the Z form?

An "overriding" objective of this thesis was, however, to systematise all excited states participating in excited state processes in a consistent diagram of energy terms that would allow to explain all transitions taking place in a lactone molecule upon its excitation. A supplementary task was to investigate the solvent effect on this diagram.

And last but not least: the question of the $L \rightleftharpoons Z$ equilibrium on the ground state level had to be addressed. This problem seems not to be directly related to the properties of the excited states, nevertheless this equilibrium may significantly influence the positions of energy levels of the excited states (in relation to the ground state of the lactone) changing in this way activation energies and facilitating (or hindering) corresponding transitions. Another reason for careful investigation of this issue was possible presence of zwitterions resulting from "natural" equilibrium, as zwitterions present in the ground state in solution could be excited and afterwards would have to be taken into account in interpretation of the results.

Some of the results of the present thesis as well as some experimental methods used in it have been already published^{6, 34, 76-78} and were presented on numerous conferences.

References and notes

- 1 U. Brackman, *Lambdachrome Laser Dyes*, Lambda Physik GmbH, Göttingen, 1986, p. III-123
- 2 A. Piutti and R. Piccolli, *Berichte* **31** (1898) 2112
- 3 R. Meyer and W. Sundmacher, *Berichte* **32** (1899) 2112
- 4 E. Noelting and K. Dziewoński, *Berichte* **38** (1905) 3516
- 5 K. H. Drexhage, *Laser Focus* **9** (1973) 35
- 6 J. Karpiuk, Z. R. Grabowski and F. C. De Schryver, *Proc. Indian Acad. Sci. (Chem. Sci.)* **104** (1992) 133
- 7 K.-H. Drexhage, in *Dye Lasers*, 2nd edition, pp 144-193 (edited by F. P. Schäfer); Springer, Berlin (1977)
- 8 M. Vogel, W. Rettig, R. Sens and K.-H. Drexhage, *Chem. Phys. Lett.* **147** (1988) 452
- 9 K. G. Casey and E. L. Quitevis, *J. Phys. Chem.* **92** (1988) 6590
- 10 T.-L. Chang and H. C. Cheung, *Chem. Phys. Lett.* **173** (1990) 343
- 11 T.-L. Chang and H. C. Cheung, *J. Phys. Chem.* **96** (1992) 4874
- 12 D. Deutsch, *Z. Physik. Chemie* **136** (1928) 353
- 13 D. A. Hinckley, P. G. Seybold and D.P. Borris, *Spectrochim. Acta* **42A** (1986) 747
- 14 U. K. A. Klein and F. W. Hafner, *Chem. Phys. Lett.* **43** (1976) 141
- 15 R. W. Ramette and E. B. Sandell, *J. Am. Chem. Soc.* **78** (1956) 4872
- 16 Further investigations have shown that the Z form of rhodamine B in ethanol has absorption maximum at 543 nm.
- 17 I. S. Ioffe and V. F. Otten, *Zh. Obshchei Khimii* **31** (1961) 1511

-
- 18 I. S. Ioffe and V. F. Otten, *Zh. Org. Khimii* **1** (1965) 336
- 19 I. S. Ioffe and V. F. Otten, *ibid.* p. 340
- 20 I. S. Ioffe and V. F. Otten, *ibid.* p. 343
- 21 A. Gutsze and H. Waleryś, *Acta Phys. Polonica* **23** (1963) 581
- 22 J. E. Selwyn and J. I. Steinfeld, *J. Phys. Chem.* **76** (1972) 762
- 23 J. Ferguson and A. W. H. Mau, *Chem. Phys. Lett.* **17** (1972) 543
- 24 J. Ferguson and A. W. H. Mau, *Australian J. Chem.* **26** (1973) 1617
- 25 P. J. Sadkowski and G. R. Fleming, *Chem. Phys. Lett.* **57** (1978) 526
- 26 N. S. Poleuktov, V. N. Dobryazko and S. B. Meshkova, *Zh. Anal. Khimii* **27** (1972) 1408
- 27 I. Rosenthal, P. Peretz and K. Muszkat, *J. Phys. Chem.* **83** (1979) 350
- 28 M. J. Snare, F. E. Treloar, K. P. Ghiggino and P. J. Thistlethwaite, *J. Photochem.* **18** (1982) 335
- 29 D. A. Hinckley and P. G. Seybold, *Spectrochim. Acta* **44A** (1988) 1053
- 30 D. A. Hinckley and P. G. Seybold, *J. Chem. Educ.* **64** (1987) 362
- 31 Y. Sueishi, Y. Sugiyama, S. Yamamoto and N. Nishimura, *Bull. Chem. Soc. Jap.* **67** (1994) 572
- 32 D. D. Desai and N. H. Pandhaye, *Curr. Sci.* **32** (1963) 356; the data according to *Beilstein's*, vol. E V 19/8, p. 669
- 33 F. Barigelletti, *Chem. Phys. Lett.* **140** (1987) 603
- 34 J. Karpiuk, Z. R. Grabowski and F. C. De Schryver, *J. Phys. Chem.* **98** (1994) 3247
- 35 K.-H. Knauer and R. Gleiter, *Angew. Chem. Inter. Ed. Engl.* **16** (1977) 113
- 36 H. Willwohl, J. Wolfrum and R. Gleiter, *Laser Chem.* **10** (1989) 63
- 37 Y. Sueishi, Y. Sugiyama, S. Yamamoto and N. Nishimura, *J. Phys. Org. Chem.* **6** (1993) 478
- 38 R. Sens, *Strahlungslose Desaktivierung in Xanthen- Oxazin- und Carbazinfarbstoffen*, Thesis, University of Siegen, 1984
- 39 H. Jacobi and H. Kuhn, *Z. Elektrochem. Ber. Bunsenges. Phys. Chem.* **66** (1962) 46
- 40 H. Kuhn, in *Progress in the Chemistry of Organic Natural Products*, ed. by D. L. Zechmeister, Vol. 16, Springer, Vienna 1958 -59, p. 411
- 41 S. Bergamasco, G. Calzaferri and T. Hädener, *J. Photochem.* **53** (1990) 109
- 42 R. F. Kubin and A. N. Fletcher, *J. Luminesc.* **27** (1982) 455
- 43 T. Karstens and K. Kobs, *J. Phys. Chem.* **84** (1980) 1871
- 44 H. Alobaldi, F. Alberkdar, Z. Hafidh and S. Alalkway, in *Laser Induced Processes in Molecules* (edited by K. L. Kompa and S. D. Smith) Berlin, 1979, pp. 108 - 110
- 45 V. E. Korobov, U. V. Shubin and A. K. Chibisov, *Chem. Phys. Lett.* **45** (1977) 498
- 46 A. K. Chibisov, H. A. Kezle, L. V. Levshin and T. D. Slavnova, *J. Chem. Soc. Chem. Comm.* **1972** 1292
- 47 R. N. Nurmukhametov, N. I. Kunavin and G. T. Khachaturova, *Izvest. Akad. Nauk SSSR Ser. Fiz.* **42** (1978) 517
- 48 R. W. Chambers and D. R. Kearns, *J. Phys. Chem.* **72** (1968) 4718
- 49 R. W. Chambers, T. Kajiwara and D. R. Kearns, *J. Phys. Chem.* **78** (1974) 380
- 50 H. A. Kezle, L. V. Levshin and V. V. Bryukhanov, *Zh. Prikl. Spekt.* **24** (1976) 809
- 51 A. P. Kostyshina and A. T. Pilepenko, *Zh. Prikl. Spekt.* **13** (1970) 444
- 52 V. V. Rylkov and E. A. Cheshev, *Opt. Spekt.* **63** (1987) 778
- 53 U. Krüger and R. Memming, *Ber. Bunsenges. Phys. Chem.* **78** (1974) 679

-
- 54 Studies on transient absorption of rhodamines are reviewed in more detail in Chapter V of this thesis.
- 55 V. V. Rylkov and E. A. Cheshev, *Opt. Spekt.* **63** (1987) 1030
- 56 V. L. Ermolaev and V. A. Lyubimcev, *Opt. Spekt.* **56** (1984) 1026
- 57 I. López Arbeloa and K. K. Rohatgi-Mukherjee, *Chem. Phys. Lett.* **129** (1986) 607
- 58 M. Vogel, W. Rettig, R. Sens and K.-H. Drekhage, *Chem. Phys. Lett.* **147** (1988) 461
- 59 G. Jones II, W. R. Jackson, C.-Y. Choi and W. R. Regmark, *J. Phys. Chem.* **89** (1985) 294
- 60 Z. R. Grabowski, K. Rotkiewicz, A. Siemiarczuk, D. Cowley and W. Bauman, *Nouv. J. Chim.* **3** (1979) 443
- 61 T.-L. Chang and W. Borst, *J. Phys. Chem.* **93** (1990) 4724
- 62 C. Reichardt and E. Harbush-Goemart, *Liebigs Ann. Chem.* **1983** 721
- 63 W. Rettig and A. Klock, *Can. J. Chem.* **63** (1984) 1649
- 64 K. Rechthaler and G. Köhler *Chem. Phys.* **189** (1994) 99
- 65 T. López-Arbeloa, F. López-Arbeloa, P. Hernández Bartolomé and I. López Arbeloa, *Chem. Phys.* **160** (1992) 123
- 66 K. Kemnitz, N. Tamai, I. Yamazaki, N. Nakashima and K. Yoshihara, *J. Phys. Chem.* **91** (1987) 1423
- 67 I. López-Arbeloa and K. K. Rohatgi-Mukherjee, *Chem. Phys. Lett.* **128** (1986) 474
- 68 F. López-Arbeloa, T. López-Arbeloa, M. J. Tapia Estévez and I. López-Arbeloa, *J. Phys. Chem.* **95** (1991) 2203
- 69 K. G. Casey and E. L. Quitevis, *Proc. SPIE-Int. Soc. Opt. Eng.* **910** (1988) 144
- 70 K. G. Casey, Y. Onganer and E. L. Quitevis, *J. Photochem.* **64** (1992) 307
- 71 S. J. Strickler and R. A. Berg, *J. Chem. Phys.* **37** (1962) 814
- 72 T. M. Grigoryeva, V. L. Ivanov, N. Nizamov and M. G. Kuzmin, *Dokl. Akad. Nauk* **232** (1977) 1108
- 73 T. M. Grigoryeva, V. L. Ivanov and M. G. Kuzmin, *Dokl. Akad. Nauk* **238** (1978) 603
- 74 O. A. Ponomaryev, A. O. Doroshenko, Y. F. Pedash and H. O. Mkhedlov-Petrosjan, *Zh. Fiz. Khimii.* **63** (1989) 2219
- 75 V. I. Vlaskin, A. J. Gorolenko, S. V. Melnitchuk, N. Nizamov, S. A. Tichomirov and G. B. Tolstorozev, *Dokl. Akad. Nauk* **302** (1988) 1141
- 76 J. Karpiuk, *J. Luminesc.* **60-61** (1994) 474
- 77 J. Jasny, J. Sepioł, J. Karpiuk and J. Gilewski, *Rev. Sci. Instrum.* **65** (1994) 3646
- 78 J. Karpiuk and Z. R. Grabowski, in *Proceedings of the Conference Fast Elementary Processes in Chemical and Biological Systems, Lille, 26-30 June 1995, France*, ed. C. Troyanovsky, American Institute of Physics, in print

CHAPTER 2

EXPERIMENTAL METHODS AND INSTRUMENTATION

2.1. Introduction

In this chapter a survey is given of the methodology and instrumentation used in the spectroscopic measurements that provided the data presented and discussed in this thesis. Also the procedures applied to obtain the lactones in a form of solids are described. Some of the methods and measurement techniques, and especially the software for computer controlled instruments, were developed originally during the research work within this thesis and now are successfully used in the Photochemistry and Spectroscopy Laboratory of the Institute of Physical Chemistry of the Polish Academy in Warsaw. Certain part of the measurements (e.g. those performed with aid of the single photon counting technique as well as some measurements of the temperature dependencies of the fluorescence) has been carried out in the Laboratory of Molecular Dynamics of the Catholic University of Leuven, Belgium, led by Prof. F. C. De Schryver. This explains doubling of some methods and instruments.

2.2. Materials used in the investigations

2.2.1. Lactones

The lactone forms of all rhodamines studied were synthesised starting from corresponding rhodamine salts. The procedures and purification methods described below do not pretend to be the most efficient ones. Only the synthesis of the lactone form of rhodamine B was previously described. The starting materials for synthesising of the lactones of rhodamine DR10 (LDR10), tetramethylrhodamine (LRMET) and rhodamine J3 (LJ3), in the form of corresponding chloride salts, were kindly obtained from Prof. K.-H. Drexhage from the University of Siegen, Germany. The lactone of rhodamine 101 (LR101) was obtained using laser grade perchlorate salt (Lambda Physics) and the lactone of rhodamine B - using the chloride salt of the dye.

(a) *Lactone of rhodamine DR10*

The lactone form of rhodamine DR10 was synthesised by conversion of its chloride salt by stirring the saturated aqueous solution of the dye containing 0.01 n NaOH with toluene. Rhodamine DR10 hardly dissolves in water and the rate of extraction was very moderate. After stirring, the water layer and the toluene layer have been separated from each other and the toluene was evaporated. An attempt to crystallise the lactone in cyclohexane gave rather unsatisfactory results. The cyclohexane was evaporated and the obtained red product was dried under vacuum over P₂O₅. Thin layer chromatography proved that only one substance was present in the sample. The product dissolved in methanol gave the absorption spectrum identical with that of the salt of the dye. On dissolving the product in butyronitrile, the

absorption spectrum analogous to that of rhodamine B lactone was observed (with some blue shift) and no absorption in the visible was recorded.

(b) Lactone of tetramethylrhodamine

To the saturated aqueous solution of the chloride salt of tetramethylrhodamine containing 0.01 n NaOH, an equal amount of toluene was added. After stirring the solution for 1 hour, leading to a significant decolouration of the water layer, both layers have been separated. The product obtained after evaporation of the toluene was hot dissolved in cyclohexane and crystallised twice from cyclohexane. The slightly red crystals were dried under vacuum over P₂O₅. The absorption spectrum of the product in methanol and the absorption spectrum of the dye were identical in the range 16000 cm⁻¹ - 35000 cm⁻¹.

(c) Lactone of rhodamine B

The lactone form of rhodamine B has been synthesised according to the method described by Klein and Hafner¹. The product was recrystallised from cyclohexane several times and then subsequently dried under vacuum over CaCl₂. The absorption spectrum of the cyclohexane solution agreed with that reported by Klein and Hafner.

(d) Lactone of rhodamine 101

Rhodamine 101 has been converted to its lactone form by hot extraction of the dye with toluene from the saturated solution of rhodamine 101 perchlorate in 0.01 M NaOH. After the toluene fraction has been enriched with the colourless lactone, the toluene layer was separated from the water layer and the solvent was evaporated. The slightly violet product was subsequently dried under vacuum over P₂O₅. On dissolving the product in an aprotic solvent, such as 1,2-dimethoxyethane, no absorption in the visible was observed. In turn, dissolution in methanol resulted in an absorption spectrum identical with that of rhodamine 101 perchlorate salt.

(e) Lactones of other rhodamines

During this study we have also obtained and occasionally used lactone forms of rhodamine J3 (structure as rhodamine B substituted at phthalide phenyl ring with 4 chlorine atoms) and rhodamine S (structure as rhodamine B but without phthalide phenyl ring). Lactone of rhodamine J3 was obtained after stirring for 10 minutes water solution of the dye with toluene, subsequent evaporation of the latter, and drying under vacuum over P₂O₅. Lactone of rhodamine S was synthesised following the procedure described for rhodamine B.

2.2.2. Solvents

The studies of the lactone forms of rhodamines required solvents of special purity. In particular, the solvents should be free of any traces of protic impurities. These impurities most probably facilitate protonation of the lactone molecule at the oxygen atom of the phthalide system. This reaction is accompanied by the hydrolysis of the lactone (C - O) bond and the subsequent creation of the elongated π -electron system that is characteristic for ionic forms of rhodamines. Such an ionic product is very easy to detect due to its absorption spectrum with a characteristic band in the visible region. The quality of the solvents was checked by

measuring the absorption of the LRB solution in a given solvent in the visible. We have found that after successful purification, even in very polar solvents the absorption from the ionic forms (mainly cation) of LRB could be reduced very significantly (this is very important in view of the lactone-zwitterion equilibria postulated in the literature - see Chapter 3). Only the solvents that yielded an absorption below certain limit were used in the measurements. For details see Chapter 3.

Only spectroscopic, HPLC quality, specially distilled solvents or solvents passed through the column with basic Al_2O_3 were used in the investigations. Table 2.1 lists the solvents used in this study, together with their abbreviations used in this thesis, the manufacturers as well as the remarks concerning the category and the purification method (where required) of the solvent in question.

Table 2.1

Solvents used in this thesis and methods of their purification

Solvent	Abbreviation	Manufacturer	Category	Purification method
Cyclohexane	CH	Merck	f. fluoresc.	1)
Butyl ether	BE	Merck	f. spectr.	
Ethyl ether	EE	Merck	f. fluoresc.	
Chlorobenzene	CB	Aldrich	f. spectr.	Al_2O_3
Dioxane	DI	Merck	f. spectr.	
Ethyl acetate	EA	Merck	f. spectr.	
Methyltetrahydrofuran	MTHF	Aldrich	f. synth.	2)
1,2-dimethoxyethane	DME	Aldrich	HPLC	
Tetrahydrofuran	THF	Merck	f. spectr.	
Dichloromethane	DCLM	Merck	f. fluoresc.	3)
Pyridine	PY	Aldrich	f. spectr.	
Butyronitrile	BN	Merck	f. synth.	4)
Benzonitrile	BZN	Aldrich	f. spectr.	
Propionitrile	PN	Merck	f. synth.	4)
Acetonitrile	AN	Aldrich	HPLC	
N,N-dimethylformamide	DMF	Merck	f. spectr.	5)
Dimethylsulfoxide	DMSO	Merck	f. spectr.	
Methanol	MeOH	Merck	f. fluoresc.	
Ethanol	EtOH	Merck	f. fluoresc.	

- 1) distilled over sodium;
- 2) preliminary dried over NaOH and subsequently distilled twice over CaH_2 ;
- 3) boiled for 5 hours with CaCl_2 and molecular sieves 4A, and subsequently distilled;
- 4) distilled 3 times: over KMnO_4 , over P_2O_5 , and over CaH_2 ;
- 5) spectroscopic grade DMF, dried over molecular sieves A4, and subsequently distilled under vacuum

2.3. Absorption and emission spectra

Electronic absorption spectra were measured with Zeiss Specord M40, Perkin Elmer Lambda 6 and Shimadzu 3100 spectrophotometers. Absorption measurements at higher temperatures have been performed using special absorption cell with a water jacket.

Emission and excitation spectra were measured with a Jasný spectrofluorimeter² or with SPEX Fluorolog 212 spectrofluorimeter. The emission spectra have been corrected for the spectral response of the detection systems. The quantum yields were measured using quinine sulphate in 0.1 n H₂SO₄ as a standard ($\Phi = 0.51$) and corrected for the refractive index of a given solvent³. The absorbance of the solutions investigated in luminescence measurements, was typically 0.1 - 0.2 at the excitation wavelength, and was higher while studying concentration dependencies. The absorbance of solutions used in transient absorption measurements was sometimes slightly higher but did not exceed 0.6 in 1 cm absorption cell.

The quantum yields were calculated according to the equation (1.1):

$$\Phi_i = \frac{A_s I_i n_i^2}{A_i I_s n_s^2} \Phi_s \quad (2.1)$$

where: i denotes the quantities referring to the investigated substance and s - those referring to the standard; other symbols have the following meaning: Φ is the quantum yield, A - the absorbance at the excitation wavelength, I - the integrated intensity of the corresponding emission band, n denotes the refractive index.

In cases where two emission bands overlap, a procedure of separation in two components was applied. The shape of each band could be estimated from measurements where apparently one emission band occurs. Such shapes were assumed and subsequently the separate bands were extracted. In cases where either strong overlap occurs or where contributions from two emissions differ significantly from each other a large error was possible and therefore in such cases the quantum yields of total luminescence were estimated only.

In temperature measurements of luminescence, the relative intensities were given unless explicitly otherwise stated.

2.4. Measurements of fluorescence decays

The measurements of fluorescence decays in nanosecond and subnanosecond regions were carried out by means of two techniques: (i) the sampling technique using boxcar signal averager and (ii) the single photon timing technique. Below a short description of both experimental setups is given.

2.4.1. Sampling technique

The experimental setup for measurements by means of the sampling technique was described elsewhere⁴. Below, a block diagram of the apparatus is presented:

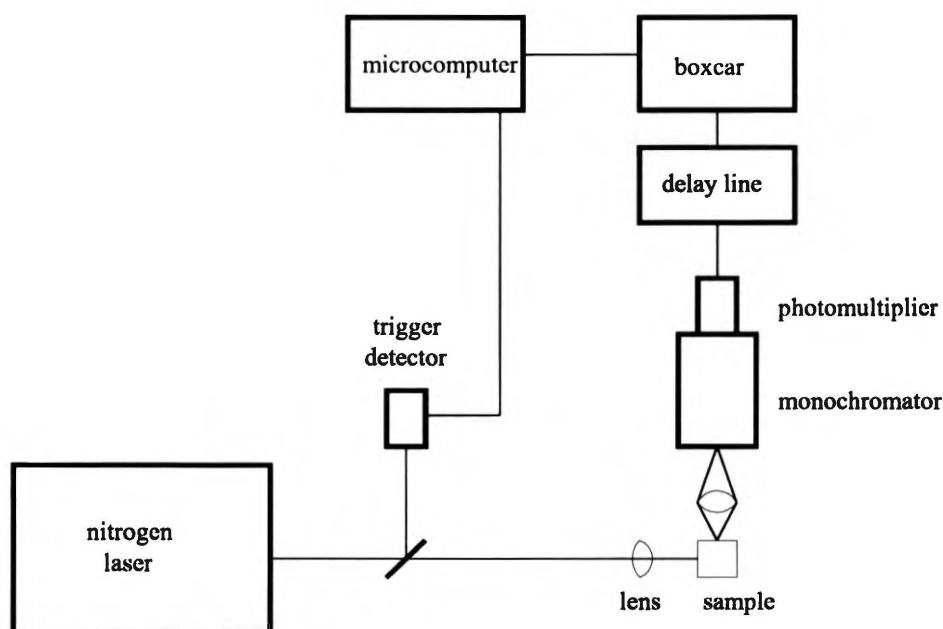


Fig. 2.1: Schematic diagram of the apparatus used for luminescence decay measurements by means of the sampling technique.

The nitrogen laser (ZWG, MSG 350; FWHM of the laser pulse was about 0.6 ns) was used to excite the sample. The fluorescence of the sample was collected in a 90° geometry on the entrance slit of the Jasny M32 prism monochromator². The signal from the photomultiplier (RCA, 1P28) after passing through a delay line (wave-guide type, KABID) was processed by a boxcar (ZWG, BCI 280) and then - after digitising by a specially developed interface card, transmitted to the Commodore C-64 microcomputer. The boxcar was triggered by a photodiode detecting the laser light pulse. During our research we have found that a special wiring of the photomultiplier was necessary in order to avoid the "ringing" of the signal and to ensure linear response of the detector. Such a "ringing" is most often caused by current oscillations in the photomultiplier circuit. The best way to eliminate it was to remove the base of the photomultiplier and to solder the disc ceramic capacitors directly to the shortened wires coming out from the tube. The signal obtained after these improvements was not contaminated by the current oscillations. The output signal from the photomultiplier was sampled with the sampler of gate duration 220 ± 50 ps. Typically, a measurement point was an average of 4 or 8 laser pulses. As the application of a photodiode for recording the intensity of the laser pulse and for normalising the signal intensity by the second gate of the boxcar (10 ns) did not improve significantly the signal-to-noise ratio, in most cases only the signal from the sampler was recorded.

The fluorescence decays were deconvoluted using a home-written program based on the method of iterative convolutions⁵ and Marquardt algorithm⁶. Usually, such software uses the method of least squares data reduction. An important point in the minimisation is to choose proper weighting factors which are equal to the reciprocal of the square of standard deviation. In the measurement techniques based on the counting of single photons (actually photoelectrons) one can assume Poisson distribution of the measured value and subsequently the square of standard deviation is equal to the measured value. This assumption is no longer

valid in the case of the signals delivered by a boxcar, and the weighting factors had to be assumed. We have found that in this case application of square roots of the measured value gave better results than the measured value itself.

2.4.2. Single photon timing technique

Decay measurements using the single photon timing (SPT) technique were performed with an instrument based on a synchronously pumped, cavity dumped DCM (640 nm) or rhodamine 6G (590 nm) dye laser (Spectra Physics models 375B, 344S and 454) that were operated with a mode locked Ar⁺ laser (Spectra Physics model 2020-05)⁷. UV pulses (320 nm and 295 nm, respectively) were generated through an angle-tuned KDP crystal. Repetition of the excitation pulses was 800 kHz. Fluorescence was passed through a polariser set at the magic angle and was detected through an American Holographic DB 10 double subtractive monochromator by a Philips XP2020Q photomultiplier tube. Pulse pile-up distortion was avoided by working at an average counting rate of 0.01 or less photon per excitation pulse. The start signal for the time-to-amplitude converter (TAC) was taken from a fast photodiode monitoring a fraction of the fundamental frequency of the laser beam. Constant fraction discriminators were used to eliminate background pulses and to provide correct voltage signals from the TAC. The output pulse from the TAC was fed into a biased amplifier to sample a section of the TAC range and expand it to cover the full voltage range of the multichannel analyser (MCA) (Canberra Model 8100) working in the pulse height analysis mode. Data collected in 512 channels of the MCA were transferred to a PC/AT computer for further processing. The response function of the detection system was recorded by measuring the decays of the reference compounds with known fluorescence decay times at the same wavelength and under the same conditions as the fluorescence measured for the investigated compound⁸. The references used were: xanthione in isooctane ($\tau = 37$ ps), 1,2-dimethyl-POPOP in methylcyclohexane ($\tau = 1.13$ ns) when measured in the spectral range below 540 nm and erythrosine in water ($\tau = 95$ ps) in the 550 - 610 nm range.

Fluorescence decays were first analysed in single curve analysis with a DECAN deconvolution program using a reference convolution method and based on the Marquardt algorithm⁶. The software for global analysis calculation was essentially the same as used by Jansen *et al.*⁹. The criterion for the fit in global analysis was $|Z(\chi^2)| < 3$.

2.4.3. Time-resolved fluorescence spectra

Time resolved spectra were recorded by means of the sampling technique with the instrument described above and boxcar equipped with a sampler of gate duration 220 ± 50 ps. The time resolution was ± 1 ns. The spectra were recorded in a fixed delay mode after manual adjusting of the proper delay time.

2.5. Transient absorption measurements

Transient absorption spectra were measured using an original computer controlled nanosecond transient spectrophotometer for laser flash spectroscopy (TAN 2) constructed by

Dr. Jan Jasny¹⁰. The spectrophotometer is based on the nitrogen (337 nm) laser (PTI, PL 2300) and on the dye laser pumped with the nitrogen laser. Typical parameters of the nitrogen laser used here are: repetition rate < 10Hz, pulse width (FWHM) < 1 ns, and pulse energy approximately equal 1 mJ.

Operation of the spectrophotometer is illustrated in a simplified diagram (Fig. 2.2). Nitrogen laser radiation is divided into two beams by a beam splitter. One of them, a sample excitation beam, before focusing is adequately delayed in a fixed optical loop. Residual excitation light passing through the sample is filtered off in front of the detectors. The second beam pumps the dye laser. The tunable radiation produced by the dye laser (termed hereafter a monitoring or a probing beam), enters the variable optical delay line (VODL) after collimation by a telescope. Having passed through the VODL, the monitoring light is focused

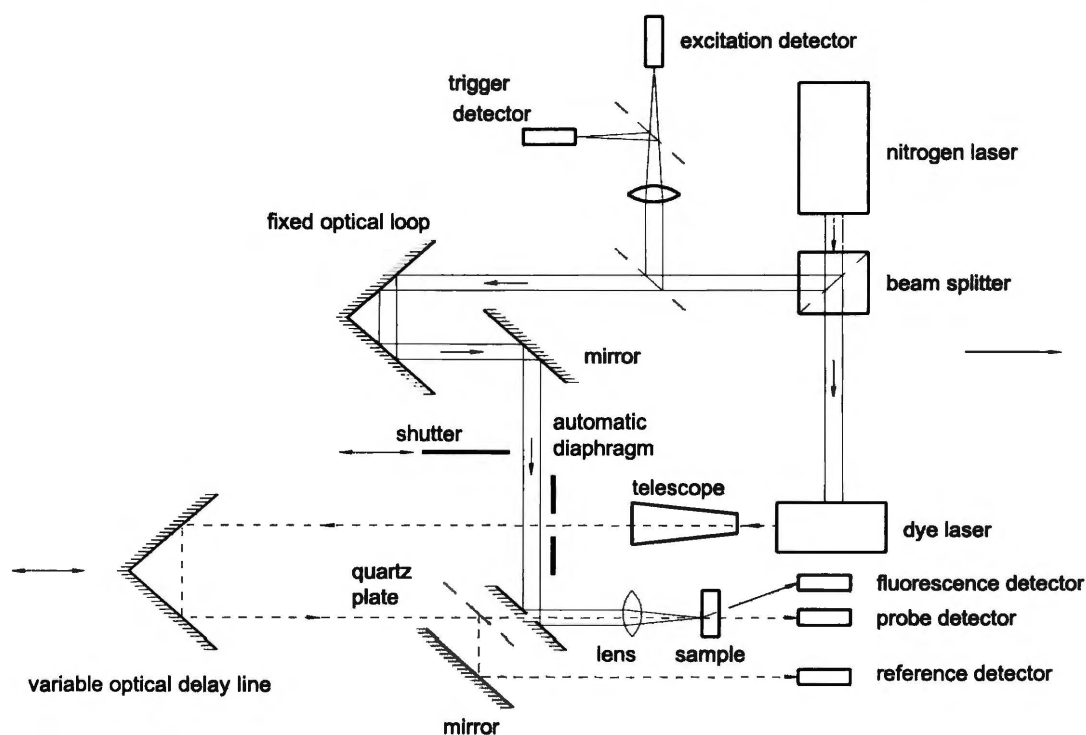


Fig 2.2: General scheme of the optical system of the TAN 2 nanosecond spectrophotometer.

on the sample and finally detected by the probe detector. If VODL is adjusted to have the shortest optical path, the monitoring pulse enters the sample about 2.5 ns before the excitation laser beam; by the longest optical path on the 2.5 m long guide rail the monitoring pulse enters the sample about 100 ns after the excitation beam. Before entering the sample, part of the monitoring beam is reflected by a transparent quartz plate towards the reference detector. Reference signal serves both to normalise the signal seen by the probe detector and to control the aperture of an automatic diaphragm placed just after the telescope. In a routine procedure the differences between the absorption of the excited and that of the unexcited sample, ΔA , for a selected wavelength of the monitoring beam and for a given delay of VODL, are measured. For this purpose, on the way of the excitation beam an electrically controlled shutter was installed. Since the investigated samples very often emit their own luminescence (e.g.,

fluorescence), an additional fluorescence detector near the probe detector has been installed. The signal from the fluorescence detector is taken into account in evaluation of the real value of ΔA . The signal to noise ratio may be significantly improved by averaging of all measurements for which the energy of nitrogen laser pulses lies within the chosen limits. This energy is monitored by an excitation detector. The measurement procedure starts after receiving the signal from the trigger detector.

The detection of light pulses in the spectrophotometer is performed by photodiodes working in photovoltaic mode, having low sensitivity with respect to electrical noises. Electric charge of each photodiode, proportional to the energy of the light pulse, is changed to an electric signal by using a charge-to-voltage converter. In addition, electrical noises are reduced by a two-pole Butterworth filter. The electric signal is then integrated, digitised by an analogue-to-digital converter and transmitted to a PC.

The intensity of the dye laser beam is controlled by means of a diaphragm changing the intensity of the dye laser beam by changing its cross section by about 200 times within 15 steps. The diaphragm opens or closes stepwise if the intensity of the probing or the reference beam is too low or too high as compared to the limits set in the program. The signal to noise ratio is also improved by rejecting all measurements for which the pulses exceed the limits set for the energy of the pumping laser.

A very important and useful feature of the spectrophotometer is the ability to move the sample along a Lissajoux figure simulating in this manner mixing of the sample. Pump and probe experiments are usually performed for gas phase or liquid samples where excited region could be easily refreshed, because of possible accumulation of a photoproduct, by flow or stirring. To make possible the measurements of solid samples (e.g. low temperature glasses, polymer films), a special mechanism has been constructed by Dr. J. Jasny¹⁰. It moves the sample in the plane perpendicular to the optical axis, so that the focus of the beam draws a Lissajoux figure. This figure has been chosen in such a way that the speed of the movement never falls to zero. Monitoring of a new area of the sample during each laser shot (which for the liquid solutions replaces the solution mixing) is of significant importance for rigid solutions or investigations of the compounds that are photochemically unstable.

The operation of the instrument is fully controlled by a PC connected to the electronic control panel by means of the 8255 card. The software operating the spectrophotometer has been written in Turbo Pascal. It consists of several routines that i.a. enable initialising of the instrument, changing of its operational parameters, carrying out the measurement, displaying the measured results in the real time mode on the screen as well as a quasi-manual control of the spectrophotometer.

A typical measurement procedure for one experimental point consists of triggering the laser, reading out the measurement values from the photodiodes served by a multiplexer, and - if they are within the limits set by the program - calculation of the optical density of the sample and displaying the value on the screen in a graphical form. The fluorescence intensity (measured by a separate photodiode) is subtracted from the measured intensity of the probing

beam and this quantity, after normalisation to the intensity of the reference beam, is used to calculate the optical density. The measurement cannot start when the sample emits too intense luminescence and the photodiode (measuring the fluorescence) becomes saturated. The problem is usually overcome by using neutral density filters, put between the sample and the fluorescence and the probe detector (see Fig. 2.2). Higher intensity required in this case for the probing beam is achieved by opening the automatic diaphragm.

The spectra were recorded by scanning the monitoring light over the spectral range (usually from 420 nm to 750 nm) by means of changing the wavelength of the dye laser. The kinetic curves of transient absorption were measured by changing a delay of the monitoring beam in relationship to the excitation beam. The delay was changed by shifting the roof prism on the rail guide. All these operations were automated and computer controlled.

2.6. Temperature measurements

The temperature of the sample was controlled by various thermostats assuring an accuracy of ± 1 K. Phosphorescence measurements were carried out at 77 K by immersing the cell with the sample in liquid nitrogen.

References and notes

-
- ¹ U. K. A. Klein and F. W. Hafner, *Chem. Phys. Letters* **43** (1976) 141
 - ² J. Jasny, *J. Luminesc.* **17** (1978) 149
 - ³ D. F. Eaton, *Pure & Appl. Chem.* **60** (1988) 1107
 - ⁴ J. Karpiuk and Z. R. Grabowski, *Chem. Phys. Letters* **160** (1989) 451
 - ⁵ H. E. Zimmerman, D. P. Werthemann and K. S. Kamm, *J. Am. Chem. Soc.* **96** (1974) 439
 - ⁶ D. W. Marquardt, *J. Soc. Ind. Appl. Math.* **11** (1963) 431
 - ⁷ (a) N. Boens, M. Van den Zegel, F. C. De Schryver and G. Desie, *From Photophysics to Photobiology*; Edited by A. Favre, R. Tyrrel and J. Cadet, Elsevier, Amsterdam, 1987, p. 93; (b) M. Van den Zegel, N. Boens, D. Daems and F. C. De Schryver *Chem. Phys.* **101** (1986) 311
 - ⁸ N. Boens, M. Ameloot, I. Yamazaki, F. C. De Schryver, *Chem. Phys.* **121** (1988) 73
 - ⁹ L. D. Janssen, N. Boens, M. Ameloot and F. C. De Schryver, *J. Phys. Chem.* **94** (1990) 3564
 - ¹⁰ J. Jasny, J. Sepioł, J. Karpiuk and J. Gilewski, *Rev. Sci. Instrum.* **65** (1994) 3646

CHAPTER 3

PHOTOPHYSICS OF THE LACTONE FORMS OF RHODAMINES

3.1. Absorption spectra

3.1.1. Ground-state equilibria

In contrast to the zwitterionic and cationic forms of rhodamines which absorb strongly in the visible and emit fluorescence very efficiently, lactone forms of these dyes - due to the interruption of the π -electronic system characteristic for the xanthene moiety - do not possess any chromophore being able to absorb in the visible¹. Therefore, any absorption in the 450 nm - 600 nm region of solutions prepared by dissolving the lactone form would indicate a presence of ionic forms of the dyes in the ground state. Fig. 3.1 shows absorption spectra of three molecular species of rhodamine B occurring in diethyl ether under different conditions:

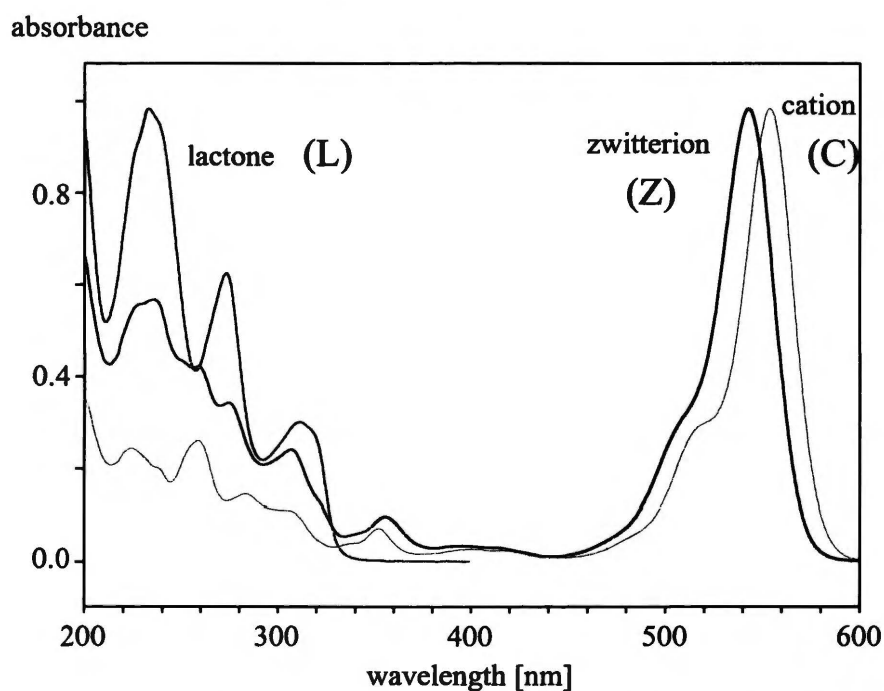


Fig. 3.1: Absorption spectra of different molecular forms of rhodamine B in diethyl ether (recorded for one lactone sample solution). The zwitterion (bold line) was generated by adding methanol to the sample. The cation (thin line) was obtained by adding 0.1 n H_2SO_4 to the ether/methanol solution. The spectrum (Z) shows some contribution from the lactone form (seen in the UV region) still present in the solution.

Spectrum (L) was obtained for the lactone dissolved in diethyl ether. Spectrum (Z) was recorded after adding few drops of methanol to the absorption cell containing the sample, and it represents a sum of absorption from the zwitterion form and the lactone form still present in the solution. Spectrum (C) was obtained for the above ether/methanol solution after adding a few drops of 0.1 n H_2SO_4 , under conditions where all molecules have been converted into the cations. The contribution from the lactone explains significant difference between the (Z) and the (C) spectrum in the UV region. Absorption maxima of the first absorption band of the

ionic forms, together with those of the respective lactone form for all four rhodamines studied have been collected in Table 3.1. For the purpose of comparison with lactones (see below), absorption maxima of corresponding amines have also been shown:

Table 3.1.

Positions of the first absorption maximum, λ_{\max} [nm], of various molecular forms of rhodamines and of respective aromatic amines.

Rhodamine	lactone ¹⁾	amine ²⁾	zwitterion ³⁾	cation ⁴⁾
DR10	303	295	517	527
RMET	310	298	538	549
RB	316	304	544	555
R101	317	-	568	577

1) in cyclohexane or dibutyl ether; 2) in cyclohexane or heptane; 3) in ethanol or methanol; 4) in ethanol with addition of one drop of 0.1 n H₂SO₄ to 3 ml solution.

All samples of rhodamines used in absorption measurements have been prepared by dissolution of the lactone crystals in respective solvents. The absorption bands of samples prepared by dissolving hydrochloride (DR10, RMET and RB) or perchlorate (R101) salt in ethanol ($c \approx 10^{-6}$ M) in the visible agreed well (position of the maximum, shape) with those obtained after dissolving the lactone form in ethanol. The absorption spectra of the cation forms have been measured after adding 1 drop of 0.1 n H₂SO₄ to the cell containing an ethanol solution of the respective rhodamine lactone. The distinction between the cation and the zwitterion is very important because these two kinds of species are formed on two different routes. The presence of the zwitterion might be caused by a possible (temperature or solvent dependent) ground state equilibrium between the lactonic and the zwitterionic form, whereas the cation in the aprotic media can originate only from protonation of dissolved lactone molecules by traces of protic impurities, almost always present, especially in more polar solvents. Formation of coloured complexes in RB lactone solutions in contact with cell windows was suggested by Snare *et al.*². We have not observed this effect, as well as remaining authors of papers reporting the ground state equilibria have not mentioned such an observation. Possible presence of zwitterions in the ground state in a larger amount would complicate the interpretation of results. Therefore, absorption spectra in the visible are of particular importance with respect to the ground state equilibria. Possibility of such equilibria was investigated for RB by Hinckley *et al.*³⁻⁵. The main conclusion drawn by the authors in regard to aprotic solvents was that the **Z** form of RB is absent in these solvents and present in equilibrium with the **L** form in protic solvents (see Section 1.2). At approximately the same time the occurrence of the **L** \rightleftharpoons **Z** equilibrium in butyronitrile-propionitrile mixture was reported for R101 by Barigelletti⁶. The question of possible ground state **L** \rightleftharpoons **Z** equilibria was of primary importance with respect to investigation of excited states appearing in the

sample upon excitation of the lactone molecule, as in some cases luminescence from the excited states of zwitterions was observed. Therefore, at preliminary stages of our work, it was critical to know which forms occur in the solution and are subsequently excited by the incident light.

It has been found that the quality of a solvent has an enormous effect on absorption spectra of the lactone solution in the visible. In some solvents, especially before purification, significant absorption in the visible was observed, which could be completely eliminated by purification of the solvent. Typical example were solutions of rhodamine B in butyronitrile. This solvent with excellent physical properties is commercially available in a poor quality only and has to be carefully purified. Usually, it has been distilled over KMnO_4 , over P_2O_5 , and over CaH_2 (once or twice), and it has been found that by careful distillation it was possible to decrease the absorption of RB in the visible band below the detection limit of the spectrophotometer (0.001 absorbance unit) at $1.5 \cdot 10^{-4}$ M concentration of lactone in butyronitrile.

The question of possible ground state equilibria was investigated more thoroughly in the case of R101⁷. The investigated solutions were checked carefully for the absorption in the visible region. In low polarity solvents like toluene or dibutyl ether a residual absorbance with a maximum at 583 nm or 585 nm, respectively, has been observed. By analogy with RB⁸ this absorbance may be ascribed to formation of dimers of the coloured form. In DME or MTHF no absorption in the visible has been found within the accuracy of the absorption spectrophotometer (0.001 absorbance unit) at the lactone concentration $[\text{L}] = 8.4 \cdot 10^{-5}$ M, which corresponds to an absorbance of 1.04 at 317 nm ($\epsilon_{317} = 12400 \text{ M}^{-1} \text{ cm}^{-1}$). Using the value of the molecular absorption coefficient for the zwitterion in EtOH, $\epsilon_{568} = 95000 \text{ M}^{-1} \text{ cm}^{-1}$ ⁹, and the value $A \leq 0.001$ absorbance units as an estimation for the upper limit of the concentration of zwitterions in the ground state, the value $[\text{Z}] \leq 1 \cdot 10^{-8}$ M was obtained. The ground state equilibrium constant $K(\text{L} \rightleftharpoons \text{Z}) \leq 1.2 \cdot 10^{-4}$ and the resulting $\Delta G^0 > 21.6 \text{ kJ} \cdot \text{mol}^{-1}$ (which corresponds to 1800 cm^{-1}) in 1,2-DME (at 293 K). This value of ΔG^0 in DME exceeds by about $12.0 \text{ kJ} \cdot \text{mol}^{-1}$ (1000 cm^{-1}) the value given by Barigelletti⁶ for a solution of the inner salt of R101 in BN/PN mixture.

Our measurements of LR101 in BN/PN mixture (4:5, v/v, as used in ref. ⁶) indicate the presence of the cation form of R101 rather than of the zwitterion one. In contrast to Barigelletti who reported the presence of an absorption band with a maximum at 568 nm and ascribed this band to zwitterion, we observed a (small) peak at 577 nm. Doubling the lactone concentration (measured in proportion to the intensity of the first absorption band of the lactone at 320 nm) only a 25% increase of the absorbance at 577 nm was observed. This could be explained by saturation of the protic impurities protonating the lactone molecules. After adding 1 drop of 0.1 n H_2SO_4 to the cell containing 3 ml of the BN/PN solution of LR101 the solution became deeply purple and the absorption spectrum changed completely. Addition of subsequent drops of the acid did not change the absorption spectrum. The maximum of the

peak in the visible (most intense) was at 577 nm and the spectrum in the UV indicated a full transformation of the lactone into the coloured form.

We have also compared solutions of LR101 in butyronitrile and in methanol. Both solutions were prepared in such a way that they exhibited the same absorbance in the visible ($A \approx 0.015$). The absorption maxima in the visible were, however, located at different wavelengths: at 568 nm in MeOH and at 575 nm in BN. The fluorescences excited at $\lambda = 320$ nm were also different, both in intensity and in position of the fluorescence maximum (at 582 nm in BN and at 588 in MeOH). The integrated intensity of the fluorescence from BN solution was approximately 15 times larger than that from the MeOH solution. This topic is discussed below in section 3.2.

On the basis of these findings we believe that the dominant source of the absorption in the visible in BN/PN solution is the cation form of the molecule produced through protonation by protic impurities present in the solvent. Hinckley *et al.*³⁻⁴ have postulated that the necessary conditions for stabilisation of zwitterion in a given solvent are: (i) hydrogen bonding and (ii) sufficient dielectric/polarisability capabilities of the solvent. Our results suggest, however, that in spite of failing the fulfilment of the first requirement in aprotic solvents, the observation of the $L \rightleftharpoons Z$ equilibrium in these media might be possible. Therefore, we do not exclude the presence of the zwitterion resulting from a possible equilibrium with the lactone form, especially on the basis of a small blue shift of the absorption maximum accompanied by a decrease of the band intensity with an increase of temperature, even if thermal expansion of the solvent has been taken into account (576 nm at 293 K, 574 nm at 323 K and 572 nm at 343 K). Energy difference of the two species is anyway higher than that given by Barigelletti⁶.

Assuming the molar absorption coefficient for cationic species of R101 to be equal to that of the zwitterion (i.e. $95000 \text{ M}^{-1}\text{cm}^{-1}$) we could estimate the total concentration of the ionic forms in a $2.8 \cdot 10^{-5} \text{ M}$ LR101 solution in BN/PN to be $3.7 \cdot 10^{-7} \text{ M}$. This roughly corresponds to the value found by Barigelletti; it has been shown here, however, that it cannot be ascribed entirely to the zwitterion. This in turn further increases the ΔG^0 value at 293 K for this system, as compared to that in ref. ⁶. *A priori* assumption that only 25% of the absorption in the visible is to be ascribed to zwitterion would yield the $\Delta G^0 = 13.8 \text{ kJ}\cdot\text{mol}^{-1}$ (1150 cm^{-1} compared with 830 cm^{-1} given in ref. ⁶). The real value could be even higher.

3.1.2. Absorption spectra of the lactone forms

The spectra of the lactone solutions in aprotic solvents have principally the same character for the lactones studied (Fig 3.2, part (I)). All the spectra exhibit in region 220 nm - 400 nm three broad bands with the fourth band arising at about 200 nm. Comparison of the absorption spectrum of LRB with that of the analogue N-phenylrhodamine lactam (part (II) of Fig. 3.2, the structure of the lactam was given in Fig. 1.5, p. 8) shows that the phthalide part of the rhodamine lactone has a minor influence on the absorption spectrum of the molecule. In fact, the absorption spectrum of phthalide exhibits its first band at about 286 nm (35000 cm^{-1} ,

$\epsilon \approx 1800$, an order of magnitude lower than the lactone absorption)¹⁰ and would not influence the position of the first absorption band of the lactone. Furthermore, perpendicular conformation of the phthalide with respect to the xanthene moiety minimises possible coupling between these two chromophores.

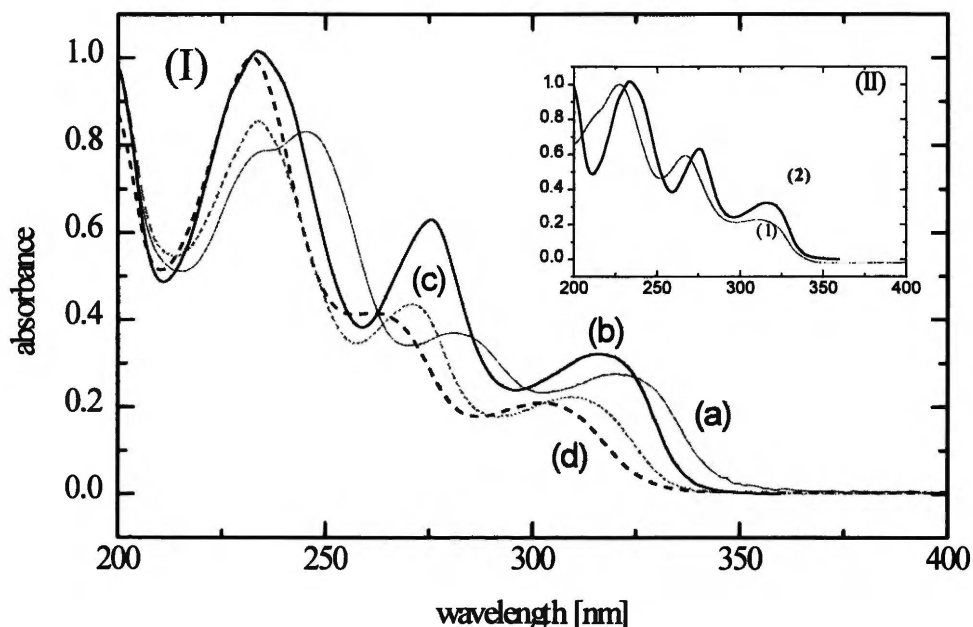


Fig. 3.2: Absorption spectra of the lactone forms of rhodamines in butyronitrile (normalised to the highest absorption peak). (I): LR101 ((a), continuous thin line), LRB ((b), bold line), LRMET ((c), dashed line) and LDR10 ((d), thick dashed line); (II) N-phenylrhodamine lactam and LRB (2) in butyronitrile.

Table 3.2.

Absorption maxima of three first bands of the lactone forms of rhodamines as a function of the solvent.

Rhodamine	LDR10	LRMET	LRB	LR101
Solvent	λ_{\max} [nm]	λ_{\max} [nm]	λ_{\max} [nm]	λ_{\max} [nm]
dibutyl ether				233 246 276 316
diethyl ether	232 260 297			231 243 276 314
dioxane				234 247 278 318
1,2-DME	232 262 302		234 275 315	230 250 279 316
THF			234 275 314	233 245 278 317
dichloromethane		234 271 309	234 275 315	
butyronitrile	232 262 303	234 272 310	234 276 316	234 245 281 320
acetonitrile	232 262 302	234 271 310	234 276 317	234 245 280 321
DMSO	269 309		277 320	280 322

The bands in absorption spectra of lactone forms exhibit shifts that are in line with the degree of alkylation of the amino nitrogen. On the other hand, the position of the first absorption band as a function of the substitution pattern of the nitrogen atom shows a close correlation to the position of the maxima of corresponding aromatic amines (see Table 3.1). This allows us to postulate that the first absorption band is localised within the part of the molecule that structurally corresponds to the relevant aromatic amine, shifted to lower energy by the excitonic splitting of the two identical amine moieties.

The absorption spectra of LR101 in aprotic solvents of different polarity (Fig 3.3) are similar to those of LRB. The first absorption band exhibits slightly positive solvatochromism (shift by about 500 cm^{-1} on going from dibutyl ether to butyronitrile). The band ends with a low intensity tail extending to about 400 nm (which may indicate a presence of a weak, Franck-Condon forbidden CT absorption band). The positions of the absorption maxima of three first bands of individual lactones in various solvents have been shown in Table 3.2.

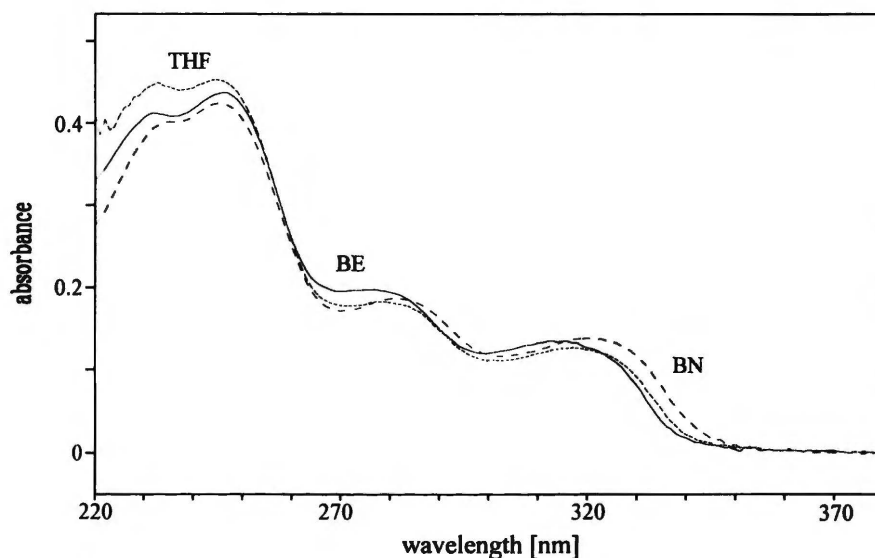


Fig. 3.3: Absorption spectra of LR101 in butyronitrile (BN, dashed line), tetrahydrofurane (THF, dotted line) and butyl ether (BE, continuous line).

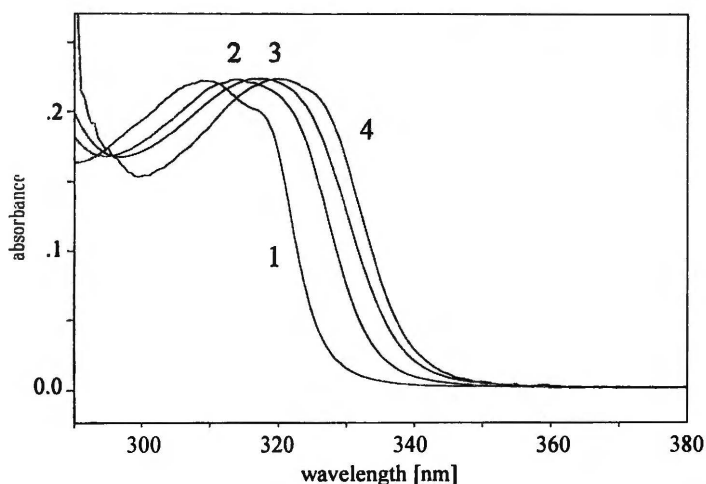


Fig. 3.4: Solvatochromism of the first absorption band of LRB (1 - 3-methyl pentane, 2 - dioxane, 3 - acetonitrile, 4 - pyridine).

The spectra are sensitive to the solvent, and, in particular, the long-wave absorption band exhibits a red shift with increasing solvent polarity in all the lactones. Fig. 3.3. shows the solvatochromism of the absorption spectrum of LR101, and Fig. 3.4 - the solvatochromism of the first absorption band of LRB. The bands shown in the latter Figure reveal also an interesting feature in a form of a shoulder on the red side of the band occurring in less polar solvents. The

shoulder was observed in absorption spectra reported by Klein and Hafner¹¹. It can (i) result from vibrational structure of the single absorption band that is revealed in less polar solvents or (ii) can originate from two transitions to the excited states with two different electronic structures. Appearance of the shoulder would require in the second case that the two transitions differ in their dependence of transition energy on the solvent polarity. Separation of the two transitions in less polar solvents would result in a broadening of the whole absorption band. As this is not the case, we believe the first case (vibronic structure) applies.

3.2. Fluorescence spectra at room temperature

Fluorescence spectra of the solutions of lactone forms of rhodamines in different solvents at room temperature (Fig. 3.5, 3.6) are strongly solvent dependent.

Depending on the substitution pattern at the amino group in the lactone molecule one can divide the solvents into three groups. The first one includes low polar solvents like toluene, dibutyl or diethyl ether where the fluorescence spectra consist of one broad band. Second group constitute medium polarity solvents like chlorobenzene, butyl or ethyl acetate, DME or THF. In these solvents a second emission band appears.

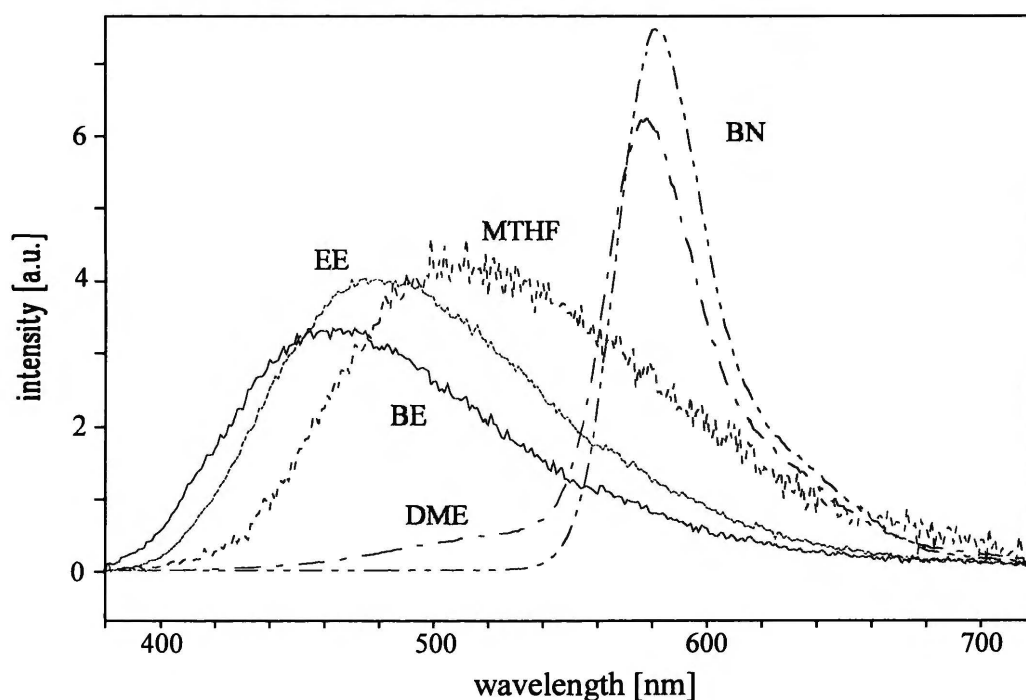


Fig. 3.5: Fluorescence spectra of LR101 at room temperature in various solvents. Abbreviations: BE - butyl ether, EE - ethyl ether, MTHF - 2-methyltetrahydrofuran, DME - dimethoxyethane, BN - butyronitrile.

In the case of LR101, double luminescence occurs also in dioxane. Increase in solvent polarity causes red shift and gradual disappearance of the short-wavelength band, and the fluorescence spectrum seems to be composed of only one band, which is accompanied by a strong increase in the observed quantum yield of the long-wavelength luminescence. For LDR10, this picture occurs in highly polar solvents only (DMF, DMSO), whereas in LR101

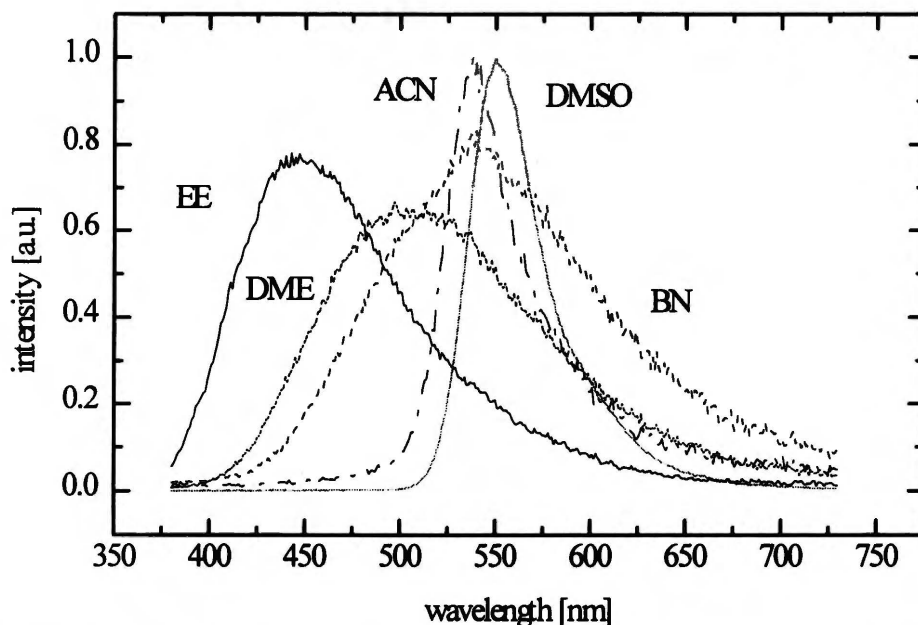


Fig. 3.6: Fluorescence spectra of LDR10 at room temperature in various solvents. Abbreviations: EE - ethyl ether, DME - dimethoxyethane, BN - butyronitrile, ACN - acetonitrile, DMSO - dimethyl sulfoxide.

single long-wave band occurs in pyridine, butyronitrile, propionitrile, acetonitrile and in DMSO. Solvent polarity can therefore be also linked with the appearance of the long-wave band and with its intensity. In the following we will adopt the nomenclature used previously¹¹ and refer the higher energy band to as the **L** (Lactone) band and the lower energy band to as the **Z** (Zwitterion) one, since the **Z** band can on the basis of its shape and spectral position be ascribed to come from the excited zwitterion formed in the excited state.

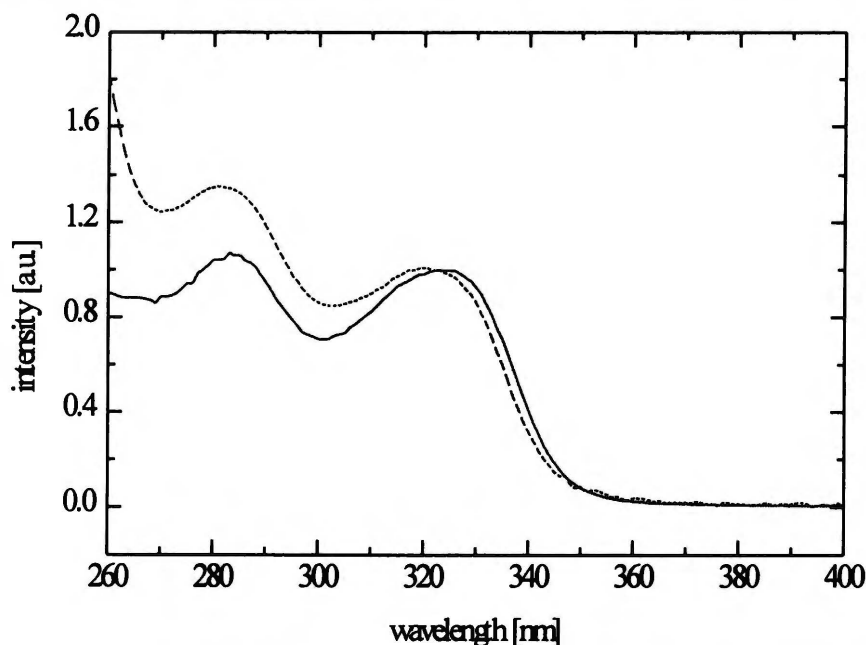


Fig. 3.7: LR101 in butyronitrile, room temperature: fluorescence excitation spectrum recorded at $\lambda_{\text{obs}} = 581 \text{ nm}$ (solid line) together with the absorption spectrum (dashed line).

The excitation spectra of both luminescences recorded for LR101 in BN and for LDR10 in ACN together with the respective absorption spectrum are shown in Fig. 3.7 and Fig. 3.8.

Other excitation spectra (recorded at various temperatures and other lactones) agree with the respective absorption spectra.

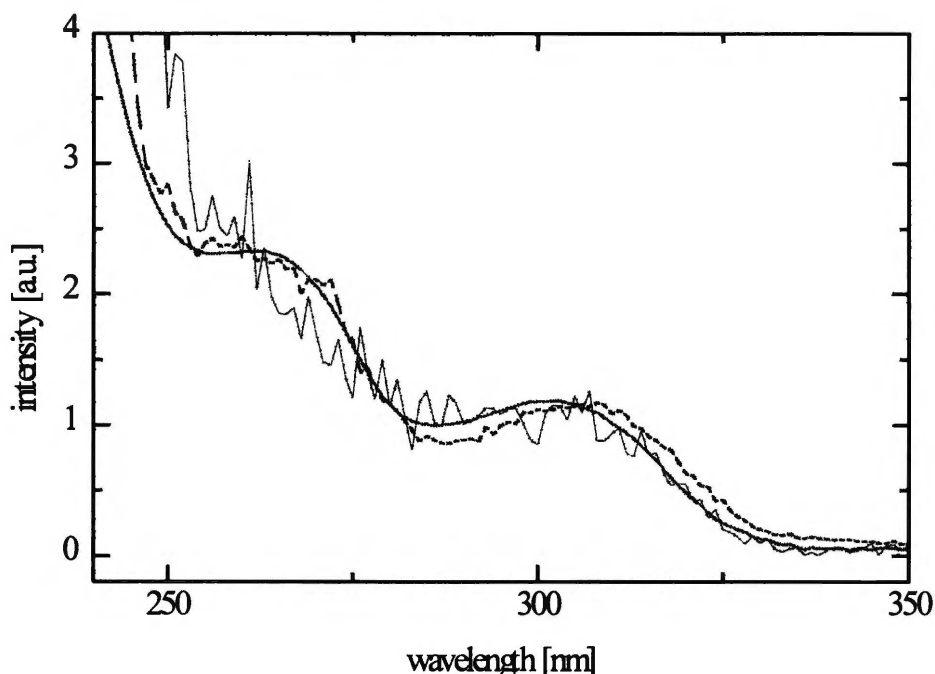


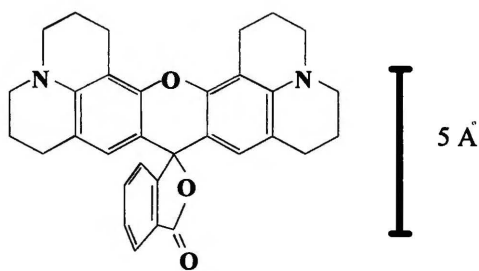
Fig. 3.8: LDR10 in acetonitrile, room temperature: fluorescence excitation spectra recorded at $\lambda_{\text{obs}} = 480$ nm (solid line), $\lambda_{\text{obs}} = 540$ nm (dashed line) together with the absorption spectrum (bold).

This proves that both **L** and **Z** luminescences are emitted from the excited states that are reached after the absorption of light by the lactone molecule.

The **L** band exhibits large Stokes shifts (for LRB, already in cyclohexane there is a shift ≈ 7000 cm^{-1}) and is very sensitive to the solvent polarity. For LR101, for instance, the maximum of the **L** band shifts from 21500 cm^{-1} in dibutyl ether to 19160 cm^{-1} in THF. Remarkable is also the Stokes shift between the first distinct absorption band and the fluorescence spectrum, in the case of MTHF being almost 12000 cm^{-1} . The shift of the **Z** band as a function of the solvent is very moderate (maxima at 17250 cm^{-1} and at 16800 cm^{-1} in DME and DMSO, respectively). Other lactones show also similar behaviour.

In order to estimate the dipole moment of the state emitting the **L** band (hereinafter referred to as the ${}^1\text{L}_{\text{CT}}$ excited state) we have neglected the polarisability effects and assumed that the lifetime of the ${}^1\text{L}_{\text{CT}}$ state is larger than the solvent reorientation relaxation time. Then, using the model given by Liptay¹², the dipole moment was estimated from the slope of linear plot of position of the maximum of **L** band, $\tilde{\nu}_{\text{max}}$, vs. a function describing the solvent polarity, $f(\epsilon, n) = (\epsilon - 1)/(2\epsilon + 1) - (n^2 - 1)/2(2n^2 + 1)$. Fig 3.9 illustrates the plot for LR101.

Taking the value of 0.7 nm for the Onsager cavity radius we obtained the value 26 D for the difference between the excited and ground state dipole moment for the ${}^1\text{L}_{\text{CT}}$ state in LR101. Assuming dipole moment for the ground state of the lactone molecule as negligible we obtain $\mu_{\text{exc}} = 26$ D. Such a large value indicates a full separation of charges over a distance of 5 Å:



LR101

This value is also similar to that found for the CT excited state of LRB¹¹. Using the same assumption and methods we have found the dipole moments for the ¹L_{CT} state in LDR10 and LRMET to be 25 D and 26 D, respectively.

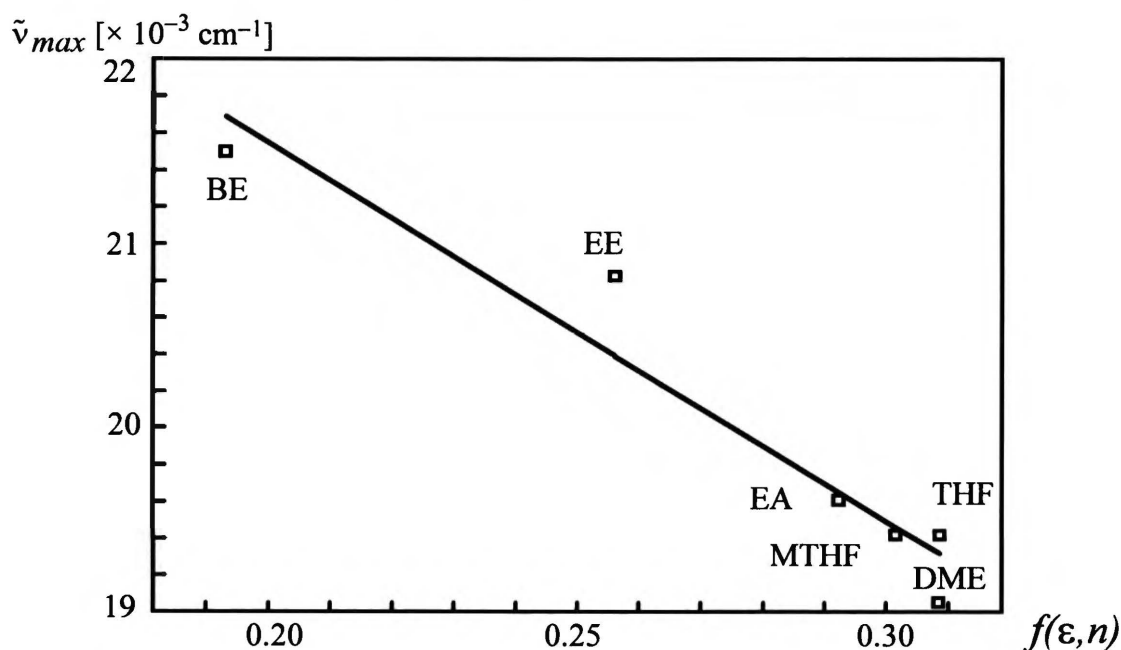


Fig. 3.9: Solvatochromic shifts of the maximum of lactone band of LR101 as a function of the solvent polarity. (See Table 2.1 for symbols denoting the solvents)

In analogy to the lactone of rhodamine B, we ascribe the L fluorescence band observed in other lactones to a highly polar excited state being formed with an electron transfer from the xanthene moiety to the phthalide one, which is not accompanied by the C-O bond cleavage.

In contrast to the L band, the Z fluorescence does not exhibit such a solvent dependence and therefore the dipole moment change on transition corresponding to this band is rather small compared with the lactone form. Using charge distribution calculated by Bergamasco *et al.*¹³ for the xanthene system in the ionic form of rhodamine, the difference of the dipole moments in the excited state and in the ground state of the zwitterion can be safely estimated to be less than 5 D. Assuming the dipole moment for ground state of zwitterion of other rhodamines being similar to that found for rhodamine B¹⁴ one can conclude that the dipole moment of the ¹Z₁ state is definitely lower than that of the ¹L_{CT} state. This in turn would indicate a significant difference in electron density distribution of both excited states and consequently - their different electronic structures.

Upon changing the wavelength of the excitation light, no differences in the ratio of the intensities of both bands have been found for all lactones studied. Measurements were carried out in the concentration range of 10^{-4} - 10^{-6} M to check a possible influence of concentration on the observed results. No dependence of the fluorescence quantum yields on the solute concentration in this range was found and the concentration typically used in the measurements was that of 10^{-5} M.

As an example of photophysical parameters of rhodamine lactones, quantum yields of the **L** and the **Z** luminescence together with other photophysical data of LR101 in various solvents have been summarised in Table 3.3:

Table 3.3
Photophysical properties of LR101 in various solvents

Solvent	$\tilde{\nu}_{\max}^A$ [cm ⁻¹]	$\tilde{\nu}_{\max}^{FL}$ [cm ⁻¹]	$\tilde{\nu}_{\max}^{FZ}$ [cm ⁻¹]	Φ_L	τ_L [ns]	Φ_Z	τ_Z ¹⁾ [ns]
Dibutyl ether	31750	21500	---	0.023	---	---	---
Diethyl ether	31750	20830	---	0.034	9.8	---	---
MTHF	31550	19690	---	0.033	9.2	---	---
Tetrahydrofurane	31550	19160	17250	0.006	7.0	0.015	0.13 ²⁾
Dimethoxyethane	31550	19420	17300	0.004	3.51	0.020	0.40 ³⁾
Pyridine	30950	19050	17100	<0.0005	---	0.168	3.60
Butyronitrile	31250	---	17210	<0.0005	---	0.201	4.03
Propionitrile	31250	---	17180	---	---	0.252	4.30
Dimethylformamide	31050	---	16980	---	---	0.225	4.20
Ethyl alcohol	17650	---	16950	---	---	0.98	4.37

¹⁾ In the case of tetrahydrofurane and dimethoxyethane a fitting with 3-exponential decay was applied. One decay time was kept constant and equal to τ_L in order to take into account the overlap of the **L** and the **Z** band.

²⁾ The shortest component ($A_1 = 0.45$). Second component recovered in the deconvolution was 3.29 ns ($A_2 = 0.07$).

³⁾ Average value of two decay components (0.21 ns and 0.59 ns, amplitudes 0.165 and 0.146, respectively)

Abbreviations:

A - absorption; F - fluorescence; L - lactone; Z - zwitterion

The samples were excited as follows: stationary measurements - at the maximum of the first absorption band; lifetime measurements - 320 nm.

In all lactones the quantum yield of the **L** fluorescence decreases with increase of the solvent polarity whereas the quantum yield of the **Z** fluorescence increases dramatically along with its decay time. This suggests the occurrence of an efficient (intramolecular) quenching mechanism of fluorescence in less polar solvents and a stabilisation of the zwitterion excited state with increase of solvent polarity. This tendency was displayed by all the lactones studied.

Table 3.4 presents total quantum yields of luminescence (Φ_T) for LRB in various solvents. The quantum yields of the lactone (Φ_L) and the zwitterion (Φ_Z) luminescence - similarly as in the case of LR101 - have been evaluated by resolving the overlapping bands with use of known shapes of both. Noticeable are the differences in Φ_Z in acetonitrile and in dichloromethane when compared with the values reported by Klein and Hafner¹¹ ($\Phi_Z(KH)$). As the fluorescence spectrum in AN consists almost exclusively of one band, the discrepancy cannot be related to the manner of separation of **L** and **Z** bands. We therefore believe the reason could be related to the direct excitation of the cations of RB present in a small amount in the lactone solution due to presence of traces of proton-donating impurities. This situation is much more probable in the case of DCLM, as this solvent contains almost always the traces of HCl.

Table 3.4

Quantum yields of fluorescence of LRB in various solvents at 293 K¹⁾

Solvent	Φ_T	Φ_L	Φ_Z	$\Phi_Z(KH)$
DME	0.040			
Dioxane	0.048			0.052
DCLM	0.18			0.35
BN	0.036	0.012	0.024	
BZN	0.079	0.016	0.063	
AN	0.12	≤ 0.001	0.12	0.22
DMSO	0.13	≤ 0.001	0.13	

¹⁾ Quantum yield data given for LRB in this thesis may differ by the factor 1.078 (= 0.55/0.51) from those published in ref. ¹⁵ which results from the fluorescence quantum yield of quinine sulphate in 0.1 n H₂SO₄ erroneously assumed in this reference to be 0.55 instead of 0.51¹⁶. The data in this thesis were calculated using 0.51 for fluorescence quantum yield of quinine sulphate in 0.1 n H₂SO₄. The value 0.55 is the fluorescence quantum yield of quinine sulphate in 1 n H₂SO₄.

3.3. Fluorescence decays at room temperature

Fluorescence decays depend also very strongly on the solvent used and are emission wavelength dependent. Generally, the decays measured in the **L** band could be fitted as a monoexponential decay yielding - for LR101 - the lifetimes shown in Table 3.3. On the other hand, decays measured in the **Z** band were more complicated and generally had to be fitted by bi- or triexponential decays. Especially in cases where a double luminescence occurs, one has to assume a considerable overlap of both luminescences within the **Z** band. The temperature dependence of the fluorescence (see below) indicates that even in cases where apparently only one band (**Z**) is displayed, there still can be two strongly overlapping bands, **L** and **Z**, with the lactone band being small, however detectable (see Chapter 4). In order to separate the contribution from the **L** band, decays in the **Z** band were analysed by keeping the longest decay time constant and equal to the decay time recovered for the **L** band. The global analyses performed for the LR101 decays in DME, and for LRB and LRMET in various solvents confirm the necessity of adding a second component (τ_2) in the analysis of the decays of the

zwitterion fluorescence after the contribution from the overlap with the L band has been separated. The non-exponentiality of the decays of Z fluorescence in solvents where the zwitterion excited states are quenched has been extensively investigated for LRB¹⁵, and it seems to be an inherent property of the system. The decay curves measured at fluorescence maxima in solvents where Z fluorescence is observed with relatively high quantum yield (LR101 in BN, pyridine; LRB in BZN, AN; LDR10 in DMSO) could be fitted with a single decay time. Below, detailed results of the lifetime study are presented.

3.3.1. LRB

Decays of LRB in the lactone band have been measured in a series of aprotic solvents of various polarity. All decays measured at room temperature could be fitted with monoexponential decay functions. Generally, the decay times agree with those reported by Klein and Hafner¹¹. We have found, however, slightly lower values for τ_L in some solvents. Table 3.5 presents decay times measured for LRB in various solvents, together with the respective values given by Klein and Hafner. The decay curves in the L band were recorded at 490 nm.

Table 3.5

Fluorescence decay times measured in the L band for LRB in various solvents at 293 K. τ_L values reported by Klein and Hafner¹¹ are given for comparison.

Solvent	this work	Klein & Hafner
Dioxane	13.8	14.4
DME	10.49	-
DCLM	14.6	16.3
BN	5.75	-
BZN	9.31	-
AN	1.72	2.3
DMSO	1.77	

An example of a decay curve collected in the L band for LRB in butyronitrile together with a monoexponential fit and statistical treatment of residuals has been shown in Fig. 3.10.

A much more complicated situation occurs when decays in the Z band in aprotic solvents are considered. (Fig. 3.11). They are generally not monoexponential and are very sensitive to the temperature (see below). In order to investigate possible reasons of this kinetic picture we have checked whether it is caused by a trivial overlap of two fluorescence bands each of them decaying with its own characteristic lifetime, and have tried to fit them with two-exponential functions. While this model could be successfully applied, for instance, in the case of LRB in BZN at room temperature, two exponential functions gave rather unacceptable fits for the decays of LRB/BN system at all temperatures as well as for decays of LRB/BZN at elevated temperatures. By this we mean not only the $\chi^2 > 1.2$ in single curve analysis, regularities in residuals and in autocorrelation function but, first of all, the fact that the

recovered longer lifetimes differed - out of the error limits - from those measured in the lactone band, and were significantly different among themselves along the Z band. This suggested that the non-exponentiality cannot be due only to the overlap of two monoexponential decays.

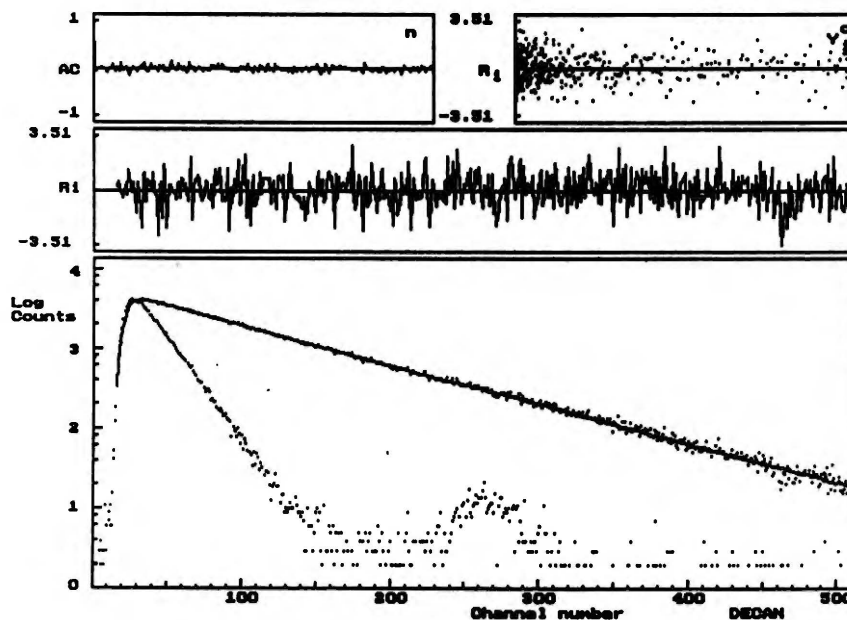


Fig. 3.10: LRB in butyronitrile: fluorescence decay curve collected in the L band (at $\lambda = 490$ nm) together with a monoexponential fit ($\tau = 5.76$ ns). The instrument response function was taken by collection of the decay of POPOP in methylcyclohexane ($\tau = 1.13$ ns) at the same λ . Time increment per channel was 68 ps. Above the decay curve, weighted residuals (R_i) have been plotted against the channel number, and the autocorrelation function (AC) and a plot of weighted residuals against the calculated values (Y_i) have been shown.

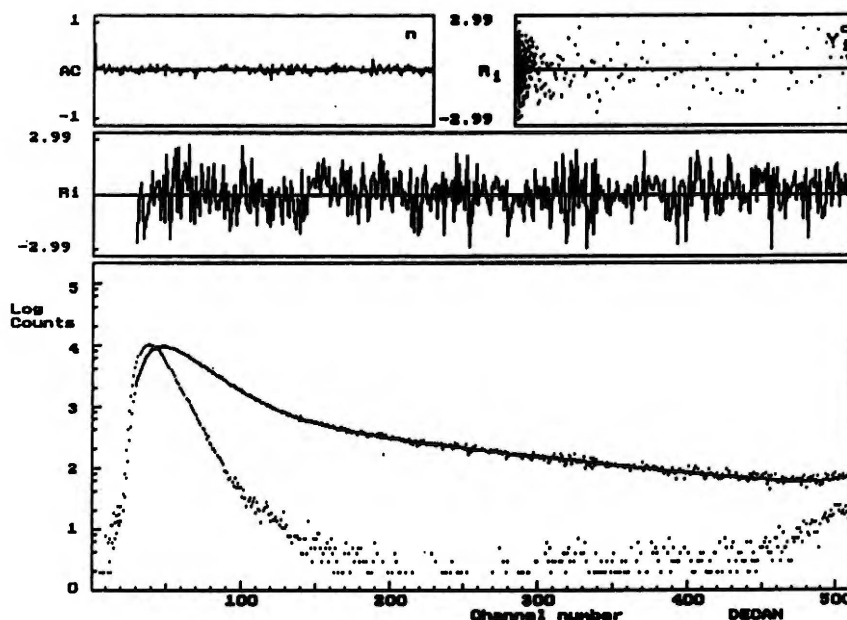


Fig. 3.11: LRB in butyronitrile: fluorescence decay curve collected in the Z band (at $\lambda = 560$ nm) together with a triexponential fit ($\tau_1 = 0.66$ ns, $\tau_2 = 1.52$ ns, and $\tau_3 = 5.76$ ns). The instrument response function was recorded by collection of the decay of erythrosine in water ($\tau = 0.095$ ns) at the same λ . Time increment per channel was 34 ps. Other plots have the same meaning as in Fig. 3.10.

The significant overlap of two fluorescences could not, however, be neglected and therefore it has been decided to analyse the decays with triexponential functions with certain constraints both in single curve and in global analysis. The constraint in single curve analysis was that one of the lifetimes was kept constant and equal to that of the lactone fluorescence measured under the same conditions. Global analysis was performed using one decay curve collected in the lactone band together with several (typically 4 to 6) decay curves taken in the zwitterion band at different wavelengths between 550 nm and 600 nm.

During global calculations the decay recorded at 490 nm was fitted with a monoexponential function and the zwitterionic decays were fitted by two- or triexponential functions with one of the lifetimes linked to that of the L fluorescence. Results of global analysis calculations for LRB in DCLM, BN and BZN, and for LRMET in DCLM have been collected in Table 3.6.

Table 3.6

Results of global analysis calculations for LRB and for LRMET in several solvents at 293 K, together with the contributions (Q_i) from the components decaying with longest τ^1 .

Solvent	Amplitude	λ (nm)	490	550	560	570	580	590
LRB/DCLM	A_1 ($\tau_1 = 2.98$ ns)	-		0.173		0.176		0.113
	A_2 ($\tau_2 = 14.60$ ns)	0.55		0.0037		0.0036		0.0037
	$Q_2^2)$			0.095		0.091		0.138
LRB/BN	A_1 ($\tau_1 = 0.66$ ns)	-		0.208	0.217	0.232	0.241	
	A_2 ($\tau_2 = 1.52$ ns)	-		0.017	0.014	0.013	0.009	
	A_3 ($\tau_3 = 5.76$ ns)	0.69		0.013	0.008	0.007	0.008	
	Q_3			0.315	0.219	0.189	0.210	
LRB/BZN	A_1 ($\tau_1 = 2.74$ ns)	-		0.368		0.408		0.462
	A_2 ($\tau_2 = 9.31$ ns)	0.582		0.047		0.016		0.021
	Q_2			0.302		0.118		0.134
LRMET/BN	A_1 ($\tau_1 = 0.19$ ns)	-		0.411	0.443	0.417	0.421	
	A_2 ($\tau_2 = 1.76$ ns)	-		0.012	0.013	0.013	0.012	
	A_3 ($\tau_3 = 4.43$ ns)	0.689		0.028	0.026	0.030	0.040	
	Q_3			0.556	0.518	0.565	0.637	
LRMET/DCLM	A_1 ($\tau_1 = 1.01$ ns)	-		0.141	0.158	0.159	0.157	
	A_2 ($\tau_2 = 2.51$ ns)	-		0.028	0.034	0.035	0.034	
	A_3 ($\tau_3 = 15.46$ ns)	0.404		0.0049	0.0053	0.007	0.0095	
	Q_3			0.263	0.251	0.303	0.376	

1) The longest component in the following data was always equal to the decay time of the $^1L_{CT}$ state.

2) The contributions Q_i from components decaying with a decay time τ_i were calculated according to the formula $Q_i = A_i \tau_i / \sum_i A_i \tau_i$

These results show that in the case of shorter decay times of the Z fluorescence, such as for LRB in butyronitrile (BN) or LRMET in DCLM, the zwitterionic fluorescence - after the overlapping component with a long lifetime (τ_3) was accounted for - cannot be regarded as a

monoexponential one. The component with a decay time τ_2 - although with a minor contribution - was necessary to obtain acceptable fits both in single curve and in global analysis. The same qualitative conclusion could be drawn from measurements of LRB in BN at higher temperatures (see Chapter 4). The non-exponentiality of the decay indicates that formation and decay of the 1Z_1 state does not underlie a simple successive kinetics. Possible reasons are discussed below.

The contribution from the component decaying with the decay time τ_3 in BN or with the decay time τ_2 in DCLM or BZN does not change significantly along the **Z** band (Table 3.6). The only regular change occurring in the contribution is its small increase at longer wavelengths, an effect that can be ascribed to participation of the **L** band, being much broader than the **Z** band and therefore extending more towards longer wavelengths. Larger increase of Q_3 in the case of LRMET/BN where the maximum of **Z** band is blue-shifted as compared with LRB, supports this conclusion. Hence, the τ_3 component would originate from the overlap of two bands rather, and would not be an inherent property of the decay of the **Z** component. This fact may to certain extent be a confirmation of the assumption that the presence of the component with longer decay time is caused by an overlap of two bands only and not by a direct equilibrium of the $^1L_{CT}$ and the 1Z_1 state (or by an unidirectional transformation involving these states).

Degassing of the sample by freeze-pump-thaw technique did not change significantly the observed decays. For instance, for LRB solution in BN at 293 K a triexponential fitting in the **Z** band was also necessary yielding τ_1 and τ_2 values of 0.6 and 1.6 ns, respectively. τ_3 both in **Z** and in **L** band (monoexponential fit) was 7.2 ns. This explains the fact that the samples may have not been degassed prior to the measurements.

3.3.2. LR101

The fluorescence decay times obtained for decays collected in the lactone and in the zwitterion band are shown in Table 3.3. Also in this molecule, the fluorescence decays measured in the **L** band could be fitted with a monoexponential function. On the other hand, decays measured in the **Z** band were more complicated and generally had to be fitted by two or triexponential decays. Especially in cases where a double luminescence occurs, one has to assume a considerable overlap of both luminescences within the **Z** band (as for LRB). The temperature dependence of the fluorescence (see Chapter 4) indicates that even in cases where apparently only one band (**Z**) is displayed, there still can be two strongly overlapping bands, **L** and **Z**, with the lactone band being small, however detectable.

In order to separate the contribution from the **L** band, decays in the **Z** band were analysed by keeping the longest decay time constant and equal to the decay time recovered for the **L** band. The global analysis performed for the decays of LR101 in DME confirms the necessity of adding a second component (τ_2) in the analysis of the decays of the zwitterion fluorescence after the contribution from the overlap with **L** band has been separated. The decay curves measured at fluorescence maxima in the solvents where **Z** fluorescence is

observed with relatively high quantum yield (BN, pyridine), could be fitted with a single decay time (similarly as for LRB in benzonitrile, when the quenching of Z fluorescence does not occur, except for taking into account the overlap of two bands for LRB/BZN system). An example of a decay curve collected in Z band for LR101 in butyronitrile together with a monoexponential fit has been shown in Fig. 3.12.

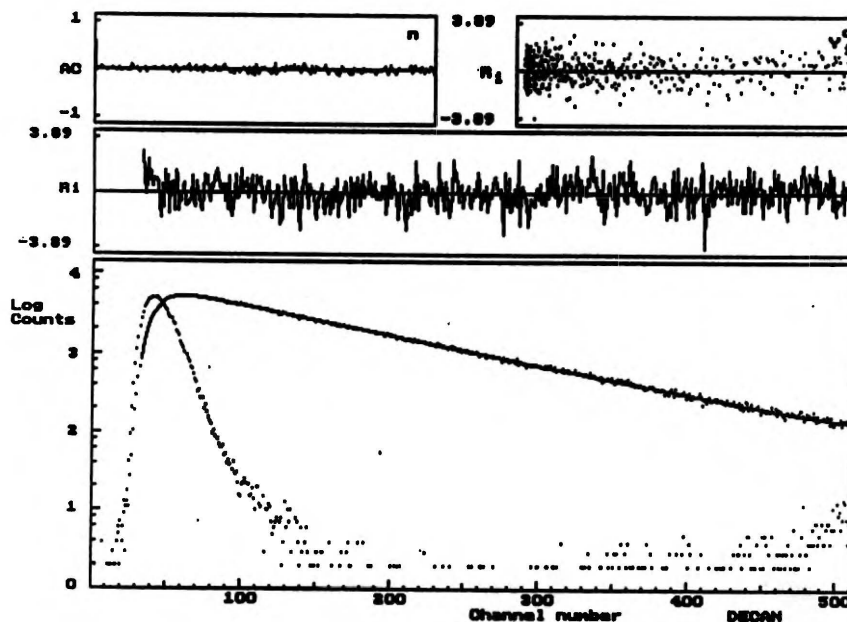


Fig. 3.12: LR101 in butyronitrile: fluorescence decay curve collected in the Z band (at 560 nm) together with a monoexponential fit = 4.0 ns). The instrument response function was taken by collection of the decay of erythrosine in water ($\tau = 0.095$ ns). Time increment per channel was 34 ps. Other plots have the same meaning as in Fig. 3.10.

Non-exponential decays and shortening of the lifetime of zwitterion fluorescence of xanthene systems were reported by Vogel *et al.*¹⁷ and in particular by Kemnitz *et al.*¹⁸. The latter paper reports on investigations of fluorescence dynamics of rhodamine B, rhodamine 101 and pyronine B adsorbed on organic crystals surfaces. The measurements with single crystals of various surface quality revealed that distorted adsorption sites are responsible for reduced fluorescence lifetimes. Comparing the fluorescence properties of these dyes, the authors deduced that the shortening of the decay time was probably caused by an enhanced internal conversion to the ground state resulting from a folding of the xanthene skeleton in the non-ideally flat sites of the crystal surface and postulated that the increased non-radiative decay is promoted by forces exerted at irregular distorted adsorption sites. An interesting effect of elongation of the decay times by thin layer of water on the crystal/dye system was interpreted in such a way that water weakens the bond to the surface (partial solvation) and therefore enables the rhodamine molecule to accommodate more planar conformation of the xanthene system. These observations are reinterpreted in Chapter 6 of this thesis.

3.3.3. Efficiency of population of the zwitterion

Very interesting are the observed changes in fluorescence quantum yield and in the decay times of the 1Z_1 excited state formed upon excitation of the lactone molecule in aprotic

solvents. The zwitterionic forms of rhodamines are well known for their high fluorescence quantum yields in alcohol solutions (e.g. R101 - 0.96, RB - 0.65¹⁹). The fluorescence quantum yield measured for the emissions from zwitterions generated upon excitation of the lactone molecule deviate, however, very much from the quantum yields reported for the emission of zwitterions in alcohols excited directly in the ground state and are in the range from 0 up to 0.27. Taking into account that apart from the ¹Z₁ state also the ¹L_{CT} state is populated, does not explain such low values. This difference may originate from the fact that either (i) the Z form is populated with a low efficiency, or (ii) the ¹Z₁ state is quenched, or (iii) it can be a combination of these two factors. Significant shortening of the decay times in less polar solvents suggests occurrence of a quenching mechanism that is connected with the dielectric properties of the surrounding medium. Using the example of LR101, the reasons for the decrease of the quantum yield and of the decay time as compared with directly excited zwitterions are investigated below.

The decay time of the Z form of LR101 in EtOH ($\tau = 4.37$ ns) at room temperature was found to be close to that for R101 in BN/PN solution as derived from figure 3 in ref. ⁶ ($\tau = 4.5$ ns) and lower than that given in ref. ²⁰ (slightly above 5 ns, but in deoxygenated solution). The decay time of fluorescence in propionitrile (PN) is almost equal to that found for EtOH solution in this study. This allows us to conclude that the zwitterionic excited state is not quenched in PN as it is most probably sufficiently stabilised against the process causing the non-radiative deactivation observed in less polar solvents. Assuming the radiative rate constant for the zwitterion fluorescence to be equal in these both solvents, the quantum yield of fluorescence in PN, $\Phi_Z = 0.252$, would indicate that the zwitterionic excited states are populated in this solvent with approximately 25% efficiency (η_Z). For EtOH one can write:

$$k_r = \frac{\Phi}{\tau} \quad (3.1)$$

where k_r , Φ and τ are radiative rate constant, fluorescence quantum yield and decay time, respectively for the zwitterion excited directly in EtOH. For other solvents, where only the lactone is excited, we can write:

$$\Phi_{ob} = \eta_z \Phi \quad (3.2)$$

where Φ_{ob} is the observed luminescence yield from the zwitterion excited state and η_z - the efficiency of population of the zwitterion excited state. Replacing Φ by $k_r / (k_{nr} + k_r)$ where k_{nr} is the non-radiative rate constant we obtain:

$$\Phi_{ob} = \eta_z \frac{k_r}{k_{nr} + k_r} = \eta_z k_r \tau_{ob} \quad (3.3)$$

$$\eta_z = \frac{\Phi_{ob}}{k_r \tau_{ob}} \quad (3.4)$$

where τ_{ob} is the main decay time component in the decay analysis of the zwitterion luminescence (τ_1). Assuming that $k_r = 2.2 \cdot 10^8$ s⁻¹ for LR101 and is independent of the solvent, the efficiencies of population of the zwitterion excited state could be calculated. These

quantities turned out to be very similar in different solvents (Table 3.7) which would suggest that the population efficiency of the zwitterion excited state does not depend on the solvent.

The efficiency of population of the 1Z_1 state in various solvents was earlier estimated for LRB by Klein and Hafner¹¹. They postulated that the 1Z_1 state is formed in solvents of sufficient polarity only. Based on the measured fluorescence quantum yields of both luminescences they determined the fraction of molecules relaxing to the $^1L_{CT}$ and the 1Z_1 state and concluded that quantum efficiency of population depends on the solvent: in solvents up to $\Delta f \approx 0.2$ (where $\Delta f = (\epsilon - 1)/(2\epsilon + 1) - (n^2 - 1)/(2n^2 + 1)$, a solvent polarity function), the lactone excited state is populated with the constant efficiency of about $\eta_L = 0.05$, and 95% of the excited molecules are deactivated *via* other states (probably triplets, they did not give, however, a more detailed description), so the zwitterion form is not populated.

Table 3.7

Efficiencies of population of the excited state of zwitterion form of rhodamine 101 and rhodamine B in different solvents calculated according to eq. (3.4):

Solvent	DME	pyridine	BN	PN	AN	DMSO	DMF
η_z (LR101)	0.22	0.21	0.23	0.25			0.24
η_z (LRB)	-	-	0.16		0.26	0.27	

According to ref. ¹¹, on increasing Δf a sudden drop in population of the excited states of the lactone form takes place and is accompanied by a corresponding increase in efficiency of population of the excited zwitterion form (η_z reaches the value close to 1.0). Grigoryeva *et al.*²¹ have independently determined the efficiency of population of the 1Z_1 state of LRB in chloroform. They estimated $\eta_z(\text{LRB})$ by comparison with the fluorescence quantum yield of RB in EtOH. Using the solution of RB in EtOH and the solution of LRB in chloroform with equal optical densities in the region 310 - 330 nm ($D \approx 0.2$), where the samples were excited, they have found that the ratio of fluorescence maxima was equal to 0.23. Then, having taken into account the lifetimes of the zwitterion fluorescence in EtOH and in chloroform (3.4 ns and 3.3 ns, respectively), and the fact that the fluorescence quantum yield of RB in EtOH is 1.8 times less when excited in the UV region²², they have determined $\eta_z(\text{LRB}) = 0.13$. They have not taken into account, however, the photochemical process leading to the ionic form the lactone undergoes in some solvents containing chlorine atoms in the molecule (they even show changes in absorption spectra of the LRB in chloroform after irradiation for 40 s and 80 s - a period of time necessary for recording the fluorescence spectrum!), especially if the solvents are not well purified. We have found, this relates to CH_2Cl_2 , as well as to chloroform. Therefore, the efficiency of population determined by Grigoryeva *et al.*²¹ is rather doubtful. Also the approach taken by Klein and Hafner and their conclusions relating to the efficiency of population of the excited states are false as they have not taken into account the

fact that the zwitterions are formed in all solvents, even under conditions where they are not revealed by their fluorescence spectrum.

3.3.4. Time-resolved fluorescence spectra

In order to check connectivity between the **L** and **Z** states and to obtain more information on the fate of particular excited species, time resolved spectra of the LR101 solution in DME and of the LRB solution in butyronitrile at room temperature were measured with a time resolution of 1 ns. The spectra recorded at the moment of maximal intensity of the **Z** fluorescence, as well as after 10, 20, and 30 ns for LR101 and after 5, 10, 20 and 40 ns for LRB, respectively, are depicted in Fig. 3.13.

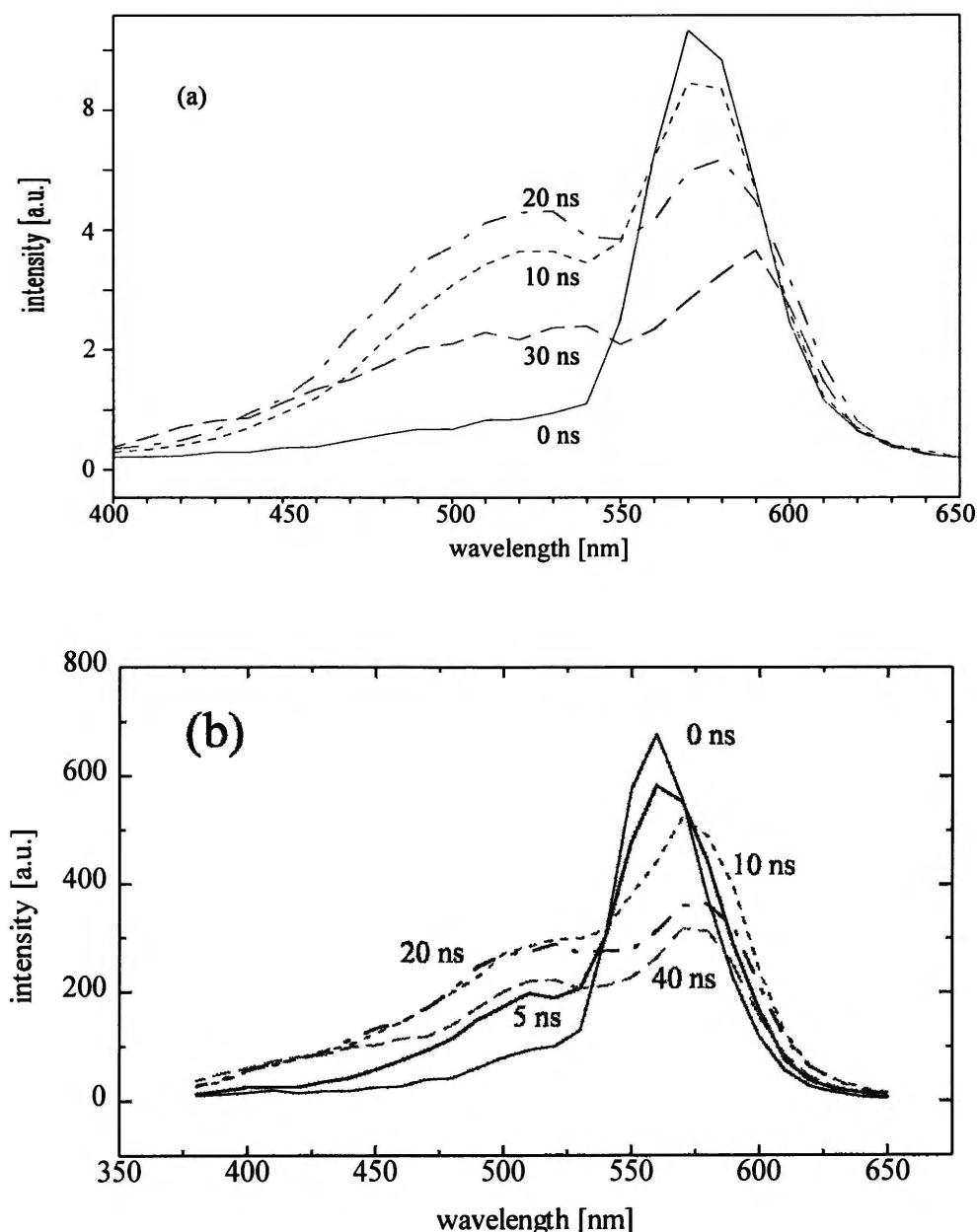


Fig. 3.13: Time-resolved fluorescence spectra of rhodamine 101 lactone in DME (a) and of rhodamine B in butyronitrile (b) at room temperature. The intensities of the spectra are arbitrary; important are the changing ratios of the two bands. The spectra were not corrected for the spectral response of the detection system.

Surprisingly, the **Z** fluorescence is still displayed after much longer time than indicated by the main short decay time recovered from the decay analysis (0.40 ns for LR101/DME and 0.66 ns for LRB/BN). The 1Z_1 state must hence be populated not only directly after excitation in a very fast process (this population is rapidly quenched, e.g. within 0.40 ns for LR101/DME) but also *via* another longer lived state. The natural explanation would be an equilibrium of the **Z** and **L** forms in the excited state or at least the population of the **Z** form from the $^1L_{CT}$ state. This is, however, hardly to assume in view of the measured (main) decay times of both forms. A direct excited state $^1L_{CT} \rightleftharpoons ^1Z_1$ equilibrium would result in decaying of the 1Z_1 state commonly with the $^1L_{CT}$ state, and in a build up of the **Z** fluorescence. The type of treatment of the kinetic data applied for the **Z** band (i.e. the separation of the spectral overlap of both fluorescences) did not allow for extracting this effect. Increase of the ratio of intensities of the **Z** and the **L** band at longer delay times (e.g. 30 ns for LR101/DME and 40 ns for LRB/BN) represents also an argument contradicting a direct $^1L_{CT} \rightleftharpoons ^1Z_1$ equilibrium, because in the case of the equilibrium the intensity ratio (**Z/L**) should remain rather constant.

Kinetic curves of transient absorption and especially observation of a charge-transfer triplet state (see Chapter 5) allow us to postulate that the delayed **Z** luminescence may come from the 1Z_1 state populated from a triplet state. Occurrence of iso-emissive points of the **L** and the **Z** luminescences in broad temperature ranges might suggest that although there is no direct $^1L_{CT} \rightleftharpoons ^1Z_1$ equilibrium, an equilibrium with participation of the triplet charge-transfer state may occur.

References and notes

- ¹ K.-H. Drexhage, in *Dye Lasers*, 2nd edition, pp 144-193 (edited by F. P. Schäfer); Springer, Berlin (1977)
- ² M. J. Snare, F. E. Treloar, K. P. Ghigino and P. J. Thistlethwaite, *J. Photochem.* **18** (1982) 335
- ³ D. A. Hinckley, P. G. Seybold and D.P. Borris, *Spectrochim. Acta* **42A** (1986) 747
- ⁴ D. A. Hinckley and P. G. Seybold, *Spectrochim. Acta* **44A** (1988) 1053
- ⁵ D. A. Hinckley and P. G. Seybold, *J. Chem. Educ.* **64** (1987) 362
- ⁶ F. Barigelletti, *Chem. Phys. Lett.* **140** (1987) 603
- ⁷ J. Karpiuk, Z. R. Grabowski and F. C. De Schryver, *J. Phys. Chem.* **98** (1994) 3247
- ⁸ I. Rosenthal, P. Peretz and K. Muszkat, *J. Phys. Chem.* **83** (1979) 350
- ⁹ U. Brackman, *Lambdachrome Laser Dyes* Lambda Physik GmbH, Göttingen, 1986, p III-123
- ¹⁰ I. L. Belaitz and R. N. Nurmukhametov, *Zh. Fiz. Khimii* **44** (1970) 29
- ¹¹ U. K. A. Klein and F. W. Hafner, *Chem. Phys. Lett.* **43** (1976) 141
- ¹² W. Liptay, *Z. Naturforsch.* **20a** (1965) 1441
- ¹³ S. Bergamasco, G. Calzaferri and T. Hädener, *J. Photochem.* **53** (1990) 109
- ¹⁴ Y. Sueishi, Y. Sugiyama, S. Yamamoto and N. Nishimura, *Bull. Chem. Soc. Jap.* **67** (1994) 572

-
- 15 J. Karpiuk, Z. R. Grabowski and F. C. De Schryver, *Proc. Indian Acad. Sci. (Chem. Sci.)* **104** (1992) 133
- 16 J. N. Demas and G. A. Crosby, *J. Phys. Chem.* **75** (1971) 991
- 17 M. Vogel, W. Rettig, R. Sens and K.-H. Drexhage, *Chem. Phys. Lett.* **147** (1988) 452
- 18 K. Kemnitz, N. Tamai, I. Yamazaki, N. Nakashima, K. Yoshihara, *J. Phys. Chem.* **91** (1987) 1423
- 19 R. F. Kubin and A. N. Fletcher, *J. Luminesc.* **27** (1982) 455
- 20 T. Karstens and K. Kobs, *J. Phys. Chem.* **84** (1980) 1871
- 21 T. M. Grigoryeva, V. L. Ivanov, N. Nizamov and M. G. Kuzmin, *Dokl. Akad. Nauk* **232** (1977) 1108
- 22 M. I. Snegov and A. S. Cherkasov, *Izv. Akad. Nauk, Fiz. Seria*, **39** (1975) 2249
- The decrease in quantum yield of fluorescence excited in UV as compared with that excited in the long-wave band can be explained by the fact that the ethanol solution of RB contains both forms in equilibrium - 71% of zwitterions and 29% of lactone molecules. The lactone molecules may significantly contribute to the absorption spectrum of RB in UV, so UV irradiation of the alcoholic solution would lead to the excitation of significant amount of lactone molecules, as opposed to the irradiation with the visible light.

CHAPTER 4

TEMPERATURE STUDIES

4.1. Introduction

The photophysics of the rhodamine lactones turned out to be very sensitive to the temperature changes. Fluorescence spectra measured at various temperatures revealed the whole richness of the photophysics of the lactone molecules and allowed us to draw important conclusions about the mechanism of the excited state processes. In general, lowering of temperature caused decrease of **L** fluorescence and increase of **Z** fluorescence. Also the decay curves changed very much on changing the temperature - with decrease of temperature the decay times of **L** fluorescence decreased and those of **Z** fluorescence increased. It has been found that the condition of the medium (mainly its polarity) may be of essential importance for the processes occurring in a given system. Below we present a selection of the experimental results obtained for different rhodamines and discuss possible mechanisms of the processes occurring in the lactones upon excitation.

4.2. Fluorescence spectra as a function of temperature

Fig. 4.1 and 4.2 show the evolution of the fluorescence spectrum of LR101 in ethyl ether as a function of temperature. Single **L** band displayed at room temperature (maximum at 480 nm) is shifted towards longer wavelengths on lowering the temperature (maxima at 487 nm at 273 K, at 495 nm at 253 K, at 502 nm at 233 K, and at 510 nm at 208 K), and at 208 K a second fluorescence band, the **Z** band, begins to appear (Fig. 4.1). The shift of the **L** band is accompanied by irregular intensity changes of this band.

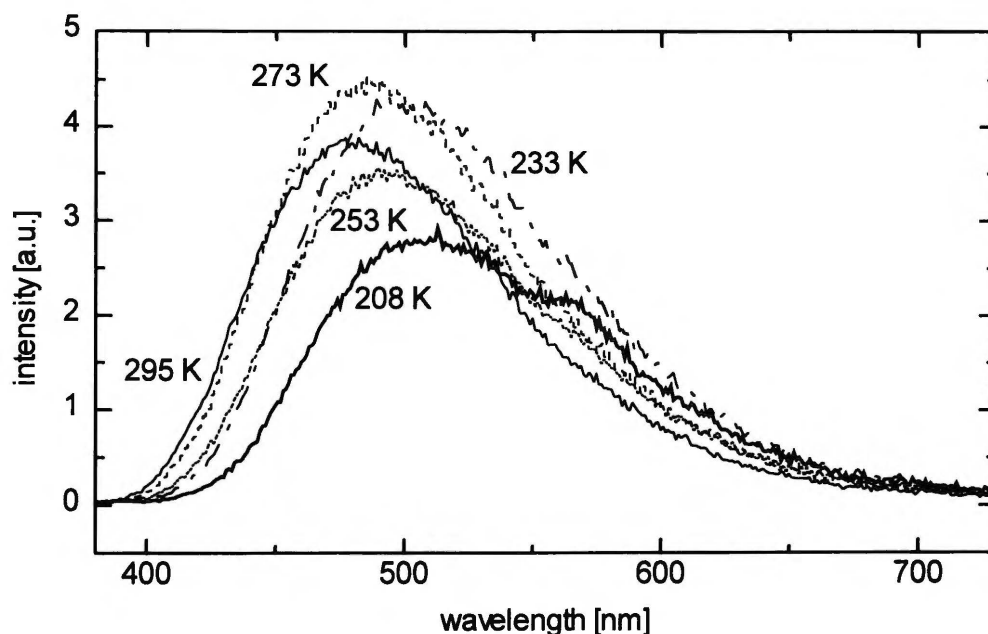


Fig. 4.1: Luminescence spectra of rhodamine 101 lactone (LR101) in diethyl ether in the temperature range 295 K - 208 K. In spectrum recorded at 208 K an appearance of the **Z** luminescence is clearly seen.

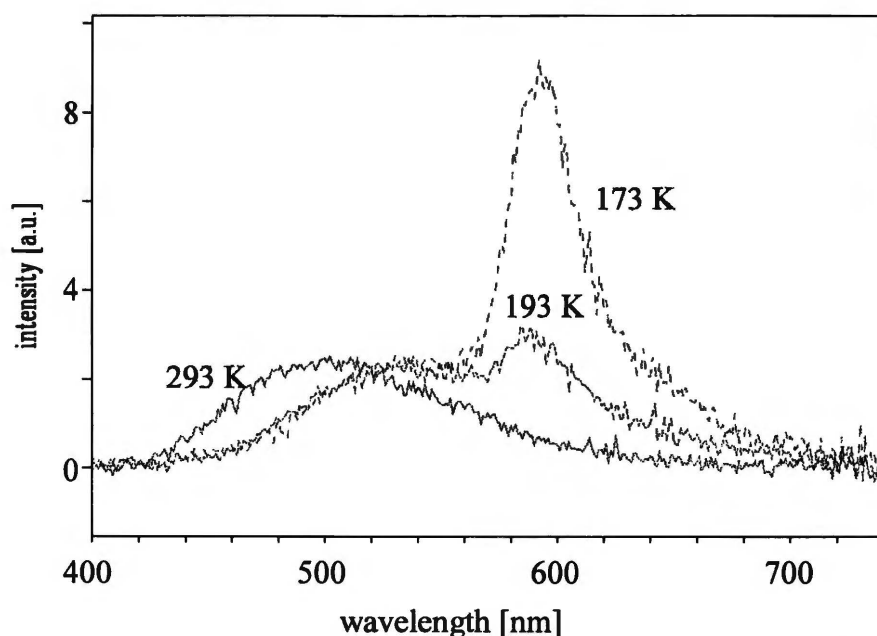


Fig. 4.2: Luminescence spectra of rhodamine 101 lactone (LR101) in diethyl ether below 200 K. The spectrum recorded at 293 K was given for the purpose of comparison.

Further evolution of the fluorescence spectrum of LR101 in diethyl ether is shown in Fig. 4.2. The L band is still shifted and the Z band becomes more intense. The intensity can be significantly enlarged in dimethoxyethane (transition to DME is equivalent to an increase in solvent polarity), where LR101 displays double luminescence at room temperature (Fig. 4.3).

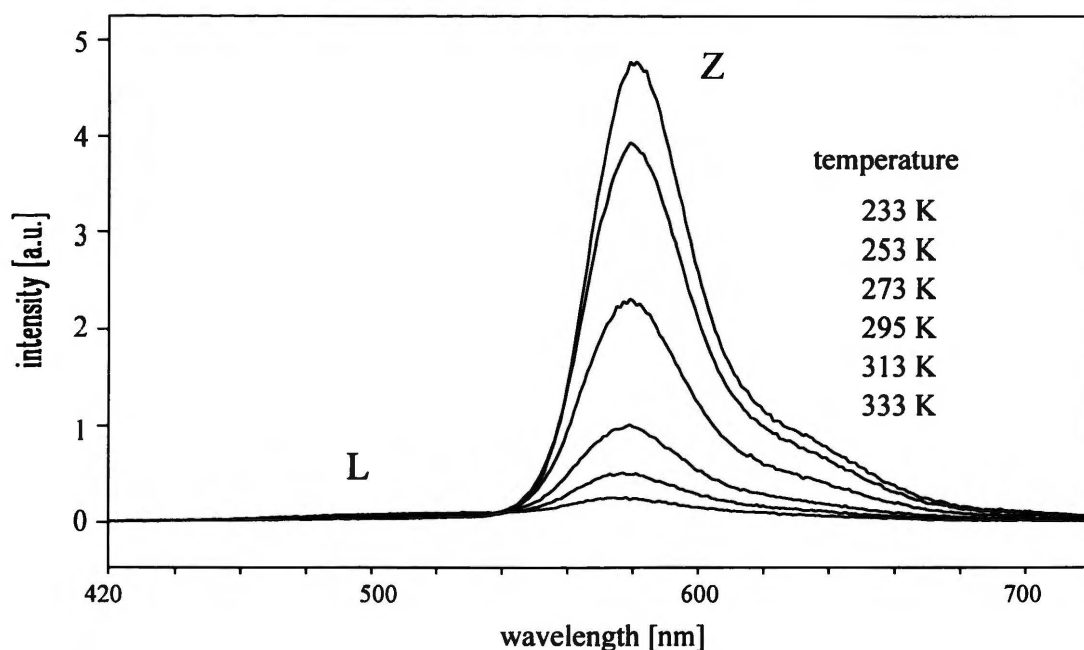


Fig. 4.3: Luminescence spectra of rhodamine 101 lactone (LR101) in dimethoxyethane as a function of temperature. Higher intensities of the Z band correspond to lower temperatures. The spectra exhibit an iso-emissive point at 537 nm.

The same observations were made for other rhodamine lactones (Fig. 4.4). On the basis of the fluorescence measurements carried out at various temperatures of the sample one can conclude that on lowering of temperature the fluorescence quantum yield¹ of the L band, Φ_L , decreases and that of the Z band - Φ_Z - increases. Decrease of Φ_L is accompanied by a red

shift of the L band, an increase in the intensity of the Z band, on the other hand, causes almost no shift of the fluorescence maximum. For instance, in the LRB/BN system, the maximum of the Z band is located at 562 nm in the temperature range 238 K - 295 K and does not shift with changing the temperature. A very interesting feature is the occurrence of an iso-emissive point in the fluorescence spectra (e.g. in the case of LRB in BN at 524 nm) in quite broad temperature ranges.

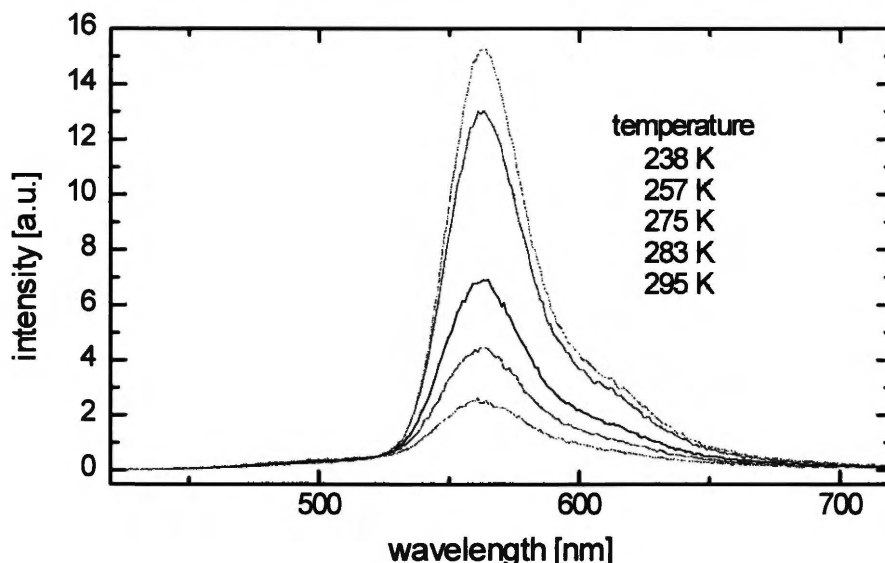
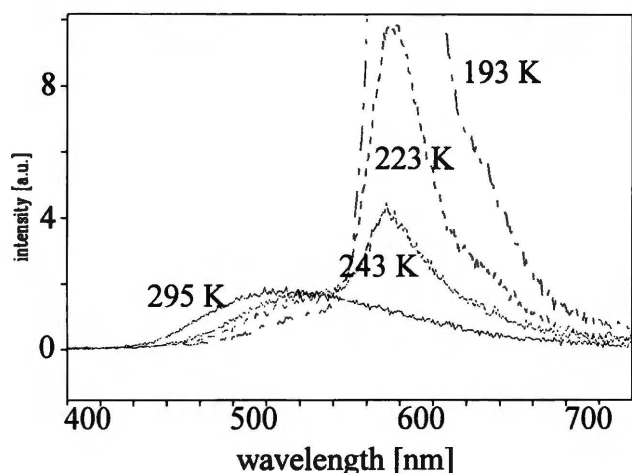


Fig. 4.4: Luminescence spectra of rhodamine B lactone (LRB) in butyronitrile as a function of temperature. Higher intensities of the Z band correspond to lower temperatures. The spectra exhibit an iso-emissive point at 524 nm.

Following the spectral changes observed in LR101/EE system on lowering the temperature, the conclusion can be drawn that **the excited zwitterion form of rhodamine is formed always, and under conditions where it is not observed - this form undergoes a rapid non-radiative deactivation.** This conclusion is supported by the fact that low observed fluorescence efficiencies are accompanied by short decay times of Z fluorescence (e.g. LR101/DME or LR101/THF at room temperature, see Table 3.3). Temperature dependent measurements of LR101 in other solvents (Fig. 4.5) and of other lactones confirm also this conclusion.



T [K]	$\epsilon(T)$
295	7.0
243	8.2
223	8.9
193	10.3

Fig. 4.5: Luminescence spectra of rhodamine 101 lactone (LR101) as a function of temperature in methyltetrahydrofuran (MTHF). The Z fluorescence was observed in MTHF already at 253 K. The table above shows temperature dependence of the dielectric constant $\epsilon(T)$ for MTHF².

The phenomenon of appearance of the **Z** fluorescence and a dramatical increase of its quantum yield on lowering the temperature was also observed in other rhodamine lactones (Fig. 4.6). The lactones with different substituents at amino groups start to display the **Z** fluorescence in different solvents and at different temperatures. The appearance of the zwitterionic fluorescence seems to be especially connected with the ionisation potential of the substituent at amino group as well as with the polarity the solvent attains at the temperature

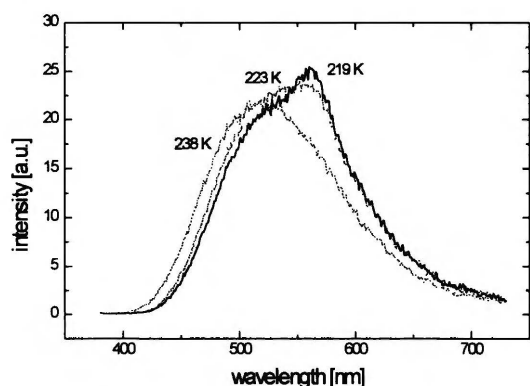


Fig. 4.6: Luminescence spectra of rhodamine B lactone (LRB) in dimethoxyethane (DME), recorded in the temperature range where the zwitterion fluorescence starts to appear.

temperature when the dielectric constant of the solvent is $\epsilon = 10.4$ ⁴. Fig. 4.6 shows the spectra of LRB in dimethoxyethane recorded in the temperature range where the zwitterion fluorescence starts to appear.

The spectra presented above prove clearly that the **Z** form in excited state (1Z_1) is formed always, and the **Z** fluorescence can be observed under such conditions only, where the 1Z_1 state is sufficiently stabilised by the solvent against the non-radiative deactivation. On the other hand, the spectra of LR101 measured as a function of temperature in BN or in PY (Fig. 4.7) (and especially, the iso-emissive points observed in a broad temperature range) show that even in the case when apparently a single luminescence band is observed, this band may consist of two luminescences strongly overlapping with each other.

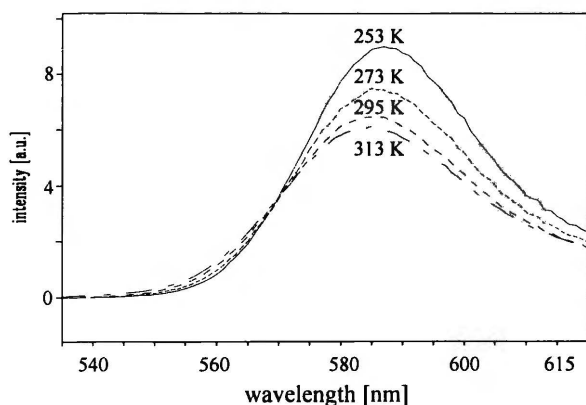


Fig. 4.7: Luminescence spectra of rhodamine 101 lactone (LR101) in pyridine as a function of temperature.

when the **Z** fluorescence starts to be displayed. The polarity increases on lowering of temperature. The decrease of the decay time of this fluorescence with increasing temperature (Table 4.1) indicates a solvent-controlled intramolecular quenching of the zwitterion. In the case of LR101 the **Z** fluorescence starts to appear in media of dielectric constant $\epsilon \sim 7 - 8$ ($\epsilon = 7.0$ for ethyl ether at 193 K³ and $\epsilon = 7.9$ for MTHF at 253 K²), and LRB (diethylamino type substituent at amino nitrogen atom) starts to display the **Z** fluorescence in DME at the

This also confirms a further shift of the **L** fluorescence due to larger stabilisation of the $^1L_{CT}$ state than that of the 1Z_1 state, with the increase of solvent polarity. As the fluorescence decay curves in these solvents (measured at the fluorescence maxima) at room temperature could in principle be fitted as a monoexponential decay, the contribution from the $^1L_{CT}$ emitting state should be not significant. Decay measurements at higher temperatures, especially at the short-wave edge of the fluorescence band of LR101 in BN

show, however, that there are two luminescences with different decay times within the observed band. The results of the measurements performed for different parts of the spectrum of LR101 in BN have been collected in Table 4.1.

Table 4.1.

Results of the deconvolution of the decay curves of LR101 in BN at various temperatures measured in different parts of the fluorescence spectrum¹⁾

Temperature [K]	$\lambda = 540 \text{ nm}$				$\lambda = 560 \text{ nm}$				$\lambda = 580 \text{ nm}$			
	τ_1	A_1	τ_2	A_2	τ_1	A_1	τ_2	A_2	τ_1	A_1	τ_2	A_2
295	-	-	-	-	4.00	0.184	0.94	0.024	4.03	0.190	0.90	0.010
313	4.04	0.180	0.80	0.039	4.05	0.179	0.85	0.039	4.08	0.188	0.80	0.016
$Q_i^{2)}$	0.96		0.04		0.96		0.04		0.98		0.02	
333	3.77	0.109	0.71	0.138	3.85	0.170	0.71	0.042	3.87	0.189	0.70	0.023
Q_i	0.81		0.19		0.96		0.04		0.98		0.02	
353	3.25	0.122	0.80	0.127	3.27	0.169	0.80	0.041	3.27	0.194	0.80	0.020
Q_i	0.80		0.20		0.94		0.06		0.98		0.02	

1) The decays were fitted with two-exponential function. τ values are given in ns.

2) The contributions Q_i from components decaying with a decay time τ_i were calculated according to the formula $Q_i = A_i \tau_i / \sum_i A_i \tau_i$

The results of deconvolution of the decay curves of LR101 in BN at various temperatures measured in different parts of the fluorescence spectrum clearly show that fluorescence consisting apparently of one band is in fact composed of two bands overlapping on each other. One can also judge that the L fluorescence may become iso-energetic or even lower in energy than the Z fluorescence. Measurements of the decay curves collected at different wavelengths support the conclusion drawn from the temperature dependent measurements of fluorescence spectra that one fluorescence band can contain emissions from two excited states. Table 4.1 reports the results of fitting the fluorescence decays of LR101 in BN at various temperatures recorded in different parts of the fluorescence spectrum (the temperature dependent spectra of LR101/BN resemble very much the spectra obtained for LR101/PY system). The decays collected at 540 nm and at 560 nm (short-wave edge of the fluorescence band) show a contribution from a luminescence with a decay time of about 0.7 - 0.9 ns which has been ascribed to the L luminescence. The significant shortening of this decay time compared with less polar solvents is linked to the decrease of the quantum yield of the L luminescence and might reflect e.g. an enhancement of the radiationless deactivation of the $^1L_{CT}$ state with decreasing transition energy.

Solvent effect on the photophysics of lactones may be visualised using the example of temperature dependent measurements of LDR10. Decay times of the Z form of this rhodamine excited directly from the ground state of Z in absolute ethanol (formed after dissolution of the lactone form in this solvent) have been found independent of the

temperature (4.10 ns at 293 K, 4.14 ns at 313 K, and 4.14 ns at 333 K). Vogel *et al.*⁵ reported that decay times of an analogue rhodamine (an ester derivative of DR10) in ethanol were also unaffected by temperature (slightly lower $\tau \approx 3.9$ ns). The zwitterion formed in aprotic solvents upon excitation of the LDR10 molecule exhibits, however, temperature dependent fluorescence quantum yields and decay times. For instance, the quantum yield of Z fluorescence changes from 0.0030 at 343 K to 0.074 at 233 K in AN or from 0.0095 at 363 K to 0.064 at 293 K in DMSO. It turned out, however, that at temperatures when the two solvents have approximately the same dielectric constants (e.g. AN at 293 K and DMSO at 363 K), fluorescence quantum yields are almost identical. For instance, at 293 K $\epsilon(\text{AN}) = 37.6$ and $\Phi_Z = 0.0097$, and at 363 K, $\epsilon(\text{DMSO}) = 36.6$ ⁶, $\Phi_Z = 0.0095$. Also decay curves and decay times obtained at these temperatures were very similar, indicating - from the point of view of the non-radiative process responsible for thermally activated radiationless process in zwitterion forms - a kind of "conversion" of DMSO in AN (at 293 K) upon warming it up to 363 K.

Table 4.2.

Results of temperature measurements of rhodamine 101 lactone (LR101) in various solvents

Solvent	Temperature [K]	$\Phi_L + \Phi_Z$ ^{a)}	τ_L ^{b)} [ns]	τ_Z ^{c)} [ns]	$(\Phi_L + \Phi_Z)/\tau_Z$ [$\times 10^{-7}$]
DME	233	0.092	-	-	
	253	0.079	-	-	
	273	0.049	-	-	
	295	0.024	3.51	0.40	
	313	0.014	3.65	0.22	
	333	0.0094	4.10	0.08	
	353	0.0075	5.8	- ^{d)}	
Pyridine	295	0.168		3.60	4.67
	313	0.162		3.59	4.51
	333	0.150		3.58	4.20
	353	0.133		3.38	3.91
BN	295	0.201		4.03	4.99
	313	0.188	0.80	4.08	4.61
	333	0.164	0.71	3.87	4.23
	353	0.130	0.80	3.27	3.98
Ethanol ^{e)}	295	0.98		4.37	
	313	0.98		-	
	333	0.97		-	
	353	0.98		-	

^{a)} Only total fluorescence quantum yield is given because of a large overlap of the Z and L bands. The quantities presented are the relative intensities of the integrated fluorescence.

^{b)} τ_L represents the main component recovered from the decay analysis. Measured at 500 nm for DME and at 540 nm for BN. The decays were non-exponential due to a strong solvatochromic red shift of the L band and its overlap with the Z band.

^{c)} Measured at 580 nm.

^{d)} Below the time resolution of the instrument.

^{e)} Absolute ethanol.

Table 4.2 presents the results of temperature studies for rhodamine 101 lactone in various solvents. In contrast to the changes in quantum yields and in the decay times in aprotic solvents, the fluorescence quantum yield of the lactone solution in ethanol (where the zwitterion form in the ground state strongly dominates) excited at 320 nm has been found to be independent of the temperature (similarly as in the case of LDR10) and equal to 0.98. This value is very close to the quantum yield found for solutions of R101 salts⁷⁻⁹.

The temperature dependencies of LRB fluorescence have been measured in a series of solvents and at various temperatures. The temperature range of systematic quantitative measurements was 293 K - 343 K. The results of the temperature measurements for this dye have been shown in Table 4.3.

Table 4.3.

Results of temperature measurements of rhodamine B lactone (LRB) in various solvents.

Solvent	Temperature [K]	Φ_T	Φ_L	τ_L [ns]	Φ_Z	τ_Z [ns]	$\Phi_Z/\tau_Z^{1)}$ [$\times 10^{-7}$]
DME	293		0.043	10.49			
	303		0.041	10.30			
	323		0.037	9.90			
	343		0.037	10.20			
BN	293	0.039	0.013	5.76	0.026	0.71	3.66
	303	0.031	0.013	5.84	0.018	0.51	3.53
	323	0.022	0.013	6.02	0.009	0.22	4.09
	343	0.020	0.014	6.30	0.005	0.09	5.56
BZN	293	0.085	0.017	9.31	0.068	2.74	2.48
	323	0.059	0.018	9.67	0.040	1.48	2.70
	343	0.043	0.019	9.67	0.023	0.84	2.74
	353	0.038	0.019	9.58	0.019	0.54	3.52
AN	293	0.127	0.001	1.72	0.126	2.08	6.06
	303	0.105			0.104		
	323	0.067			0.066		
	343	0.041	0.0015	2.15	0.004	0.62	6.45

¹⁾ Average τ_Z values have been used (see description below Table 4.5).

In DME ($\epsilon = 7.2$) the spectrum in this temperature range is broad and consists of one band which shifts towards shorter waves as the temperature increases. The FWHM (Full Width at Half Maximum) of the band changes slightly from 5300 cm^{-1} at 293 K to 5500 cm^{-1} at 343 K. The fluorescence quantum yields change also in narrow limits. Changes in Φ_L in three other solvents (BN, BZN and AN) are also small with a slight trend to increase with elevation of the temperature. Fluorescence rate constants for lactone fluorescence (calculated as Φ_L/τ_L) remain practically unchanged. More dramatic changes occur in the Z band. Fig. 4.8 shows the fluorescence spectra of LRB in BZN as a function of the temperature. The spectra in BN change with temperature in a very similar manner and an iso-emissive point was also observed in this solvent. Very low quantum yield of the lactone fluorescence in AN compared with that of the zwitterion prevents any observation of such a possible iso-emissive point.

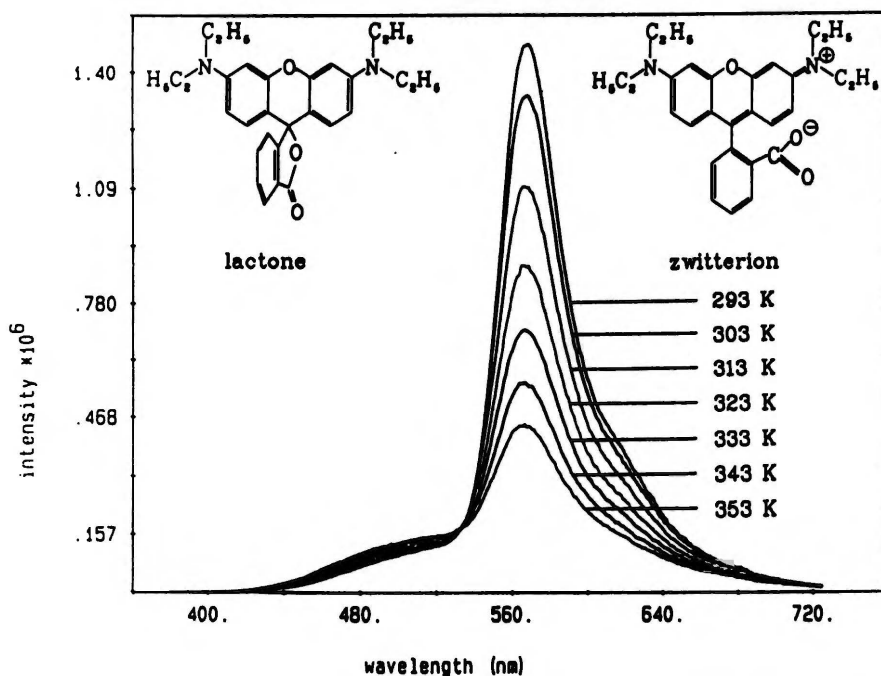


Fig. 4.8: Fluorescence spectra of rhodamine B lactone (LRB) in benzonitrile as a function of temperature.

The ratio Φ_Z/τ_Z for LRB exhibits small changes for a given solvent (neglecting the shortest decay times at highest temperature applied which might have been determined with the largest experimental error; see Table 4.5), indicating that the radiative rate constant of **Z** generally does not depend on temperature. On the other hand, the ratio $(\Phi_L + \Phi_Z)/\tau_Z$ calculated for LR101 from the data collected in Table 4.2 decreases slightly with increase of temperature, which can result either from a temperature dependence of k_r for the **Z** form or - which is more probable - is caused due to participation of the **L** fluorescence, strongly overlapping with the **Z** luminescence (see Fig. 4.9 and discussion below in this section).

The existence of iso-emissive points (see e.g. Fig. 4.3, 4.4, 4.7, 4.8) in the spectra recorded at various temperatures extending over broad temperature ranges (253 K - 333 K for LR101/pyridine, 253 K - 323 K for LR101/BN, 293 K - 353 K for LRB/BZN and 253 K - 353 K for LR101/DME) suggests a kinetic coupling of the two emitting states. The monoexponential decays observed in all cases within the **L** band and the energy difference between the luminescent states would limit such coupling to a population of the zwitterion from the lactone; otherwise a second decay time would be found in the decays collected in the **L** band, especially in cases where τ_L is shorter than τ_Z . However, the decay curves recorded for LRB in AN in the **L** band could be well fitted with a monoexponential function (at 293 K $\tau_L = 1.72$ ns, at 343 K $\tau_L = 2.15$ ns) and the decay times of the **Z** form were found equal to 2.08 ns and 0.62 ns, at 293 K and at 343 K, respectively. On the other hand, time-resolved fluorescence spectra (cf. Fig. 3.13) represent an evidence for a slow population channel of the excited 1Z_1 state. The term slow is used here to describe a process occurring on the time scale of nanoseconds. There are two possible sources for such a population: (i) the 1Z_1 state is formed directly from the $^1L_{CT}$ state, which is accompanied by a slow photodissociation reaction of the lactone ring, or (ii) the 1Z_1 state is populated from a "dark" (e.g. triplet) state,

which is formed either on deactivation of the ${}^1L_{CT}$ state or in a fast relaxation process resulting in a primary generation of the ${}^1L_{CT}$ and the 1Z_1 states.

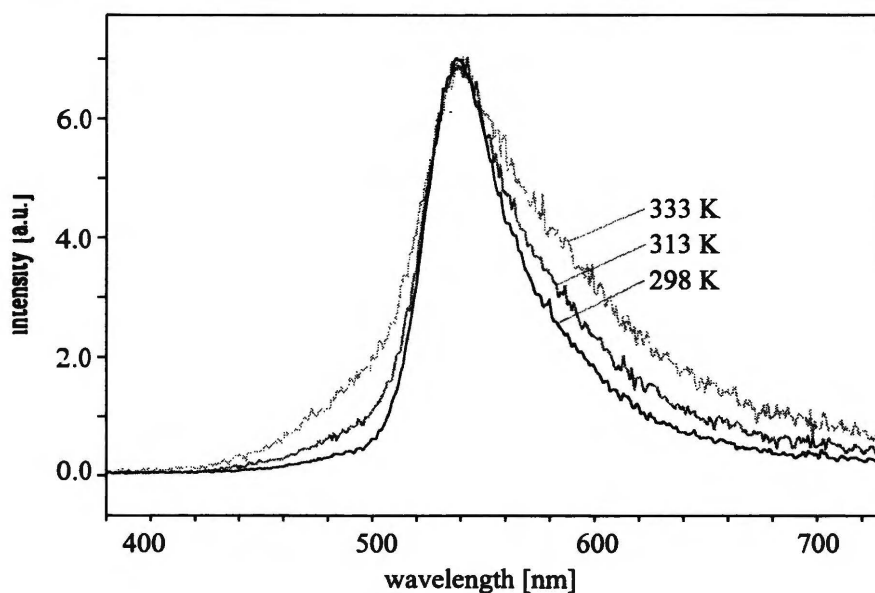


Fig. 4.9: Fluorescence spectra of rhodamine DR10 in acetonitrile as a function of temperature. The spectra have been normalised to the maximum of the Z band.

Multi-exponential decay curves were recorded in Z band only when the L fluorescence was observed. As already discussed in section 3.3.1, the multiexponentiality of the decays could result either from an obvious overlap of the L and the Z band or it could be an indication of an equilibrium of the two excited states: the ${}^1L_{CT}$ and the 1Z_1 state. Significant contribution from the overlap of the two bands prove temperature-dependent spectra of LDR10 in AN (Fig. 4.9). The spectra shown in that Figure have been normalised to the maximum of Z fluorescence and the spectra recorded at higher temperatures show clearly that the L band extends far in the red region of the spectrum. Therefore, at the present stage of understanding of the excited state processes it cannot be decided to which extent a possible excited state ${}^1L_{CT} \rightleftharpoons {}^1Z_1$ equilibrium contributes to the observed multiexponentiality of decays. Also the problem of occurrence of the iso-emissive points in the temperature dependent spectra of rhodamine lactones, though very interesting, was not, however, solved in this thesis and requires further investigations.

Luminescence near the freezing point of the solvent

The condition and dielectric properties of the medium surrounding the lactone molecule influence significantly the excited state processes. For instance, cooling down from 143 K to 93 K corresponds to the transformation of methyltetrahydrofuran (MTHF) from a polar liquid ($\epsilon = 15.4$) through a soft glass to a more rigid solvent. The transformation is accompanied by significant changes in dielectric properties of the medium and its relaxation time. This results in the evolution of the spectrum and band positions in this temperature region. The shifts of the L and the Z band of LR101 luminescence in this temperature range are reported in Table 4.4.

Table 4.4.

Shifts of the fluorescence spectrum of LR101 in MTHF with temperature.

T [K]	λ_{max}^L [nm]	λ_{max}^Z [nm]
143	a)	582
123	505	566
113	470	561
93	455	559

a) Only short-wave tail of the L band was outside of the Z band, the rest was overlapped by the Z band and the position of the maximum could not be determined.

The shift of the L band towards shorter wavelengths with decrease of the temperature (in the range 143 K - 93K corresponding in this temperature region to a decrease of the dielectric constant) was accompanied by increase in the intensity of this band. The spectral shift of the Z band by 650 cm^{-1} compared with the position of the Z band at temperatures where MTHF is still liquid (i.e. at 143 K, maximum at 582 nm) may be caused by the rigidity of the glass disabling the full conformational relaxation from the non-planar structure, characteristic for the lactone molecule, to the planar elongated xanthene system of the zwitterion. The changes in intensity of the Z band were much less than those in the temperature range 243 K - 143 K.

4.3. Luminescence in glass

Figure 4.10 shows luminescence spectra of LR101 measured in a perfectly glassed MTHF at 93 K.

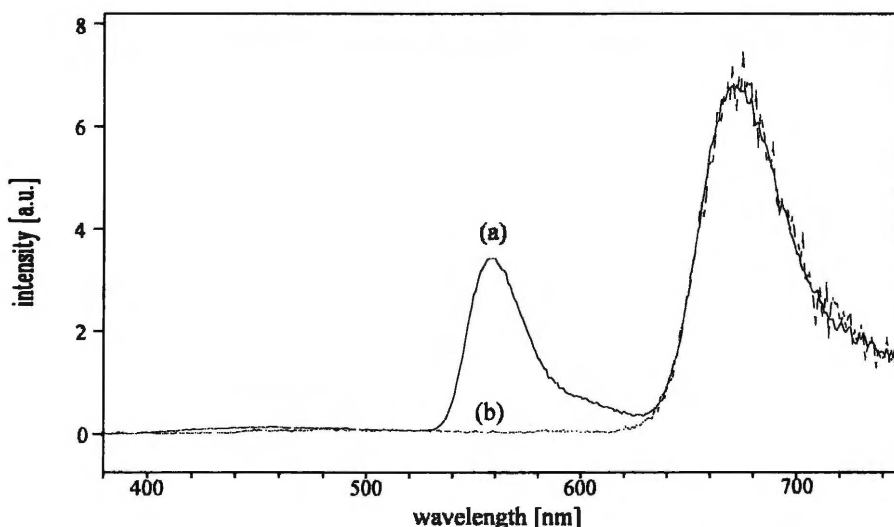


Fig. 4.10: Luminescence spectra of rhodamine 101 lactone (LR101) in MTHF glass at temperature 93 K. The glass was of very high quality and did not contain any cracks. The solution was colourless. (a) total luminescence (continuous line); (b) phosphorescence (dashed line) recorded after switching on the choppers of the spectrofluorimeter.

The spectrum consists of 3 bands with the maxima at 455 nm, 559 nm and 672 nm, respectively. The band at 455 nm may be ascribed to the L fluorescence shifted at this

temperature towards shorter wavelengths according to the polarity change of MTHF, which at this temperature exhibits a dielectric constant about 3^2 and an elongated relaxation time as compared with room temperature, so the position of the band corresponds to that in butyl ether at room temperature ($\epsilon = 3.08$). The band with a maximum at 559 nm comes from the zwitterion which is formed upon lactone ring dissociation in the excited state (see discussion above). As calculated by the PC Model molecular mechanics program and confirmed by preliminary determination of the crystallographic structure for LRB¹⁰, the conformation of the xanthene part in lactone molecule in the ground state is slightly bent in contrast to that of zwitterion, where it is planar due to the extended π -electronic system.

The band with the maximum at 672 nm was identified as the phosphorescence of the LR101 (Fig. 4.10). The excitation spectrum of the phosphorescence measured at the band maximum was the same as that of Z fluorescence and matched the absorption spectrum of the lactone. Similar phosphorescence emissions were discovered for lactones of other rhodamines (Fig. 4.11).

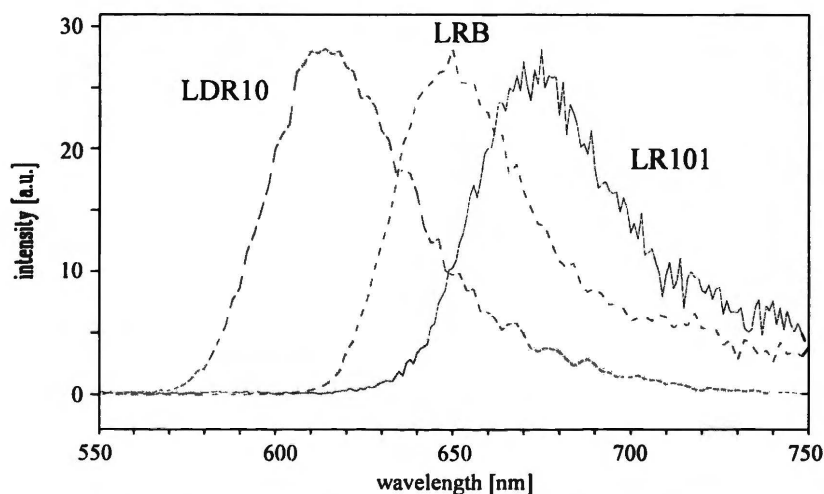


Fig. 4.11: Phosphorescence spectra of rhodamine lactones measured at 77 K. LRB and LDR10 were measured in BN, LR101 was measured in MTHF.

A very important question is the nature of the triplet state being the source of this phosphorescence, i.e. does the phosphorescence come from (i) the lactone charge transfer triplet state, (ii) a local triplet state within the lactone molecule or (iii) a triplet state of the Z form? A very large energy difference between the CT fluorescence and the phosphorescence allows us to discard the possibility (i) because the $^1L_{CT}$ and $^3L_{CT}$ should be energetically nearly degenerate. The option (ii) can be eliminated by comparison of the phosphorescence of LRB and its lactam analogue (see Fig. 1.5, R = Ph) differing from LRB by substituting the oxygen atom in the phthalide ring by the nitrogen atom with the phenyl ring attached to it ($>N-C_6H_5$)¹¹. The latter compound displays also the CT luminescence in BN, does not, however, undergo any dissociation in the excited state and displays an intense, slightly structured phosphorescence with a maximum at 425 nm, which we preliminarily ascribe to a local triplet of this molecule¹². The energy difference between the maxima of the CT fluorescence and the phosphorescence in the lactones is rather high (more than 7000 cm^{-1} for

the LR101/MTHF system at 93 K) and therefore a direct population of the emitting triplet state from the $^1L_{CT}$ seems to have a very low probability. On the basis of these arguments we postulate that the phosphorescence observed upon excitation of lactones come from the triplet state of the **Z** form. The phosphorescence bands observed agree also well with those reported by Nurmukhametov *et al.* as phosphorescence bands of zwitterion forms of rhodamines¹³. A long decay of the phosphorescence visually observed upon the excitation of the lactone, large quantum yield, as well as the results of preliminary ESR measurements for LRB that yielded low value of the zero field splitting parameter $D^* = \sqrt{D^2 + 3E^2} = 0.067 \text{ cm}^{-1}$, indicate that the spin density in the emitting T_1 state is distributed over the whole π -electron system¹⁴ and let us infer that the emitting triplet state is that of the $^3(\pi, \pi^*)$ nature¹⁵. This is supported by the value of parameter D^* found for oxonine (0.067 cm^{-1}) and the assignment of the lowest triplet state of oxonine to (π, π^*) states¹⁶. The value of parameter D^* agrees also with that reported for rhodamine B by Yamashita *et al.*¹⁷ (0.065 cm^{-1}). An interesting feature of the phosphorescence is its solvent-dependent shift observed, for instance for LRMET in BN ($\lambda_{\text{max}} = 647 \text{ nm}$) and in MTHF ($\lambda_{\text{max}} = 638 \text{ nm}$).

Total luminescence quantum yield of LR101 in MTHF glass was found equal to 1.0 within the error limit. Taking this into account, it is assumed in further discussion that all significant non-radiative transitions diminishing the luminescence quantum yield at higher temperatures occur between the 1Z_1 , the $^1L_{CT}$ and the triplet states, the radiationless deactivation to the ground state being negligible.

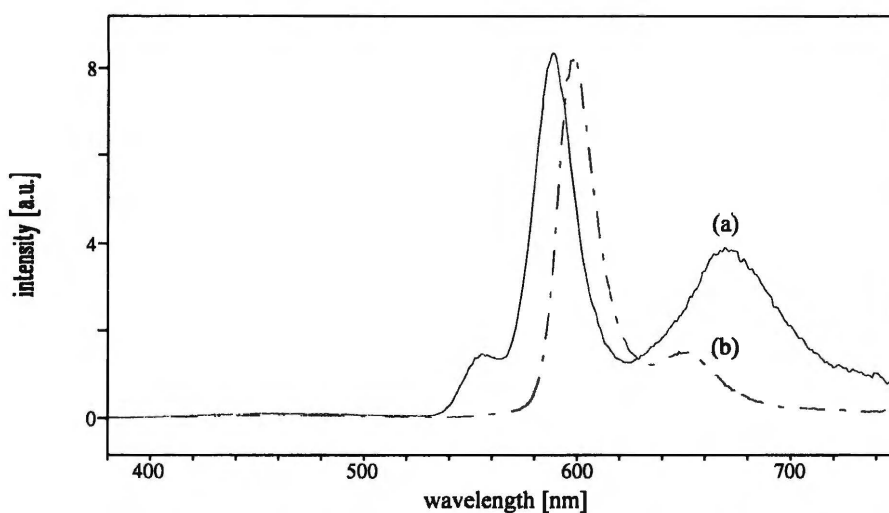


Fig. 4.12: Luminescence spectra of rhodamine 101 lactone (LR101) under conditions when the polycrystalline regions after freezing the solvent occur. (a) MTHF glass at temperature 93 K with small amount of cracks; the peak at 589 nm comes from zwitterions excited directly from the ground state that are present in the crack regions (continuous line); (b) polycrystalline dimethoxyethane snow at 77K (dash-dotted line). In both cases the samples were excited with the same UV light.

The ratio of integrated intensity of the **L** band to that of the **Z** band and to the phosphorescence band in the LR101/MTHF system was 0.03 : 0.24 : 0.73, respectively. The value 0.24 corresponds very well to the efficiency of population (η_Z) of the zwitterion form in the excited state reaction at room temperature found in other solvents (0.21 - 0.25, see Table 3.7 in this thesis). The practical consistency of these values confirms also the independence of

η_Z of the solvent. Similar intensity ratios have been found for LRB/BN and for LRMET/BN systems. The intensity of Z fluorescence to phosphorescence in LDR10/BN system was, however, different: 0.81 : 0.13.

It has been found that the luminescence emitted by LR101 from rigid solution depends critically on the condition of the glass. The luminescence from a perfect glass without any cracks is shown in Fig. 4.10. In the cases when only a few cracks were present in the glass, an additional, strong sharp band with a maximum at 589 nm appeared (Fig. 4.12 (a)).

The same effect was observed for other lactones (Fig. 4.13). On the basis of the spectral position of the band and the excitation spectrum of this luminescence we ascribe it to emission from zwitterions directly excited from the ground state. The conclusion is supported by the observation that all the snow samples were intensely coloured. The colour disappeared completely on warming up the sample and melting the snow. The new luminescence peak is also the only one displayed in the low temperature spectra of the solutions in solvents that do not yield glasses (e. g. DME, Fig. 4.12 (b)) and form polycrystalline snow after cooling them down to 77 K.

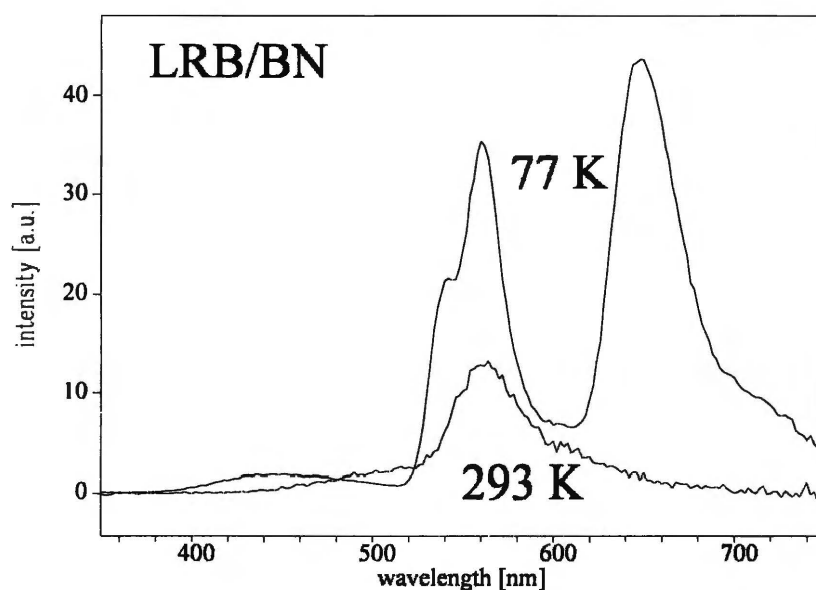


Fig. 4.13: Luminescence spectrum of rhodamine B lactone (LRB) in BN under conditions when polycrystalline regions after freezing the solvent occur, compared with the spectrum recorded at room temperature.

No phosphorescence has been detected when the solution was frozen to form a polycrystalline snow even in such solvents like BN, which - when properly cooled down - yield glasses. The same BN solution warmed up and cooled down once again to give a perfect glass displayed triple luminescence, such as that described above for the perfect MTHF glass.

4.4. Temperature studies of the decay kinetics

Part of the results of decay measurements performed for LR101 in various solvents at different temperatures was shown in Table 4.1. Similarly as in the case of LR101, elevation of temperature gives rise also in other lactones to significant evolution of fluorescence decay curves. Main changes are: (i) increase of τ_L and (ii) decrease of τ_Z (main short component

recovered from the fitting) upon elevation of temperature. Fig. 4. 14 shows a typical example - decays of LRB in BN measured at $\lambda = 560$ nm in the temperature range 293 - 343 K. Different effect observed for LR101 in BN (cf. e.g. Table 4.1) may be explained by low intensity of the L band preventing from recovery of a decay time of the L fluorescence.

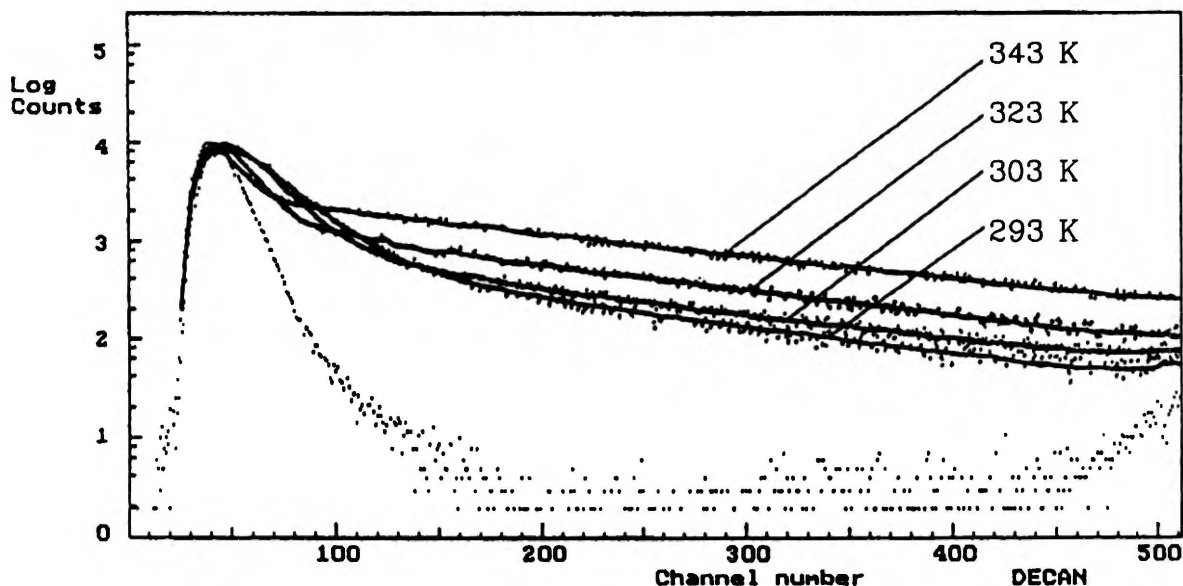


Fig. 4.14: Decays of LRB in BN measured at $\lambda = 560$ nm in the temperature range 293 - 343 K. The channel width used was 34 ps.

As the lifetimes of Z fluorescence for LR101 and LDR10 in absolute ethanol have been found temperature independent in the temperature range 293 K - 333 K, they have been used to calculate radiative rate constants. Radiative rate constants k_r for LRB, LDR10 and LR101 together with the fluorescence quantum yields and fluorescence lifetimes used to calculate them for two latter lactones have been shown in Table 4.4. k_r for LRB was taken from ref. ¹⁸.

Table 4.4.

Radiative rate constants of zwitterion fluorescence¹⁾ at 293 K.

Rhodamine	Φ	τ [ns]	k_r [$\times 10^{-8} \text{ s}^{-1}$]
LDR10	0.83	4.14	2.0
LR101	0.98	4.37	2.2
LRB	-	-	2.3 ²⁾

¹⁾ Φ and τ values have been measured for rhodamine lactones dissolved in absolute ethanol.

²⁾ k_r for LRB was taken from ref. ¹⁸.

Assuming the radiative rate constants k_r of the Z fluorescence to be independent of temperature¹⁸ and using the equation:

$$k_{nr} = (1/\tau_Z) - k_r, \quad (4.1)$$

non-radiative rate constants k_{nr} of zwitterion decay have been calculated for different solvents as a function of temperature. In calculations according to eq. 4.1, in cases where a mono-exponential fit was insufficient to describe the decay, a mean value for decay time τ_Z was used. The mean value was calculated according to the formula: $\tau_Z = (A_1\tau_1 + A_2\tau_2) / (A_1 + A_2)$. Because of the independence of k_r of temperature, changes observed in decay times of Z fluorescence reflect variations in k_{nr} . Table 4.5 reports decay times of zwitterion fluorescence together with corresponding non-radiative rate constants k_{nr} for LRB, LDR10 and LR101. Figure 4.15 shows Arrhenius plots of k_{nr} for the zwitterion generated from LRB in butyronitrile, benzonitrile, acetonitrile and DMSO.

Table 4.5

Decay times of Z fluorescence τ_Z , rate constants of non-radiative deactivation k_{nr} and calculated Arrhenius activation energies E_a for LRB.

LRB	BN				BZN				AN			DMSO			
η (cP) ¹⁾	0.515				1.111				0.325			2.003			
ϵ ²⁾	24.8				25.2				37.5			46.7			
T [K]	293	303	323	343	293	323	343	353	293	323	343	293	323	343	353
τ_Z [ns]	0.71	0.51	0.22	0.09	2.74	1.48	0.84	0.54	2.08		0.62	2.33	1.45	0.95	0.73
k_{nr} [$\times 10^{-8}s^{-1}$]	11.8	17.3	43.2	122.7	1.35	4.46	9.60	16.2	2.6		13.9	2.0	4.6	8.2	11.4
E_a [kJ·mol ⁻¹]	37.3				35.0				28.3			24.8			
LR101	DME			BN											
η (cP)	1.111			0.515											
ϵ	7.2			24.8											
T [K]	295	313	333	313	333	353									
τ_Z [ns]	0.40	0.23	0.08	4.08	3.87	3.27									
k_{nr} [$\times 10^{-8}s^{-1}$]	22.7	41.2	122.7	0.25	0.38	0.86									
E_a [kJ·mol ⁻¹]	36.2			28.5											
LDR10							AN			DMSO					
η (cP) ¹⁾							0.325			2.003					
ϵ ²⁾							37.5			46.7					
T [K]							295	313	333	295	313	333	353		
τ_Z [ns]							0.34	0.19	0.12	2.45	1.70	0.96	0.51		
k_{nr} [$\times 10^{-8}s^{-1}$]							27.4	50.6	81.3	2.1	3.9	8.4	17.6		
E_a [kJ·mol ⁻¹]							23.3			31.9					

1) Solvent viscosity at 303 K¹⁹; 2) solvent dielectric constant²⁰

The value of experimentally determined activation energy $E_a = 24.8$ kJ mol⁻¹ for LRB in DMSO corresponds well to the values given by López-Arbeloa and K. K. Rohatgi-Mukherjee²¹. Very clear is the dependence of E_a on solvent polarity. General tendency for LRB and LR101 is an increase of activation energy with decrease of solvent polarity, whereas

a reverse behaviour is observed for LDR10. The experimental data for LR101 and LDR10 are, however, insufficient to draw any quantitative conclusions and would require extension of the study on other solvents. A very interesting result is an increase of k_{nr} with decrease of solvent polarity.

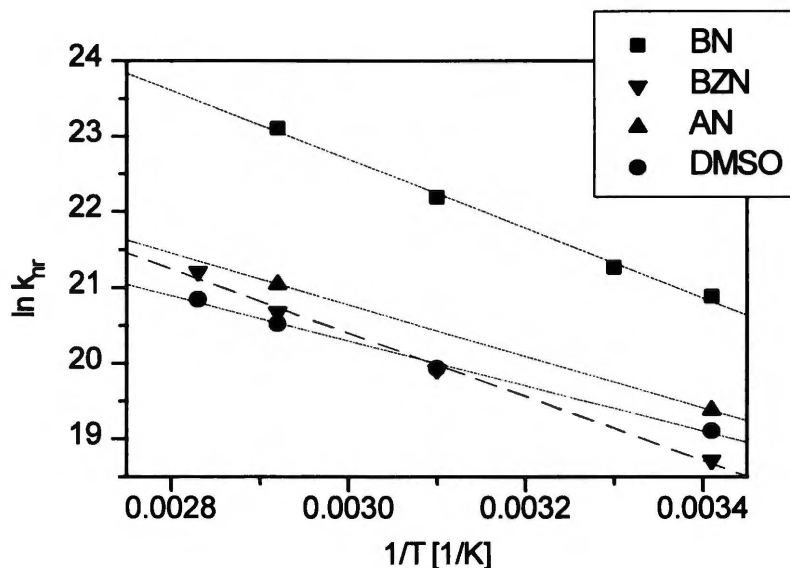


Fig. 4.15: Arrhenius plots of k_{nr} for LRB in BN, BZN, AN and DMSO.

Thermally activated non-radiative process in zwitterion and in cation form of rhodamine B has drawn attention of several workers (see Section 1.4 for a review of existing literature). The rate constant of non-radiative decay k_{nr} was studied as a function of temperature, solvent viscosity and solvent polarity. In contrast to this study, other researchers investigated RB under conditions where formation of hydrogen bonding (a necessary condition for stabilisation of the zwitterion in the ground state²²) was stimulated by the surrounding medium (mainly in alcohols; cation form was also studied in nitriles containing trifluoroacetic acid²³). The zwitterion formed upon excitation of the lactone molecule in aprotic solvents is not stabilised in such a way and is not exposed on interactions with the H^+ ions or the counterions that are present in a solution of rhodamine in a form of a salt.

The rate constant k_{nr} and the activation energy of thermally activated radiationless process in zwitterion of rhodamine B was determined in a series of normal alcohols²⁴ and in cation form of this dye in nitriles containing trifluoroacetic acid²³. It has been found that k_{nr} in alcohols decrease with solvent polarity both for **Z** and for **C** form. k_{nr} increased with solvent polarity for radiationless deactivation of **C** form in nitriles. Observed activation energy, on the other hand, was found to decrease for cation form (from 21.8 kJ·mol⁻¹ in methanol to 15.5 kJ mol⁻¹ in 1-hexanol²³) and to increase for zwitterion form (from 22.1 kJ·mol⁻¹ in 1-propanol to 43.2 kJ·mol⁻¹ in 1-decanol²³) along with decrease of solvent polarity. Our measurements show that in the case of zwitterion formed upon excitation of the lactone molecule in aprotic solvents the zwitterion is stabilised against the non-radiative process

(decrease of k_{nr}) in more polar solvents, and at the same time the activation energy of the reaction decreases. This question is discussed extensively in section 6.5.2.

Almost all papers dealing with radiationless deactivation of rhodamines tried to rationalise the thermally activated process by involving movements of amino groups at xanthene skeleton as a source of non-radiative process. In an attempt to explain observed variation in the activation energy in RB, Chang and Borst²⁵ have considered the influence of solvent polarity by taking into account the change of energy barrier of the radiationless transition and examined various models trying to explain the torsional motion on the basis of solvent viscosity with the common idea among these models being that of an energy barrier. They interpreted the barrier as the energy necessary for the diethylamino groups to rotate from the planar state to the twisted state (TICT). The same assumption was made by Vogel *et al.*⁵ who postulated structural relaxation to the TICT state in zwitterion forms of rhodamines and by Casey and Quitevis²⁴ for the cation form. The quenching of the zwitterion form of the rigid rhodamine 101 observed in this thesis and the analogy of its photophysics with other rhodamines suggest, however, that twisting or torsional motion of the amino group play an insignificant role in the non-radiative deactivation of rhodamines. This experimental fact is of great importance for photophysics of rhodamines as it provides a negative structural verification of the TICT hypothesis for rhodamine dyes. On the other hand it stimulates to search for a new explanation of the non-radiative process. An alternative new mechanism of radiationless deactivation in the **Z** form is discussed in Chapter 6.

References and notes

-
- ¹ The term "fluorescence quantum yield" is used in discussion of results obtained for lower and elevated temperatures in place of the term "fluorescence intensity", as we have found that no absorption changes occur on elevation of the temperature for LRB/BN system
 - ² T. Furutsuka, T. Imura, T. Kojima and K. Kawabe, *Technolog. Rep. Osaka Univ.* **1974** *24* (1155-1190), 367
 - ³ Ländolt - Börnstein, *Zahlenwerte und Funktionen*, Band **11.6** (1959)
 - ⁴ The dielectric constant was calculated using the empirical formula given in Ref. ⁶
 - ⁵ M. Vogel, W. Rettig, R. Sens and K.-H. Drexhage, *Chem. Phys. Lett.* **147** (1988) 452
 - ⁶ G. Grampp and W. Jaenicke, *J. Chem. Soc. Far. Trans. II* **81** (1985) 1035
 - ⁷ K.-H. Drexhage, in *Dye Lasers*, 2nd edition, pp 144-193 (edited by F. P. Schäfer); Springer, Berlin (1977)
 - ⁸ R. F. Kubin and A. N. Fletcher, *J. Luminesc.* **27** (1982) 455
 - ⁹ T. Karstens and K. Kobs, *J. Phys. Chem.* **84** (1980) 1871
 - ¹⁰ J. Lipkowski, J. Karpiuk and Z. R. Grabowski, unpublished results
 - ¹¹ Kindly obtained from prof. R. Gleiter, Heidelberg, Germany
 - ¹² It is interesting that luminescence spectrum recorded at 77 K with choppers and without choppers are identical which would indicate that in the lactam all luminescence is emitted from the triplet state similarly as in the case of phthalide (see ref. 10, Chapter 3).

-
- 13 R. N. Nurmukhametov, N. I. Kunavin and G. T. Khachaturova, *Izvest. Akad. Nauk SSSR Ser. Fiz.* **42** (1978) 517
 - 14 S. P. McGlynn, T. Azumi and M. Kinoshita, *Molecular Spectroscopy of the Triplet State*, Prentice-Hall Inc., Englewood Cliffs, N.J., 1969
 - 15 J. Herbich and J. Karpiuk, to be published.
 - 16 E. Vogelmann, H. Schmidt, U. Steiner and H. T. A. Kramer, *Z. Phys. Chem. NF* **94** (1975) 101
 - 17 M. Yamashita, H. Ikeda and H. Kashiwagi, *J. Chem. Phys.* **63** (1974) 1127
 - 18 L. B.-A. Johansson and A. Niemi, *J. Phys. Chem.* **91** (1987) 3020
 - 19 Ch. K. Mann, *Electroanal. Chem.* **3** (1969) 57
 - 20 C. Reichardt, *Solvent effects in organic chemistry*, ed. H. F. Ebel, Verlag Chemie, Weinheim, New York 1979
In the case of butyronitrile, different sources give two different values of ϵ at 293 K: 20.3 and 24.8; $\epsilon=24.8$ was used throughout this thesis.
 - 21 I. López-Arbeloa and K. K. Rohatgi-Mukherjee, *Chem. Phys. Letters* **128** (1986) 474; **129** (1986) 607
 - 22 D. A. Hinckley and P. G. Seybold, *Spectrochim. Acta* **44A** (1988) 1053
 - 23 K. G. Casey, Y. Onganer and E. L. Quitevis, *J. Photochem.* **64** (1992) 307
 - 24 K. G. Casey and E. L. Quitevis, *J. Phys. Chem.* **92** (1988) 6590
 - 25 T.-L. Chang and W. Borst, *J. Phys. Chem.* **93** (1990) 4724

CHAPTER 5

TRANSIENT ABSORPTION MEASUREMENTS

5.1. Introduction

Transient absorption spectroscopy following laser flash excitation on nanosecond time scale is a very useful technique to obtain information about the species involved in the excited state processes. This method of observation has an advantage over the time-resolved luminescence spectra, as some intermediates occurring in the course of an excited state reaction may not luminesce (e.g. radicals, radical ions or triplet states at room temperature). In other words, transient absorption spectra and kinetic curves may provide a complementary evidence for all species participating in a process under consideration. In addition, transient absorption spectra may yield a structural information on individual species.

Transient absorption measurements carried out within this thesis aimed at detection of possible intermediates participating in relaxation processes of the excited rhodamine molecule that could be observed by emission spectroscopy. Following transient absorption spectra and kinetic curves I wanted to obtain additional information concerning the mechanism of excited state reactions and to extract possible kinetic relations between the excited states of both - the lactone and the zwitterion - forms. Transient absorption was measured with TAN2 computer controlled nanosecond absorption spectrophotometer allowing to record the spectra at delay times in the range from 0 ns to 100 ns with a time resolution of 1 ns, and the kinetic curves of transient absorption in this time domain. Below, a summary of the literature relating to studies on transient absorption from lowest excited singlet and triplet states of rhodamines is given. Following this review the results obtained for the solutions of the **lactone form of rhodamine B (LRB)** are described in detail. The samples of LRB used in transient absorption studies were generally deoxygenated prior to measurements by bubbling with purified argon for at least 45 minutes. Use of non deoxygenated samples was specifically denoted.

5.2. Review of the literature

5.2.1. $S_1 \rightarrow S_n$ transient absorption

Despite of a wide application range of rhodamines, there are not many studies reporting the $S_1 \rightarrow S_n$ (singlet-singlet) transient absorption of these dyes. This relates both to the lactone and the ionic forms of rhodamines. It is the more strange in view of the fact that knowledge of spectral properties of the S_1 state would allow one, *inter alia*, to determine optimum pumping conditions in laser applications and is essential for the design of improved laser dyes. More attention has drawn rhodamine 6G¹⁻² (R6G), by far the most frequently used laser dye, which is an ethyl ester derivative of rhodamine DR10 substituted in 2' and 7' position with methyl groups (see Fig. 1.1, $R_1 = H$, $R_2 = R_3 = C_2H_5$, $R_4 = CH_3$) and does not form the lactone. First data on $S_1 \rightarrow S_n$ transient absorption of RB in trifluoroethanol

containing 0.01 M triethanolamine has been published by Hammond¹. That paper did not provide, however, a deeper insight in the excited state spectra. Studying the gain of the dye, the author reports the $S_1 \rightarrow S_n$ spectrum in the region 500 nm - 572.5 nm and concludes that the spectrum matches the ground state absorption with a certain red-shift. Only recently Beaumont *et al.*³ have published a comprehensive study on picosecond laser flash photolysis of rhodamine B, rhodamine 101 and rhodamine 6G in ethanolic and methanolic solutions. The authors report transient absorption spectra of these rhodamines, measured 66 ps after excitation (30 ps pulses were used as the excitation and the probing light), together with extinction coefficient values at the absorption maxima. Although the form of the dye investigated in that study was not *explicite* specified, on the basis of the dye concentration applied ($7.6 \cdot 10^{-6}$ M) and the conditions of measurements, one can infer that the zwitterion form was excited in the experiments. On the basis of the short delay time applied, they postulate that the observed absorption comes exclusively from the S_1 state of the zwitterion form. This assignment is made on the basis of kinetic data and derived from the fact that relaxation to the lowest vibrational level of S_1 (after excitation to S_n) is completed in rhodamines within 1 - 2 ps⁴. The authors rule out any significant contribution from the triplet state of rhodamine B to the observed absorption spectrum assuming that the rate of triplet state production will be equal to the rate of decay of the lowest excited singlet state ($3.5 \cdot 10^8$ s⁻¹ from their data for ethanol solution). [At 66 ps after excitation less than 3% of singlet states will have been deactivated.] The $S_1 \rightarrow S_n$ transient absorption spectrum of rhodamine B in ethanol reported by Beaumont *et al.* consists generally of two bands with the maxima at 430 nm and 566 nm, and the extinction coefficients are equal to $4.3 \cdot 10^4$ M⁻¹ cm⁻¹ and $3.8 \cdot 10^4$ M⁻¹ cm⁻¹, respectively. The spectra produced upon excitation at 532 nm and at 355 nm were superimposable after normalisation to the peak maxima. In view of their own data, one can, however, conclude that excitation at 355 nm may be not sufficient to reach the S_2 state of rhodamine B (see section 5.4 for a more detailed discussion). The authors note that there appears also a small absorption band above 600 nm (maximum at *ca.* 630 nm, Fig. 7, ref. 3). This band was observed for rhodamine B and for rhodamine 101 and did not occur for rhodamine 6G. The assignment of individual transitions for rhodamine B made in ref. 3 ($S_1 \rightarrow S_4$, $S_1 \rightarrow S_3$ and $S_1 \rightarrow S_2$ correspond to absorption bands with maxima at 430 nm, 566 nm and 950 nm (the latter predicted, but not observed), respectively) might indicate another than S_1 source of absorption at 630 nm. The $S_1 \rightarrow S_n$ spectra reported by Beaumont *et al.*³ for this region were, however, constructed from observed gain signal and stimulated emission spectrum, and the absorption may also be an artefact resulting from an inappropriate subtraction of the stimulated emission. The band with maximum at 430 nm reported in that paper may correspond to the $S_1 \rightarrow S_n$ band found earlier by Rylkov and Cheshev at 442 nm⁵.

Transients observed on picosecond time scale were also reported by Vlaskin *et al.*⁶ who studied the dynamics of population of the zwitterion excited state in rhodamine B and in rhodamine S (in DMF and in polymer matrices plastified with DMF) **upon excitation of the lactone molecule**. The authors presented transient absorption spectrum and the gain spectrum

of LRB in DMF recorded 20 ps after the excitation pulse and ascribed the band with a maximum at 475 nm to the excited zwitterion form. It was shown by comparison of the experimental results with the model calculations taking into account the finite width of the laser pulses (6 ps) that the rise time of the zwitterion is not longer than 1 ps. So high built up rate of the Z form and the lack of any changes in the transient absorption and the gain spectra with time was also observed on increasing solvent viscosity and in polymer matrices. This confirms that the dynamic process observed is not connected with intermolecular interactions but is controlled by the dissociation of the C-O bond and the redistribution of the electron density within the xanthene chromophore. Linear dependence of the fluorescence intensity on the intensity of the excitation pulse proved that the zwitterion is built up in a monophotonic mechanism of excitation. To our knowledge the paper by Vlaskin *et al.* constitutes the only work dealing with transient absorption of the lactone forms of rhodamines. The papers reporting $T_1 \rightarrow T_n$ transient absorption of rhodamine B (described below) have dealt exclusively with an ionic (most probably zwitterionic) form of the dye.

5.2.2. $T_1 \rightarrow T_n$ transient absorption

Transient absorption spectra of the excited triplet state of zwitterion form of rhodamine B have drawn considerably larger attention as compared with those of $S_1 \rightarrow S_n$ absorption. This is fully understandable, as the detection of triplet states of organic molecules requires much lower time resolution as in the case of excited singlet states. On the other hand, investigation of $T_1 \rightarrow T_n$ (triplet-triplet) absorption of rhodamines was of great importance for laser applications of these dyes. Krüger and Memming⁷ had found that excitation in first absorption band of RB ($\lambda = 545$ nm) did not result in formation of any short-lived (on the time scale of μ s) intermediates - neither $T_1 \rightarrow T_n$ absorption nor absorption bands of any other photoproducts could be detected. On the other hand, upon excitation with higher energy light ($\lambda < 360$ nm) they observed transient absorption band (decaying with $\tau \sim 400$ μ s) with a maximum at *ca.* 460 nm, which they assigned to triplet state of the RB molecule. The authors tried to explain this fact using the assumption that the intersystem crossing is more efficient from a higher singlet state ($S_2 \rightarrow T_2$) than from the lowest excited singlet level. The dependence of the rate constant of ISC process on excitation energy in rhodamines was mentioned for RB by Aristov and Maslyukov⁸ and investigated more thoroughly by Rylkov and Cheshev^{5, 9}. Using flash photolysis with multiphotonic excitation the latter authors have investigated the intersystem crossing process from higher excited singlet states to the triplet manifold. Measurements of quantum yields for this process allowed them to estimate the rate constants for $S_1 \rightarrow T$ and $S_n \rightarrow T$ transitions, which turned out to differ by 3 - 5 orders of magnitude in favour of higher excited states for various rhodamines (e.g. for RB: $k(S_1 \rightarrow T) \leq 3 \cdot 10^5$ s⁻¹ and $k(S_n \rightarrow T) \leq 10^8$ s⁻¹). The authors point out that at intense laser excitation, under conditions of high population rates of higher singlet states, this mechanism of triplet formation may be a predominant one and may exceed the triplet yield from the fluorescent state.

Dunne and Quinn¹⁰ have reported $T_1 \rightarrow T_n$ spectrum of 10^{-6} M ethanolic solution of RB where the triplet state of the dye was sensitised by triplet-triplet energy transfer from naphthalene. Their spectrum exhibits maxima at 419 nm, 560 nm and 630 nm (shoulder). They have also observed a longer lived photoproduct of the flash excitation¹¹. The photoproducts occurring at longer delays (on a ms time scale) after excitation of RB, DR10 and R6G ($\lambda_{exc} > 420$ nm) in water and in propanol were identified by Korobov *et al.*¹²⁻¹³ as ion radicals (both positive and negative) of corresponding rhodamines. Their results indicate that ion radicals are formed as a result of reactions involving molecules in the triplet state. As these species appear after much longer time than the time scale of our TAN 2 nanosecond spectrophotometer (100 ns), they were not a subject of experiments carried out within this thesis. $T_1 \rightarrow T_n$ spectrum reported by Korobov *et al.* (excitation light: $\lambda > 420$ nm) consists of three bands with maxima at 450 nm, 640 nm and 1000 nm. On the basis of transient absorption measurements the authors have also determined quantum yield of $S_1 \rightarrow T_1$ intersystem crossing being equal 0.006 and 0.005 for RB and DR10, respectively. These values are somewhat larger than those reported by Nurmukhametov *et al.*¹⁴ (0.0015 and 0.003, respectively) or by Dunne and Quinn¹⁰ (0.0024 for RB) but consistent with them as far as the order of magnitude is concerned. Saturation of ethanolic solution of RB with oxygen resulted in a threefold increase of quantum yield of the ISC process (0.0018 versus 0.0045)¹⁵.

To our knowledge, no solvent dependence of transient absorption spectra of rhodamines has been reported in the literature until now. Such a dependence could not be expected for solutions containing only zwitterions, as the $S_1 \rightarrow S_n$ or $T_1 \rightarrow T_n$ transitions in the zwitterion form occur most probably within the xanthene chromophore as the **Z** form of rhodamines does not exhibit significant solvent dependence of $S_0 \rightarrow S_n$ absorption. On the other hand, however, such a solvent dependence may reflect differences in rate constants of the ISC process in the case when solvent polarity shifts the energy levels of the excited states between which intersystem crossing takes place.

A summary of data on transient absorption spectra of rhodamine B and rhodamine DR10 is presented in Table 5.1.

Table 5.1

Literature transient absorption data concerning the zwitterion form of rhodamines

Dye	$S_1 \rightarrow S_n$ [nm]	$T_1 \rightarrow T_n$ [nm]	Reference
Rhodamine B	430, 566		ref. 3
	442	420 452 640 710	ref. 5
		460	ref. 7
		419 560 630	ref. 10
		450 640 1000	ref. 12
Rhodamine DR10		410 625 920	ref. 12
Rhodamine 101	450, 576		ref. 3

5.3. Transient absorption study of LRB - spectra and kinetic curves

In contrast to the zwitterion form excited directly in the ground state, transient absorption observed upon excitation of solutions containing exclusively the lactone form is very strongly solvent dependent. The dependence is demonstrated both by different shape of the spectra and by different kinetic curves of transient absorption recorded at the same wavelength in different solvents. Due to high complexity of the system and many possible intermediates which may occur upon excitation of the lactone molecule, a direct assignment of individual bands observed in spectra to corresponding molecular species and the interpretation of both the spectra and the kinetic curves was rather difficult and could be undertaken barely after a detailed investigation of both spectral and kinetic data from transient absorption measurements. It should be mentioned that our interpretation of transient absorption measurements was to a large extent supported by the data obtained from emission spectroscopy. Below, the spectra and kinetic curves of LRB are presented, followed by a study of solvent dependencies of transient absorption.

5.3.1. Low polar solvents

Transient absorption spectra of LRB in dioxane and in benzene are shown in Fig. 5.1:

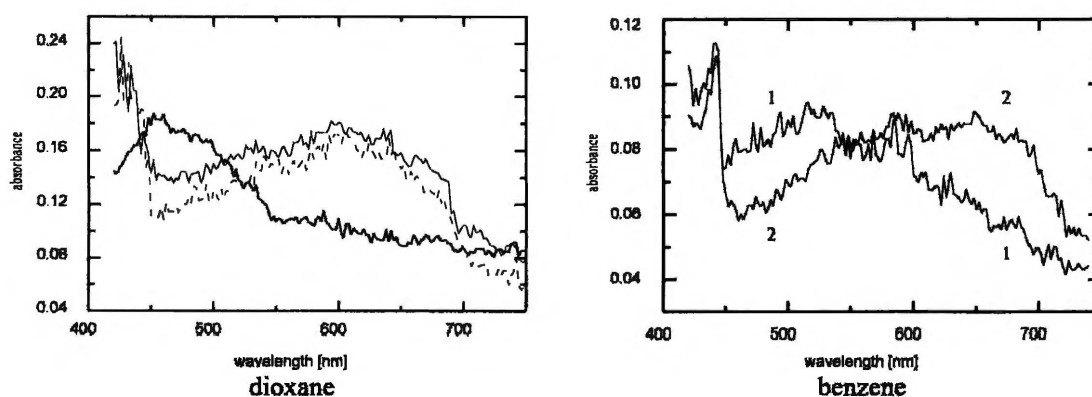


Fig. 5.1: Transient absorption spectra of LRB in dioxane (left side, $c = 4.9 \cdot 10^{-4}$ M, $T = 293$ K) recorded 1 ns (thick line), 20 ns (thin continuous line) and 60 ns (dashed line) after excitation, and in benzene (right side, $c = 1.2 \cdot 10^{-4}$ M, $T = 293$ K) recorded during the excitation (1) and 35 ns after excitation (2). Different excitation intensities were used while recording the spectra in different solvents. The samples were deoxygenated prior to the measurement. The samples were excited at 337 nm.

In both solvents the spectrum measured within 1 ns after excitation exhibits one band with a maximum in blue part of the spectrum (at 470 nm and at 510 nm in dioxane and in benzene, respectively). The spectra measured 60 ns (in dioxane) or 35 ns (in benzene) after the excitation pulse show this band slightly decreased and a new broad band arising at 600 nm - 620 nm in dioxane or at 650 nm in benzene. Kinetic curves recorded in these both bands¹⁶ show very clearly the course of absorption in particular band (Fig. 5.2). The curves observed at 452 nm exhibit a decay with decay time close to that of CT fluorescence, followed by a more or less constant absorption, which is to be ascribed to a long living intermediate state.

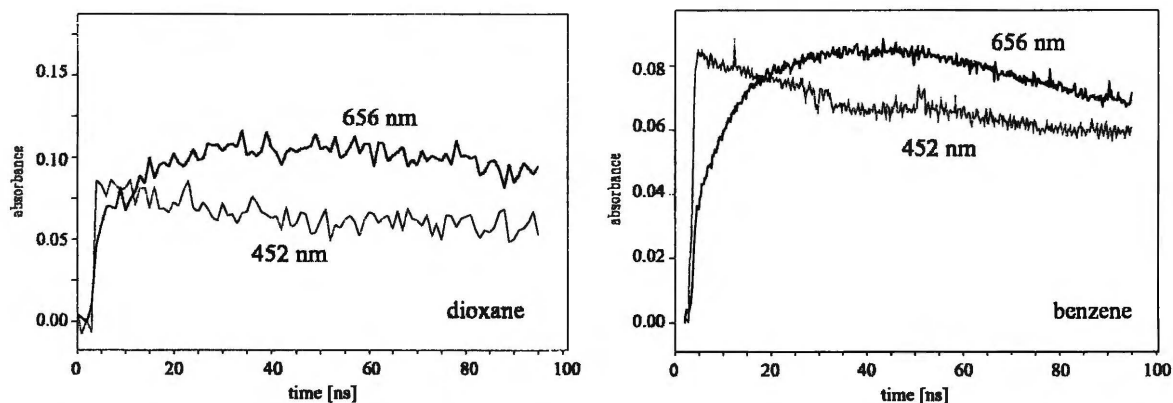


Fig. 5.2: Kinetic curves of transient absorption recorded for LRB at two different wavelengths: 452 nm and 656 nm (thick line) in dioxane (experimental points each 1 ns) and in benzene (experimental points each 0.2 ns) at 293 K. The samples were deoxygenated prior to the measurement.

The decay time of these species is much longer than the time scale of our transient absorption spectrophotometer. As only CT luminescence was observed upon excitation of LRB in these two solvents, one can conclude that absorption at 452 nm comes from the luminescent singlet state of L form ($^1L_{CT}$) (decaying part) and from a long living triplet state (constant background). Very interesting is a build up of absorption, **followed by a decay**, observed for curves recorded at 656 nm. This build up was recorded also in other low polar solvents (e.g. diethyl ether or dibutyl ether), but was not observed in more polar solvents (see below). The rise time of the transient absorption in low polar solvents could be always correlated with the decay time of fluorescence from the $^1L_{CT}$ state (cf. Fig. 5.2).

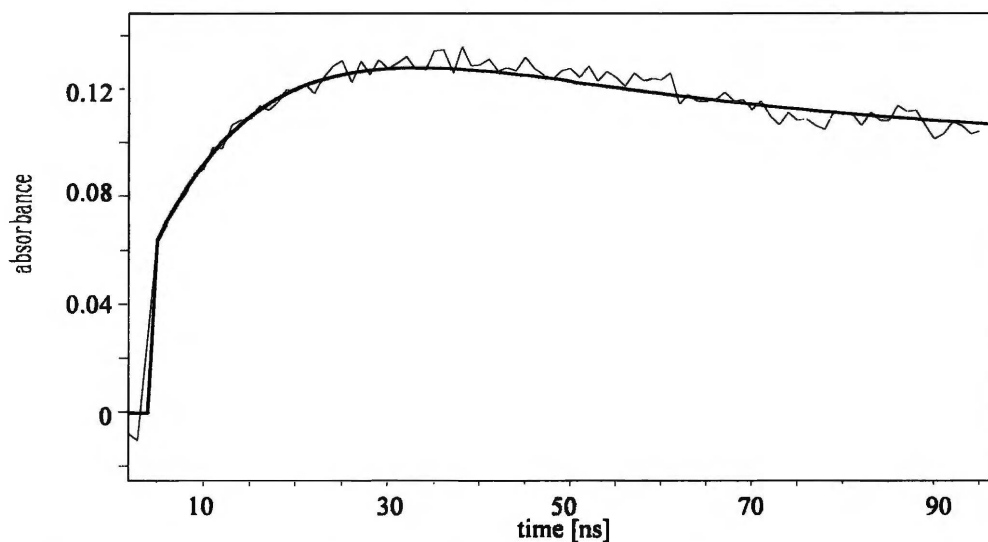


Fig 5.3: Transient absorption of LRB in dioxane measured at 656 nm together with a curve (thick line) simulating overlapping absorptions from: $^1L_{CT}$ state (decay time $\tau_1 = 14$ ns, $A_1 = 0.064$), $^3L_{CT}$ (rise time $\tau_1 = 14$ ns, decay time $\tau_2 = 34$ ns, $A_3 = 0.1$) and a long living triplet state built up with τ_1 (amplitude $A_2 = (A_1/\tau_1)/((1/\tau_2 - 1/\tau_1))$). Assignment and identification of these species are described below in Section 5.4.

In order to identify the species responsible for that effect, a simple fitting of the kinetic curve recorded for LRB in dioxane at 656 nm has been carried out. Such a course of kinetic curve suggests that at least three species are responsible for observed absorption: first one - decaying directly after excitation with τ_1 (appearing during the excitation pulse and

corresponding to the $^1L_{CT}$ state), second one - built up with a rise time equal to τ_1 and decaying with a decay time much longer than 100 ns (assumed to give a constant signal on the time scale of the measurement), and third one - built up with a rise time equal to τ_1 and decaying on the time scale of our instrument (Fig. 5.3)¹⁷. The assumption of minimum three absorbing species was necessary in order to account for the changes observed in the decay curves of LRB in weakly polar solvents. We have used a function $D(t)$:

$$D(t) = A_1 e^{-t/\tau_1} + A_2 (1 - e^{-t/\tau_1}) + \frac{A_1}{\tau_1} \frac{1}{\left(\frac{1}{\tau_1} - \frac{1}{\tau_2}\right)} (e^{-t/\tau_2} - e^{-t/\tau_1}) \quad (5.1)$$

describing transient absorption from these three species related to each other in the above way. Using the value $\tau_1 = 14$ ns (equal to the decay time of CT fluorescence measured for the LRB/dioxane system), a good fit was obtained with a decay time $\tau_2 = 34$ ns. This allowed us for an assumption that in low polarity solvents such as dioxane or benzene three species can be observed on nanosecond time scale after excitation of the LRB molecule: the $^1L_{CT}$ state, visualised by the decay of transient absorption observed at 452 nm, a state arising from the $^1L_{CT}$ state and decaying during tens of ns (tentatively denoted as $^3L_{CT}$ state), and a long living state, most probably the triplet state being a source of phosphorescence (as shown in the analysis in section 4.3, the triplet state of the **Z** form, denoted as 3Z_1). A more detailed identification of the second state will be carried out later in Section 5.4.

5.3.2. Polar aprotic solvents

Fig. 5.4 displays transient absorption spectra of LRB in butyronitrile recorded during the excitation pulse (spectrum marked by 0 ns), 1 ns and 45 ns after the excitation pulse. In butyronitrile, LRB emits dual fluorescence indicating occurrence of both the $^1L_{CT}$ and the 1Z_1 excited state. Transient absorption spectrum recorded during the excitation pulse exhibits a large band with a maximum at 460 nm that disappears almost completely within few nanoseconds.

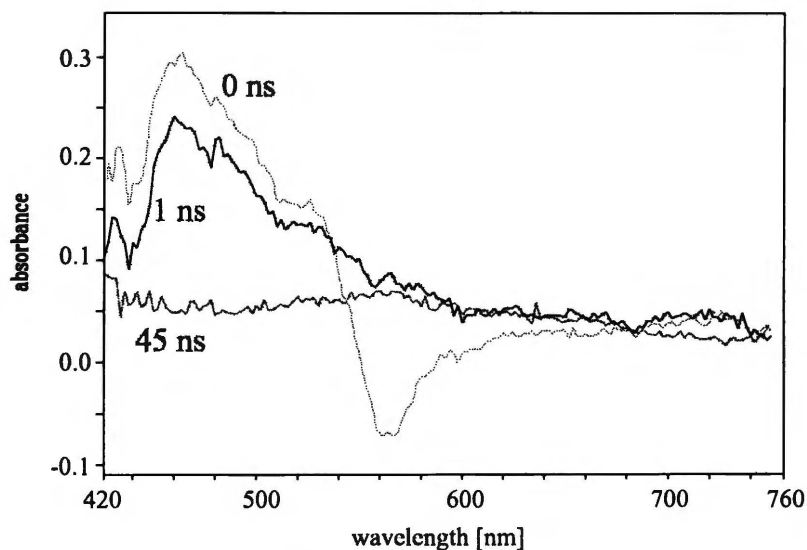


Fig. 5.4: Transient absorption spectra of LRB in butyronitrile recorded at various delay times: during the excitation pulse (FWHM = 0.6 ns) - 0 ns, 1 ns and 45 ns after excitation ($c=5.1 \cdot 10^{-4}$ M, $T=293$ K).

A negative absorption with a peak at 566 nm corresponds to a gain of the probing light. The gain occurs in the case of population reversal between the ground and the excited state (the population of the ground state of the **Z** form at $t = 0$ is equal to zero) and is due to a stimulated emission from the **Z** form. In Fig. 5.5, kinetic curves recorded for LRB solutions in butyronitrile and in acetonitrile at 568 nm (1) and 555 (2) nm, respectively, are presented. (Transient absorption spectra recorded in acetonitrile resemble those in BN). In nitriles the compound displays a double fluorescence. Probing light with the frequency resonant with that of the radiative transition between the excited (populated *via* excited state reaction) and the ground state (not populated) of the zwitterion (e.g. with $\lambda = 568$ nm) causes depopulation of the excited **Z** state and is amplified due to a stimulated emission from this state which is manifested by a "negative optical density". The decay times of the negative transient absorption correspond to the decay times of the excited **Z** state and are equal 0.7 ns (1) and 2.1 ns (2).

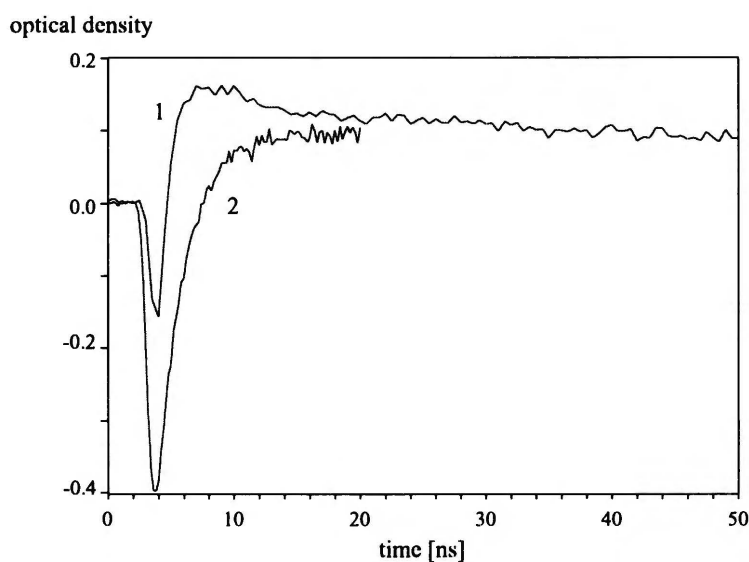


Fig. 5.5: Gain of the probing beam manifesting by a "negative" transient absorption for solutions of the lactone form of rhodamine B in butyronitrile (1, recorded at 568 nm) and acetonitrile (2, recorded at 555 nm). Curve 1 was recorded every 1 ns, curve 2 - every 0.2 ns. For each curve an appropriate interference filter was placed in front of the photodiodes measuring the intensity of the probing beam and the intensity of the fluorescence, in order to keep the fluorescence seen by each of these detectors as low as possible.

After few tens of nanoseconds, the transient absorption spectrum is rather not specific and has as a main feature a small band with a maximum at 560 nm - 565 nm (cf. Fig. 5.4). In contrast to non polar solvents, the spectra recorded for LRB solutions in BN or in AN do not reveal any significant build up of absorption above 600 nm. Before an attempt to interpret the spectra in polar solvents will be made, kinetic curves of transient absorption recorded at different wavelengths will be considered.

Fig. 5.6 presents kinetic curves of transient absorption recorded for the same sample of LRB in BN (not deoxygenated, which allows for comparison with decay times derived from the emission spectroscopy) in different regions of the transient absorption spectrum. An assumption has been made that absorption observed at a given wavelength is a sum of

absorptions from different species contributing to the recorded kinetic curve at a given delay time with different weights related to their concentrations and absorption coefficients.

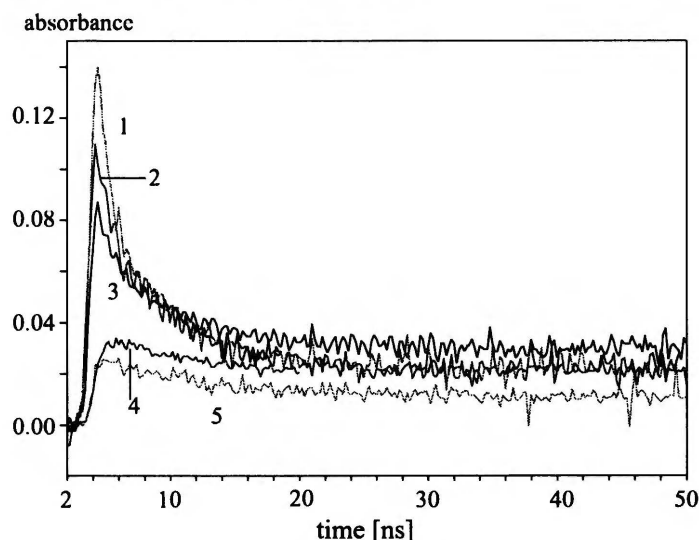


Fig. 5.6: Transient absorption kinetic curves of LRB/BN at various wavelengths: 1 - 433 nm, 2 - 477 nm, 3 - 525 nm, 4 - 656 nm, 5 - 700 nm ($c = 1.4 \cdot 10^{-4}$ M, $T=293$ K):

In order to identify the species responsible for the transient absorption bands of LRB in BN, kinetic curves were fitted with a monoexponential or with a two-exponential decay function, both of them having in addition a term describing an almost constant absorption signal at longer delay times as originating from a long living state formed with a rise time equal to the decay time used in the term (or in one of terms) describing the decay. Temporal width of the excitation pulse has been neglected (no deconvolution has been carried out). The functions were as follows:

$$\mathbf{M:} \quad D_m(t) = A_1 e^{-t/\tau_1} + A_2 (1 - e^{-t/\tau_1}) \quad (5.2)$$

$$\mathbf{D:} \quad D_d(t) = A_1 e^{-t/\tau_1} + A_2 (1 - e^{-t/\tau_1}) + A_3 e^{-t/\tau_2} \quad (5.3)$$

The results of the fitting have been collected in Table 5.2:

Table 5.2

Results of fitting of transient absorption kinetic curves of LRB in BN¹⁾:

No.	λ [nm]	Function	τ_1	τ_2	A_1	A_2	A_3
1.	433	$D_d(t)$	1.06	6.18	0.089	0.022	0.053
2.	477	$D_d(t)$	0.81	4.91	0.044	0.023	0.067
3.	525	$D_d(t)$	1.03	6.42	0.089	0.03	0.035
5.	700	$D_m(t)$		6.2	0.026	0.011	

¹⁾ Kinetic curve recorded at 656 nm is considered in section 5.3.3.

It has been found that none of the decays recorded in 420 nm - 540 nm region could be fitted with the monoexponential function $D_m(t)$. The decay times recovered from the above analysis using $D_d(t)$ function fall in two groups, first around 1 ns, and second around 6.2 ns.

These decay times correlate well with the fluorescence lifetime of the **Z** form (~ 0.7 ns) and the lifetime of the CT fluorescence (~ 5.8 ns) of LRB in butyronitrile, respectively. An elongation of the decay times recovered from transient absorption measurements can be explained by the fact that the fitting has been carried out assuming the excitation in a form of a delta function (without deconvolution of decays). The two decay times (1 ns and 6 ns) show clearly that the transient absorption band found in a polar solvent (in which a dual luminescence is observed) and decaying within few nanoseconds results from an overlap of transient absorption from both the $^1L_{CT}$ and the 1Z_1 excited state. A large contribution from zwitterion decay observed at 433 nm compared with those at longer wavelengths corresponds well to the data reported by Beaumont *et al.*³ or by Rylkov and Cheshev⁵ (see Table 5.1). On the other hand, relatively high contribution from the 1Z_1 state in decays monitored at 477 nm and at 525 nm (Table 5.2) is in contrast to the spectrum published by Beaumont *et al.* (ref. ³, Fig. 7), which shows very little absorption at these wavelengths. This cannot be caused by a multiexponential decay of the $^1L_{CT}$ state (the decay of L luminescence in BN could be very well fitted with a monoexponential function), and hence puts in doubt this region of their spectrum.

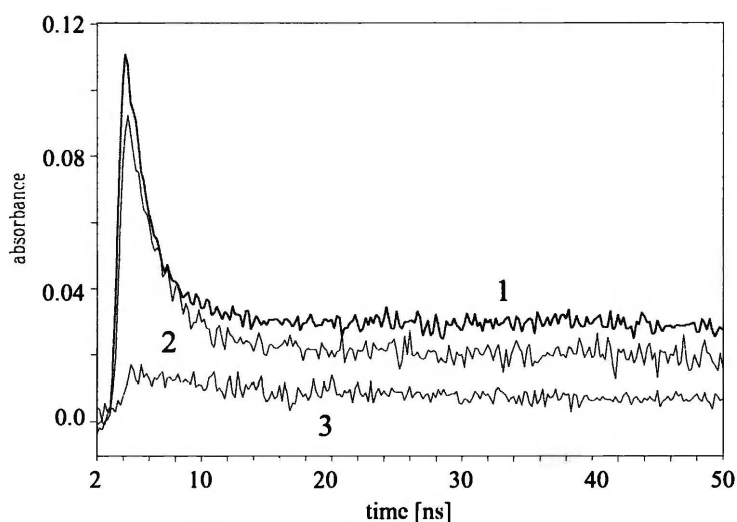


Fig. 5.7: Transient absorption kinetic curves of LRB/AN at various wavelengths: 1 - 477 nm (thick line), 2 - 525 nm, 3 - 700 nm ($c=1.0 \cdot 10^{-4}$ M, $T=293$ K):

Our data agree with the interpretation of transient absorption band of LRB in dimethylformamide by Vlaskin *et al.*⁶ who ascribed the band observed at 475 nm to absorption from the 1Z_1 state (though their spectrum shows small absorption at 430 nm - most probably due to low sensitivity of their detection system in this spectral region). Transient absorption kinetic curves recorded in AN (Fig. 5.7) and in DMF (almost no fluorescence from the $^1L_{CT}$ state in both solvents) within this thesis could be very well fitted with $D_m(t)$ function, which indicates that only the 1Z_1 state is present during the early period of the excited state process (on ns time scale). Although transient absorption spectra in AN and BN must differ due to a contribution from the $^1L_{CT}$ state in the latter solvent, a direct comparison of spectra was difficult due to a much higher intensity of the LRB fluorescence in AN, which cannot be

entirely accounted for by means of the photodiode measuring the fluorescence level (see description of TAN 2 nanosecond spectrophotometer in section 2.5), and caused deformation of the recorded spectrum. Measurements of transient absorption kinetic curves were not affected by the fluorescence light because of use of interference filters in front of the sample and are much more suitable for comparisons.

The absorption observed in polar solvents several tens of ns after excitation, comes most probably from the triplet state of the **Z** form and is discussed below in this Chapter. The absorption from the ground state of the zwitterion (formed upon e.g. radiative deactivation of the 1Z_1 excited state) was not observed, with the exception that a small maximum observed in BN at ~ 550 nm - 560 nm and at 545 nm in AN may be assigned to this transition (Fig. 5.4, spectrum recorded 45 ns after excitation). Very high transition moment (absorption coefficient above $10^5 \text{ M}^{-1}\text{cm}^{-1}$) for the absorption of zwitterion in the ground state would result in an intense absorption at 510 nm - 550 nm, provided that the zwitterion in the ground state occurs in the solution at the time of observation. As this absorption was not observed, we postulate that the **Z** form in the ground state reached in luminescence - converts very fast to the **L** form by a ring closure in the ground state.

The results described above allow us to conclude that in polar solvents at least three species may be observed in transient absorption measurements: (i) the $^1L_{CT}$ state, (ii) the 1Z_1 state, and (iii) a long living triplet state, most probably the 3Z_1 state.

5.3.3. Solvent effect on kinetics of the excited state process

In order to identify all intermediates occurring on the nanosecond time scale, a series of measurements of kinetic curves in various solvents has been carried out under the same conditions of excitation. The results of measurements at 656 nm and at 433 nm have been shown in Fig. 5.8 (a) and (b), respectively.

Table 5.3

Transient absorption of LRB as a function of the solvent, normalised to the ground state absorbance at the wavelength of excitation (337 nm):

Solvent	A*(656 nm, 0 ns)	A*(433 nm, 0 ns)	A*(656 nm, 15 ns)	A*(433 nm, 45 ns)
Dioxane	.195	.367	.325	.286
Diethyl ether	.164	.443	.375	.70
Dimethoxyethane	.181	.323	.222	.269
Butyronitrile	.090	.413	.076	.102
Pyridine	.078	.471	.072	.071
AN	.026	.602	.047	.067
DMF	.0003	.561	.0386	.104

The curves presented in Fig. 5.8 have not been normalised to the absorption of the sample at the excitation wavelength (337 nm), so it is difficult to compare them directly. Table 5.3 shows transient absorption values recorded at the peak of excitation pulse (marked

as "0 ns", which corresponds to $t = 4.6$ ns and to $t = 4.4$ ns at 656 nm and at 433 nm, respectively, on the time scale of TAN2 spectrophotometer) as well as the absorption values 15 ns and 45 ns after the excitation normalised to the ground state absorption of individual samples at 337 nm (A^* values). Such a presentation allows one to compare the populations of states giving rise to absorption at the corresponding wavelengths.

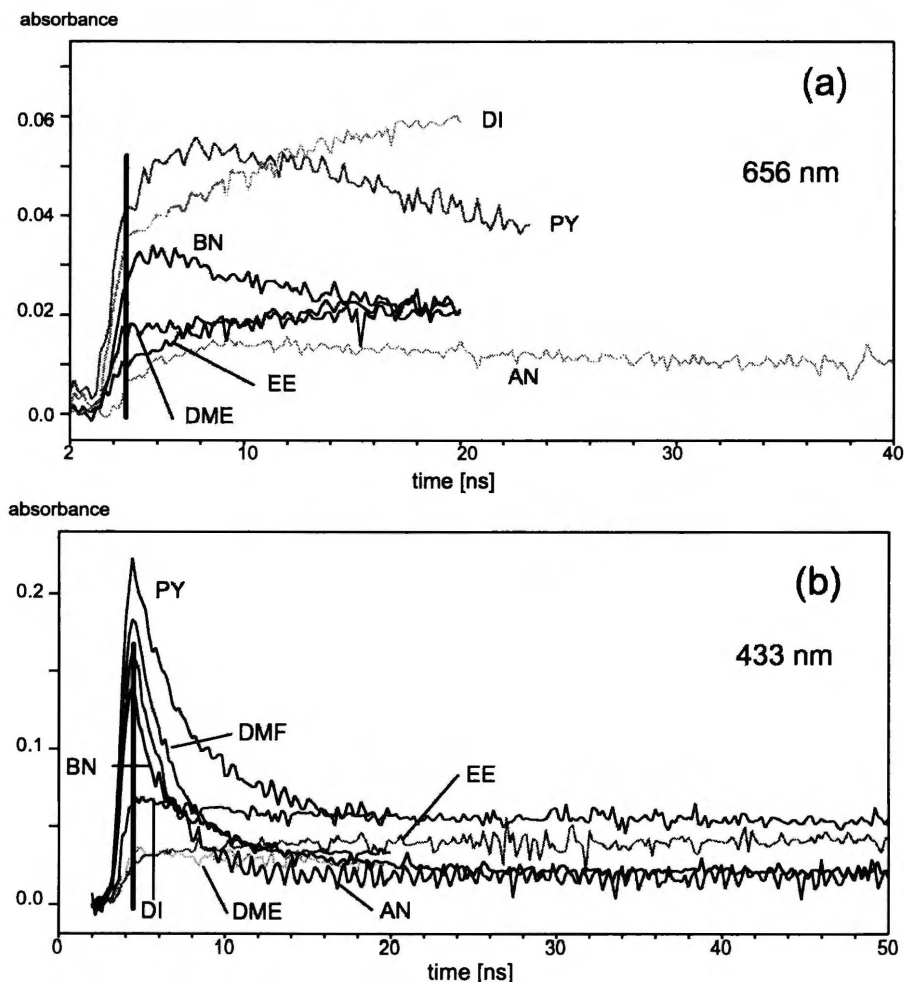


Fig. 5.8: Solvent effect on kinetic curves of transient absorption of LRB measured at $\lambda_{\text{obs}} = 656$ nm (a) and at $\lambda_{\text{obs}} = 433$ nm (b). Thick vertical line symbolises the excitation pulse (FWHM = 0.6 ns). Solvents: AN - acetonitrile, BN - butyronitrile, DI - dioxane, DME - dimethoxyethane, DMF - dimethylformamide, EE - diethyl ether, PY - pyridine. The curves have not been normalised to the absorption of the sample at the nitrogen laser line (337 nm).

While transient absorption measured at 433 nm does not exhibit large variations in different solvents, both at 0 ns delay and at longer delay times, the solvent significantly modifies kinetic curves recorded at 656 nm. The change between the low polar and the highly polar solvents exceeds 1 order of magnitude for absorption measured at 0 ns (bold values in Table 5.3). Low values of A^*_{656} in polar solvents are not due to a transient absorption gain observed in these solvents (tail of the fluorescence spectrum from the **Z** form, see e.g. Fig. 4.12) as similar differences were found for kinetic curves recorded at 700 nm. Where then such a large difference does come from? Below two possible reasons are discussed:

- (i) If at $\lambda = 656$ nm absorption from a **primary excited state** (i.e. the state reached after a fast vibrational relaxation) is observed, then different values A^*_{656} would indicate that

this state is much more preferentially populated in absorption from the ground state in dioxane ($A^*_{656} = 0.195$) than in AN ($A^*_{656} = 0.026$). Then one has to assume that the first absorption band of the lactone ground state consists of more than one electronic transition and one of these transition selectively populates the state absorbing at 656 nm. A consequence of such an assumption would be so, that the absorption to that state decreases (or shifts?) dramatically with solvent polarity (cf. AN and DMF). This is, however, difficult to accept in view of the absorption spectrum from the ground state. The absorption band(s) exhibits a bathochromic shift with increasing solvent polarity, and the above assumption would require a hypsochromic shift of the band giving rise to the state absorbing at 656 nm in excited state absorption (i.e. absorption to that state would be much larger in e.g. ethyl ether than in acetonitrile), and this is difficult to accept (also in view of a possible CT character of the transition).

- (ii) The absorption monitored at $\lambda = 656$ nm (at $t = 4.6$ ns on the time scale of the spectrophotometer) is to be assigned to a **state being a product of a very fast** (on the nanosecond time scale) **excited state process**. The probability of such a process would strongly decrease with increase of solvent polarity, as much less of its product is observed in more polar solvents ($A^*_{\text{Diox}} = 0.195$, $A^*_{\text{AN}} = 0.026$).

I believe the case (ii) applies and the differences in transient absorbance at 656 nm prove that the absorption observed at the beginning (on the ns-time scale) comes already from a product of an excited state reaction. Although the above analysis enables one to draw a conclusion on such a fast excited state process on the basis of the data from nanosecond transient absorption spectroscopy, this question deserves further experimental investigation on a much shorter time scale. Possible nature of this fast process is discussed in more detail in the following section.

The normalised absorption measured at 433 nm during the excitation pulse (second column of Table 5.3) reflects the changes in population of the $^1L_{\text{CT}}$ and the 1Z_1 excited states, as both of them intensely absorb at that wavelength. Increase of A^*_{433} in line with solvent polarity ($A^*_{\text{diox}} = 0.367$, $A^*_{\text{AN}} = 0.602$) is a consequence of higher contribution from the zwitterion singlet state resulting from its longer lifetime and a larger stabilisation in more polar solvents as well as (most probably) a larger absorption coefficient of the **Z** form.

The third column of Table 5.3 applies rather to low polar solvents, as it reflects the population of species formed in these solvents with the rise time equal to the decay time of the $^1L_{\text{CT}}$ state. Absorption at 656 nm at $t = 15$ ns after excitation is up to 10 times (cf. diethyl ether and DMF) less in polar solvents which means that the product of deactivation of the $^1L_{\text{CT}}$ state ($^3L_{\text{CT}}$) is not formed in these solvents.

The most right column of Table 5.3 shows the changes in population of long living triplet states. For their identification the reader is referred to the following section.

5.4. The excited state process - conclusions from transient absorption study

In this section an attempt is made to assign individual transitions occurring in transient absorption to species involved in the excited state reactions, to construct a picture of the entire relaxation process and to extract possible relations between various excited states of different molecular species. As concluded in previous section, the species observed in transient absorption measurements on a nanosecond time scale must be already products of a rapid excited state relaxation. A key to investigate this issue are differences in kinetic curves of transient absorption observed at 656 nm. At $t = 0$ (i.e. at the moment of the excitation pulse) there is very little absorption at that wavelength in such solvents like AN or DMF. On the other hand, the solutions of LRB in these solvents show a large absorption at 433 nm and emit an intense fluorescence from the 1Z_1 state. The decays of transient absorption of LRB in AN or DMF at 433 nm could be very well fitted as monoexponential ones with decay times well matching those of Z fluorescence (e.g. for AN: $\tau_{\text{flu}} = 2.1$ ns, $\tau_{\text{abs}} = 2.2$ ns), which implies that population of the $^1L_{\text{CT}}$ state in AN is very low (as opposed to BN where the population of the $^1L_{\text{CT}}$ state had to be taken into account in fitting the kinetic curves of transient absorption recorded at 433 nm, cf. Table 5.2). This indicates that in a highly polar environment, at 656 nm the 1Z_1 state does not absorb and consequently the absorption recorded at " $t = 0$ " at that wavelength is a fingerprint of another product of rapid relaxation of the lactone molecule. The natural choice would be the $^1L_{\text{CT}}$ state. However, in view of an efficient and apparently solvent independent population ($\sim 23\%$ in the case of LR101 in several solvents - see section 3.3.3, and 24% in the case of LRB in AN - calculated by analogous method to that from section 3.3.3) and subsequent very fast deactivation of the 1Z_1 state, the excess of absorption at 656 nm (measured at $t = 0$) in low polar solvents compared with highly polar ones may result from products of fast deactivation of the zwitterion. Ultimate products of that deactivation may be the triplet states of both forms: $^3L_{\text{CT}}$ (lactone) and 3Z_1 (zwitterion), where the latter - in addition - may be formed in a fast ISC process involving an upper excited state of the Z form. Hence, possible sources of transient absorption observed at 656 nm at $t = 0$ are: the $^1L_{\text{CT}}$ state, the $^3L_{\text{CT}}$ state and the 3Z_1 state, as none of the ground states absorbs at 656 nm and no other photoproducts (e.g. radical ions resulting from a reaction with the solvent) could be expected.

Kinetic curves of transient absorption recorded at 656 nm in solvents, where LRB displays dual luminescence (e.g. in butyronitrile or in pyridine) may be very helpful in approaching the problem. At the peak of the excitation pulse they show certain absorption (see Fig. 5.8 (a) and Table 5.3) and subsequently they exhibit a fast build up followed by a decay to a constant absorption background. Kinetic curves of transient absorption in both solvents could be well described assuming that they represent a depopulation with a decay time equal to that of the $^1L_{\text{CT}}$ state (τ_L) overlapped with a build up with the rise time equal to the decay time of the 1Z_1 state. This allows us to conclude that at 656 nm both the $^1L_{\text{CT}}$ state and the products of radiationless deactivation of the 1Z_1 state absorb. In BN, the former is responsible for the absorption appearing "immediately" with the excitation pulse while the latter are built

up with the rise time equal to the decay time of the 1Z_1 state. The hypothesis on (non-luminescent) products of radiationless zwitterion deactivation is also in agreement with results from emission spectroscopy, as both observed (**L** and **Z**) luminescences start to be emitted immediately on the sub-nanosecond time scale and the rise observed in transient absorption kinetic curve is to be ascribed to a build up of non-luminescent species. The function used in fitting describes an overlapping absorption from the $^1L_{CT}$ state (decay with τ_L) and a build up of the product of the 1Z_1 excited state deactivation (with a rise time τ_Z) that persists for a much longer time compared with the time accessible with TAN 2 nanosecond spectrophotometer. On the other hand, under very polar conditions (e.g. AN, DMF) where very little or no luminescence from the $^1L_{CT}$ state is observed, only build up with a rise time equal to τ_Z was observed at 656 nm (cf. Fig. 5.8 a). On the basis of this relationship between the rise time of this transient absorption and the decay time of **Z** luminescence it is to be concluded that the absorption observed in more polar media at 656 nm comes from the triplet state of the **Z** form (3Z_1). This is also supported by the existing data on $T_1 \rightarrow T_n$ transient absorption (see Table 5.1), suggesting occurrence of a $T_1 \rightarrow T_n$ absorption band in 620 nm - 640 nm region. Thermally activated nature of this deactivation would suggest that population of the 3Z_1 state must follow a transition to a higher triplet state (e.g. proceed on the route $^1Z_1 \rightarrow ^3Z_x \rightarrow ^3Z_1$).

The triplet states observed in non-polar and in polar solvents may be populated on two routes: directly as products of an ISC process from a higher, non relaxed electronic or vibrational level, and indirectly as products of the above mentioned intramolecular quenching of the 1Z_1 excited state, which was shown to be very efficient process in less polar solvents (see Chapter 3 and 4). Both the direct and the indirect route must be fast processes. Let us consider this problem in the following way:

Transient absorption kinetic curves exhibit at longer delay times - both in less polar and in highly polar solvents - a non decaying signal which indicates a presence of long living species (with a lifetime significantly exceeding the time scale of our instrument). Their occurrence in highly polar solvents (e.g. AN or DMF), where almost no $^1L_{CT}$ state is formed (as judged from fittings of transient absorption decays collected at 433 nm and from very low quantum yields of the **L** luminescence) indicates that they are triplet states of the zwitterion form (3Z_1). This is supported by the fact that the formation of the lactone triplet state ($^3L_{CT}$) from the 1Z_1 excited state - in addition to the change of multiplicity - would involve a ring closure reaction with very little energy loss or perhaps even with some activation energy, as the $^1L_{CT}$ and the $^3L_{CT}$ should be energetically degenerated, and the 1Z_1 state must be close to the $^1L_{CT}$ state in highly polar solvents. As such a ring closure is rather not possible, we postulate that the absorption occurring at longer delays (constant signal) comes from the 3Z_1 state both in polar and in non polar solvents. The absorbance measured in BN, PY, AN and DMF at 433 nm, 45 ns after excitation (Table 5.3) decreases with increasing solvent polarity (and with increase of the observed quantum yield of **Z** luminescence). Assuming that the $^3L_{CT}$ state is not significantly populated in these solvents, this would mean that a more efficient

triplet population would occur in line with higher quenching efficiency of the 1Z_1 state and with its shorter decay time (e.g. $A^*(433 \text{ nm}, 45 \text{ ns}) = 0.076$, $\tau_Z = 0.66 \text{ ns}$ in BN against $A^*(433 \text{ nm}, 45 \text{ ns}) = 0.047$ and $\tau_Z = 2.1 \text{ ns}$ in AN). Although more quantitative and - especially - temperature dependent data would be required, this finding is a strong evidence supporting the $^1Z_1 \rightarrow ^3Z_x$ transition as the quenching mechanism of the 1Z_1 excited state. The experimental data collected within this thesis and the time resolution of transient absorption measurements available with TAN 2 nanosecond spectrophotometer did not allow us to answer the question about the formation route of the 3Z_1 state, i.e. whether (i) it is exclusively populated on a direct $^1Z_1 \rightarrow ^3Z_1$ route (possibly via 3Z_x state) or whether (ii) an ISC process involving higher excited (both singlet and triplet) states occurs. The latter possibility cannot be excluded especially in view of some suggestions postulating for rhodamines an efficient ISC process from higher excited singlet states (see section 5.2 of this Chapter) in connection with the fact that excitation of the lactone molecule in its first absorption band (at $\sim 31500 \text{ cm}^{-1}$) provides it with a large excess of energy compared with the lowest excited singlet and the triplet state of the Z form (17500 cm^{-1} and 14850 cm^{-1} in the case of LRB, respectively). The concept of the direct route of triplet state formation ($^1Z_1 \rightarrow ^3Z_1$, via 3Z_x state) is, however, strongly supported by the fact that this state is built up with a rise time matching the decay time of the 1Z_1 state in a given solvent. It is to be pointed out that - in addition to the phosphorescence spectra (at low temperatures) - transient absorption measurements prove an efficient formation of the triplet state in the Z form of rhodamines (at room temperature). The efficiency of population of the zwitterion triplet state upon excitation of the lactone molecule is by orders of magnitude higher than that observed in alcohols¹⁴ and most probably is to be ascribed to the energy excess mentioned above and to the solvent effect on the relative energy level positions (discussed in detail in Chapter 6). Also the conformation of the lactone molecule to be excited (non-planarity of the xanthene part) may be another factor enhancing spin-orbit coupling and thus leading to an increase of the efficiency of triplet population. Extensive measurements of transient absorption as a function of temperature are needed in order to investigate the mechanism of this reaction more thoroughly.

A very important question is connected with a broad absorption band built up in less polar solvents such as hexane, dibutyl or diethyl ether, dioxane and benzene (see Fig. 5.1) with a maximum at 600 nm - 630 nm. The rise time of this absorption was found equal to the decay time of the L fluorescence in corresponding solvents, which unambiguously proves a parent-daughter relationship between the species built up and the $^1L_{CT}$ state. The state under consideration decays then within tens of nanoseconds and its decay was found much shorter in hexane than in benzene or dioxane. This state cannot be a local triplet state of any of two perpendicular moieties forming the lactone molecule (i.e. diethylaminoxanthene or phthalide) as both possible triplets are energetically much higher than the $^1L_{CT}$ state. The energy of the phthalide triplet state is larger than 25000 cm^{-1} ¹⁸, which is also close to a lowest estimation for the diethylaminoxanthene triplet state (23500 cm^{-1})¹⁹, so they would be hardly accessible from the $^1L_{CT}$ state in dioxane (maximum of fluorescence at $\sim 21000 \text{ cm}^{-1}$) at room

temperature. Also dramatic dependence of appearance and decay of this band on the solvent is an argument against a local nature of the state being its source. On the basis of these arguments we postulate that this state is an **intramolecular charge transfer triplet state** of the lactone molecule (${}^3L_{CT}$) i.e. that with the lactone ring closed and the charges separated between the xanthene and the phthalide part of the molecule. It is to be noted that CT nature of this state would result in a strong dependence of its energy on the solvent polarity, which in turn will influence population efficiency of this state. Results of preliminary temperature dependent transient absorption measurements of LRB in butyl acetate show an increase of ${}^3L_{CT}$ population with increase of temperature (decrease of polarity).

The shapes of kinetic curves of transient absorption recorded in less polar solvents at 433 nm show also that the efficiency of population of the ${}^3L_{CT}$ state seems to increase with decrease of polarity (slight decay in dioxane or in DME and a build up in ethyl ether, Fig. 5.8 (b)). However, in solvents of lowest polarity, such as hexane or cyclohexane, another mechanism of deactivation of the ${}^1L_{CT}$ state may be operative, namely a transition to a local triplet state within the lactone molecule (fluorescence maximum in cyclohexane is at $\sim 25000\text{ cm}^{-1}$).

In a summary of transient absorption study described in detail in this Chapter it is to be concluded that a change of medium allows to observe different transients occurring in photophysics of LRB. In the case of a low polar solvent these are: ${}^1L_{CT}$, ${}^3L_{CT}$ and 3Z_1 states, and in highly polar solvents - 1Z_1 and 3Z_1 states. A more detailed insight in possible links between these states, especially on the triplet level requires further investigation.

References and notes

- 1 P. R. Hammond, *I.E.E.E. J. Quantum Electron.* **QE-15** (1979) 624
- 2 D. Magde, S. T. Gaffney and B. F. Campbell, *I.E.E.E. J. Quantum Electron.* **QE-17** (1981) 489
- 3 P. Beaumont, D. G. Johnson and B. J. Parsons, *J. Chem. Soc. Faraday Trans.* **89** (1993) 4185
- 4 A. Penzkofer, W. Falkenstein and W. Kaiser, *Chem. Phys. Lett.* **44** (1976) 82
- 5 V. V. Rylkov and E. A. Cheshev, *Opt. Spekr.* **63** (1987) 778
- 6 V. I. Vlaskin, A. J. Gorolenko, S. V. Melnitchuk, N. Nizamov, S. A. Tichomirov and G. B. Tolstorozev, *Dokl. Akad. Nauk* **302** (1988) 1141
- 7 U. Krüger and R. Memming, *Ber. Bunsenges. Phys. Chem.* **78** (1974) 679
- 8 A. V. Aristov and Y. C. Maslyukov, *Izvest. Akad. Nauk SSSR Ser. Fiz.* **42** (1978) 524
- 9 V. V. Rylkov and E. A. Cheshev, *Opt. Spekr.* **63** (1987) 1030
- 10 A. Dunne and M. F. Quinn, *J. Chem. Soc. Faraday Trans. 1* **73** (1977) 1104
- 11 Occurrence of this photoproduct was also reported in: B. Stevens, R. R. Sharpe and W. S. W. Bingham, *Photochem. Photobiol.* **6** (1967) 83
- 12 V. E. Korobov, U. V. Shubin and A. K. Chibisov, *Chem. Phys. Lett.* **45** (1977) 498
- 13 V. E. Korobov and A. K. Chibisov, *J. Photochem.* **9** (1978) 411

-
- ¹⁴ R. N. Nurmukhametov, N. I. Kunavin and G. T. Khachaturova, *Izvest. Akad. Nauk SSSR Ser. Fiz.* **42** (1978) 517
- ¹⁵ A. V. Butenin, V. V. Gavriluk, B. Ya. Kogan and T. A. Mironova, *Opt. Spekr.* **67** (1989) 342
- ¹⁶ Kinetic curves of transient absorption were recorded using interference filters in order to minimise the level of fluorescence emitted by the sample and reaching the photodiodes.
- ¹⁷ Temporal width of the excitation pulse was neglected.
- ¹⁸ I. L. Belaitz and R. N. Nurmukhametov, *Zh. Fiz. Khimii* **44** (1970) 29
- ¹⁹ See the discussion of the nature of phosphorescing triplet state in section 4.3.

CHAPTER 6

DISCUSSION OF RESULTS

6.1. Ground state equilibria

The lactone form is a less known but a peer partner of both ground and excited state equilibria of rhodamines. It is the only form of rhodamines (apart from aggregates) which occurs in less polar aprotic solvents. In contrast to the earlier work¹, it has been found in this thesis that in well purified polar aprotic solvents (e.g. acetonitrile) the $L \rightleftharpoons Z$ equilibrium is so strongly shifted towards the lactone that no absorption in the visible could be detected even in concentrated (e.g. 10^{-3} M LRB in butyronitrile) lactone solutions. Appearance of a colour resulted from formation of cations due to presence of trace amounts of protic impurities. The lactone molecule could be even used as an indicator of solvent proticity (at least in the case of rhodamine B) monitored by absorption intensity of the cation absorption band. The shift of $L \rightleftharpoons Z$ equilibrium towards the lactone in aprotic solvents is in accordance with conclusions of earlier investigations² postulating hydrogen bonding as a necessary condition for stabilisation of the **Z** form. In view of the results for LR101 obtained in this thesis, the presence of the zwitterion resulting from a possible equilibrium with the lactone form in the ground state (cf. section 3.1.1) cannot be excluded. Furthermore, free enthalpy change, ΔG^0 , of the $L \rightleftharpoons Z$ equilibrium is strongly dependent on solvent polarity, as the ground states of both forms are differently stabilised by the solvent, and a significant increase of ΔG^0 on lowering solvent polarity may be expected. Higher degree of alkylation of the amino group (which corresponds to a lower oxidation potential of the xanthene moiety) most probably contributes to a larger stabilisation of the **Z** form.

Fluorescence spectra reveal that on the excited state level, both the **Z** and the **L** form can occur simultaneously in aprotic solvents, and an increase of solvent polarity results in a higher stabilisation of the excited singlet state of the **Z** form. In the excited state, hydrogen bonding seems to be apparently not necessary for the existence of the zwitterion. Instead, the solvent provides the stabilisation of the **Z** form via its dielectric and polarisability properties. Before attempting to consider the question of mutual coexistence of the **L** and the **Z** form in their excited states a question of their formation upon excitation of the lactone molecule must be addressed.

6.2. Primary excited state process

The lactone molecule can be considered as being composed of two mutually perpendicular π -electronic subsystems which are approximately non-interacting in the ground state: the dialkylaminoxanthene part and the phthalide part. High sensitivity of the fluorescence spectra to solvent polarity and a very large Stokes shift observed even in low polar solvents imply that a photoinduced electron transfer reaction in the excited state must be

involved. The free energy of the electron transfer reaction in the excited state from the xanthene to the phthalide part, ΔG^0 , may be estimated by means of Weller's equation³:

$$\Delta G^0 = E(D^{+\bullet} / D) - E(A / A^{-\bullet}) - \frac{e^2}{\epsilon d} - E_{00} \quad (6.1)$$

where $E(D^{+\bullet} / D)$ is the oxidation potential of the donor, $E(A / A^{-\bullet})$ - the reduction potential of the acceptor, $e^2/\epsilon d$ - the energy of Coulombic interaction between the two radical ions, and E_{00} - the energy of zero-zero transition in the molecule.

Using the data shown in Table 6.1, free energy change, ΔG^0 , of electron transfer reaction may be calculated (the most right column of Table 6.1).

Table 6.1

Free energy of electron transfer reaction in lactone forms of rhodamines in acetonitrile

Lactone	$E(D^{+\bullet} / D)$ ¹⁾ [eV]	$E(A / A^{-\bullet})$ ²⁾ [eV]	E_{00} ³⁾ [eV]	d Å	$e^2/\epsilon a$ ⁴⁾ [eV]	ΔG^0 [eV]
LRMET	0.78	-2.11	3.69	5	0.08	-0.88
LRB	0.75	-2.11	3.65	5	0.08	-0.87
LR101	0.56	-2.11	3.56	5	0.08	-0.97

1) assumed according to ref. ⁴, potentials were measured versus SCE.

2) taken from ref. ⁵

3) a value corresponding to 10% of absorbance in acetonitrile at the absorption maximum was assumed

4) Coulomb term in acetonitrile

In solvents less polar than AN, Coulomb term will be much higher due to a lower ϵ value, the difference $E(D^{+\bullet} / D) - E(A / A^{-\bullet})$ will, however, increase⁶ and the resulting change in ΔG^0 would be not significant. Such an exothermicity - close to 1 eV - would result in a **rapid electron transfer** from the xanthene to the phthalide part of the molecule and a **non-relaxed charge transfer state will be populated**. This state could be either a higher electronically excited state of one of the radical ion parts of the molecule or a highly vibronically excited charge transfer state being after relaxation a source of the observed luminescence. Since electron transfer preferentially occurs with a small change of the vibrational quantum number and with larger FC factors⁷, it is proposed that the first scenario applies. We suspect that this state (hereinafter referred to as L_{CT}^*), and not that one achieved directly upon excitation, is a starting point for subsequent steps. Such a hot, non-relaxed state was previously suggested by Klein and Hafner⁸ and by Grigoryeva *et al.*⁹. The former authors postulated occurrence of this intermediate state on the basis of the analysis showing a deviation from the Strickler-Berg equation, while the latter used the fact that the decay time of the excited Z form in chloroform (product of photodissociation) was much shorter than that of the ${}^1L_{CT}$ state (possible precursor). Investigating transient absorption of LRB in various solvents it has been shown in this thesis that the species observed (with the time resolution of 1 ns) during the exciting pulse have already been formed in a fast excited state relaxation process, which yields products depending on the solvent. Ultimate products of this process (as observed on a nanosecond time scale) at room temperature are the L and the Z form in their

excited states which are sources of the luminescence ($^1L_{CT}$ and 1Z_1). In the paper¹⁰ it has been differentiated between the cases where only L fluorescence and those where double fluorescence is displayed, and assumed that in the case of single L fluorescence there occurs only vibrational relaxation to the emitting CT state and the zwitterion state is not formed. The same conclusion was drawn by Klein and Hafner⁸. Present results allow us, however, to postulate that the branching in two routes of deactivation of this transient state (i.e. leading to the $^1L_{CT}$ and to the 1Z_1 state) occurs always - before the final vibrational relaxation takes place, and the lack of zwitterion fluorescence in less polar solvents is caused by a very efficient intramolecular quenching of Z form in these media (see below). This allows us to conclude that in transient absorption measurements, at $t = 0$ ns (i.e. within the excitation pulse with FWHM of 0.6 ns), products of this quenching reaction must be observed (at least under conditions where efficient quenching occurs).

A question of primary importance connected with occurrence of the two deactivation channels is, which are the factors determining the branching into these channels and what are efficiencies of population for individual excited states populated on that deactivation? An important indication for the nature of these factors is the independence of the population efficiency of the zwitterion of the solvent (see section 3.3.3), which might suggest that the partition in two reaction paths occurs beyond the control of the medium, and thus faster than the medium could respond (i.e. in a time shorter than the dielectric relaxation time of the solvent). As a consequence, the partition would have to be controlled by intramolecular factors, most probably of vibronic nature. This is in part supported by the results obtained by Vlaskin *et al.* who investigated transient absorption of LRB and narrowed down the time after which the dissociation reaction and the building up of the Z form has occurred, to 1 ps¹¹. On the other hand, the population of the $^1L_{CT}$ state seems to depend on the solvent, as indicated by transient absorption spectroscopy for rhodamine B, where population of $^1L_{CT}$ in AN is very low as opposed to BN, where it had to be taken into account in fitting of the kinetic curves of transient absorption (see Chapter 5). However, population efficiency of the $^1L_{CT}$ state represents - at least at low temperatures - a small portion (e.g. 3% for LR101 in MTHF) in the entire deactivation balance, and the main deactivation channel is the photoinduced dissociation. Detailed investigation of this problem would require application of spectroscopic methods with picosecond and subpicosecond time resolution.

6.3. Diagram of energy levels

For the purposes of the following discussion it is necessary to construct a diagram describing all energy levels and transitions occurring in the lactone molecule after the excitation. Such a diagram is shown in Fig. 6.1. Apart from the ground (L_0) and the Franck-Condon state (L_{FC}^* , achieved upon excitation) of the lactone form, this diagram contains the states that have been detected either by emission ($^1L_{CT}$, 1Z_1 , 3Z_1) or by transient absorption ($^3L_{CT}$, 3Z_1) spectroscopy. In addition, a virtual state (L_{CT}^*) reached on electron transfer

reaction and representing a non-relaxed ion pair (see section 6.2), and the ground state of the zwitterion (Z_0) have been included.

It has been shown in the foregoing chapters that relative positions of individual energy levels on the energy scale are very sensitive to solvent polarity. Assuming L_0 as the relative zero-energy level of the entire molecular system, on the ground state level, it might be expected that the position of the Z_0 state is a strong function of solvent polarity as the free enthalpy change, ΔG^0 , of the $L \rightleftharpoons Z$ equilibrium is strongly dependent on solvent polarity (see Chapter 3). The energy of the ${}^1Z_1 \rightarrow Z_0$ transition exhibits very moderate solvent dependence, as this transition occurs within the xanthene moiety, without any significant change of the dipole moment. This independence of transition energy of the solvent, connected with a strong dependence of the position of Z_0 level results in a strong solvent polarity dependence of the energy of the 1Z_1 state as measured in respect to the L_0 state.

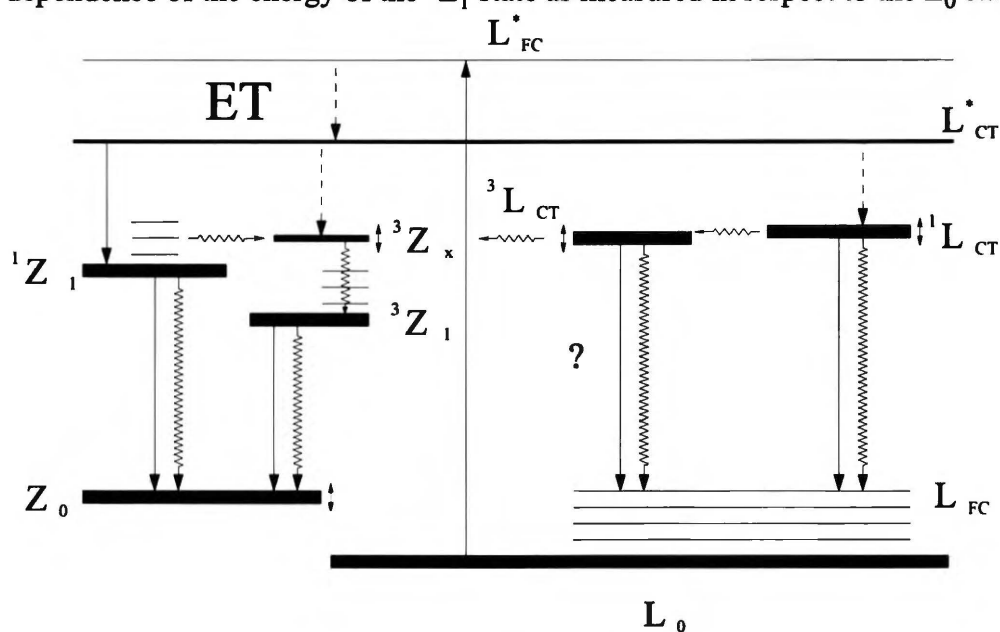


Fig. 6.1: Energy levels diagram of a rhodamine molecule. Double arrows placed at some levels indicate particular dependence of the positions of these levels on the polarity of the solvent. ET indicates the primary electron transfer reaction.

The ${}^1L_{CT}$ state is a charge transfer state with a large dipole moment, and its energy (in relation to L_0) is significantly stabilised by a more polar environment. The same happens with the triplet charge transfer state, ${}^3L_{CT}$, as it is practically energetically degenerate with the ${}^1L_{CT}$ state. The influence of solvent polarity on the position of triplet levels of the Z form is more difficult to estimate on the basis of the available experimental data, it is to be pointed out, however, that in LRB the phosphorescence maximum exhibits a red shift with increase of solvent polarity (see section 4.3). In addition, the 3Z_1 state can have orbital character different from the 1Z_1 state, which would result in a different dependence of the energy of 3Z_1 state (and also of higher triplet states of the Z form) on solvent polarity than that of the 1Z_1 state. Moreover, in view of the available experimental data¹² (also cf. section 5.2.2) and the results of theoretical calculations¹³⁻¹⁴, higher excited states of the Z form have to be considered because of their possible participation in the excited state process. The mechanism of

intramolecular radiationless deactivation on the $S_1 \rightarrow T_2$ route is e.g. well known for some heterocyclic anthracene derivatives and has been studied in detail for the N-substituted acridones¹⁵, where the authors have correlated the activation energy for the $S_1 \rightarrow T_2$ transition with a solvent polarity parameter (acceptor number of the solvent)¹⁶.

Theoretical work by Artyukhov¹³⁻¹⁴, almost unknown in the English language literature, may be very helpful in interpretation of the excited state process occurring in the rhodamine lactones on the "zwitterionic side", in particular in respect to transitions involving higher excited states of the zwitterionic form. Using semiempirical INDO method¹⁷ the author carried out comprehensive quantum-chemical calculations for zwitterionic forms of xanthene dyes including various pyronines and rhodamine with unsubstituted amino groups (rhodamine 110). His first conclusion was that the assumption of a plane geometry of the xanthene system in the ground state does not allow to obtain transition energies observed in the absorption spectra, even with reasonable variations of bond lengths and angles (calculated transition energies exceeded by 6000 cm^{-1} the observed ones, while the same method yielded good results for anthracene, phenoxazine or pyrilium). The differences could be explained neither by the interaction of the xanthene system with the counterion nor with the solvent, and the calculations have been performed for numerous non-planar geometries. The most appropriate geometry turned out to be that with pyrane ring with boat-like conformation and two benzene rings in one plane. Fundamental change in the magnitude of the orbital energy and in the structure of the lowest unoccupied molecular orbital was related to deviation of the central carbon atom (C9) from the plane. Table 6.2 shows transition energies to several excited singlet and triplet states calculated using this geometry for unsubstituted rhodamine (R110) and their oscillator strengths.

Table 6.2

Calculated transition energies in rhodamine 110 molecule according to ref. ¹⁴

State number (n)	$S_0 \rightarrow S_n$ [cm^{-1}]	$f(S_0 \rightarrow S_n)$ ¹⁾	$S_0 \rightarrow T_n$ [cm^{-1}]	$f(T_1 \rightarrow T_n)$
1	20100	0.678 <i>l</i>	14300	0.637 <i>l</i>
2	25700	0.057 <i>s</i>	20500	0.263 <i>s</i>
3	28300	0.050 <i>s</i>	24200	0.002 <i>s</i>
4	29100	0.005 <i>l</i>	27350	0.009 <i>l</i>
5	29900	0.001 <i>l</i>	29600	0.009 <i>l</i>
6	34400	0.026 <i>s</i>	31250	0.271 <i>s</i>
7	35000	0.001 <i>l</i>	32700	0.663 <i>l</i>
8	36600	0.374 <i>s</i>	32700	0.256 <i>s</i>
9	37000	0.003 <i>l</i>	32900	0.046 <i>s</i>
10	37900	0.001 <i>s</i>	34600	0.239 <i>l</i>

¹⁾ The letter given at oscillator strength indicates polarisation of the transition: *l* - in the long axis of the xanthene system, *s* - in the short axis.

Substitution of amino hydrogens by alkyl groups in pyronines results in lowering of respective energy levels, e.g. from 20700 cm⁻¹ and 14200 cm⁻¹ in pyronine 110 (non-substituted amino groups) for S₁ and T₁ state, respectively, to 18900 cm⁻¹ and 12600 cm⁻¹ in pyronine B (diethyl-substituted amino groups), and the same effect can be expected for rhodamines with alkyl-substituted amino groups (e.g. on transition from rhodamine 110 to rhodamine B).

Assuming that in zwitterion form of rhodamine B majority of the respective transitions will decrease by about 2000 - 3000 cm⁻¹, (energy difference denoted as ΔE_r), the energy delivered during the excitation of the lactone molecule (usually about 32000 cm⁻¹) allows to reach several excited singlet or triplet states of the Z form. Exact determination would require a more precise value of ΔG⁰ of the L ⇌ Z equilibrium. But even assuming upper estimations for ΔE_r = 3000 cm⁻¹ and for ΔG⁰ = +36.0 kJ·mol⁻¹ (corresponding to 3000 cm⁻¹), the excitation energy would allow the molecule to reach S₅ and T₆ states of the Z form. Higher excited states of the zwitterion can be therefore easily accessible upon excitation with regard to their energy and would be able to participate in the excited state process.

Another interesting result given by Artyukhov¹⁴ is related to singlet-triplet coupling in the Z form of rhodamines. Spin-orbit interaction (SOI) between singlet and triplet states differs significantly in rhodamine 110 and in corresponding pyronine. Sharp increase of SOI in R110 as compared with the pyronine indicates - according to Artyukhov - a large influence of carboxylphenyl part of the molecule on the magnitude of this interaction. In my opinion this influence relates mainly to the conformation of the molecule at central (9) carbon atom (see below). Dramatic differences occur also in squares of SOI matrix elements (H_{SO}²) for different excited states. For instance, for R110, H_{SO}²(S₁,T₁) = 0.028 cm⁻², whereas H_{SO}²(S₁,T₂) = 101 cm⁻², H_{SO}²(S₂,T₂) = 15.9 cm⁻², or H_{SO}²(S₃,T₁) = 16.9 cm⁻² or H_{SO}²(S₃,T₂) = 48.6 cm⁻². In particular, large value of H_{SO}²(S₁,T₂) would indicate a very strong coupling between these two states, and suggest an opportunity for an efficient transition under conditions when they are close to each other in energy. It is noteworthy that in the case of deactivation process in zwitterions formed after excitation of the lactone molecule, the energy of the ¹Z₁ → ³Z_x transition is a function of temperature. This is due to the different dependence of the energy of the ¹Z₁ and ³Z_x states as measured vs. the L₀ state as a function of solvent polarity, which in turn changes with the temperature. The question of singlet-to-triplet intersystem crossing will be discussed in more detail later in section 6.6.

6.4. Transitions between excited states - excited state equilibria?

A number of excited states observed upon excitation of the lactone molecule must of course invoke the question about their mutual relationships and a closely related problem of the influence the external environment has on these relationships (temperature, polarity, etc.). Experimental time resolution available in time-resolved measurements carried out within this thesis allows us basically to discuss only the relationships between the excited states reached as a result of the fast excited state process, i.e. the lowest excited singlet and triplet states of

both forms, and to present some indications with regard to higher excited states. In respect to dual luminescence observed under certain conditions, one of the most fundamental questions emerging in this thesis is **which is the relationship between the $^1L_{CT}$ and the 1Z_1 state and whether there occur transitions between them?** Temperature dependent fluorescence measurements ("mysterious" iso-emissive points) and time resolved fluorescence spectra clearly indicate occurrence of a connection between the states, but fluorescence decay curves and transient absorption kinetic curves measured in this thesis point out that the connection is rather not a direct equilibrium of both excited singlet states.

Decay curves measured in both fluorescence bands show that both **L** and **Z** luminescences appear without any measurable rise time (on the time scale of SPT instrument described in Chapter 2, i.e. in less than 10 ps). Transient absorption experiments by Vlaskin *et al.*¹¹ mentioned above narrowed down the process of zwitterion formation to 1 ps, which means that at least a part of zwitterions populated in their excited singlet state is produced in a very fast (subpicosecond?) process and does not originate from the $^1L_{CT}$ state. Large difference of the dipole moments of $^1L_{CT}$ and 1Z_1 states indicates significant difference in charge distributions in lactone and in zwitterion excited states. Difference in π -electron systems of both forms imply, on the other hand, marked structural differences. In particular, the carbon atom in position 9 must have different hybridisation in the lactone and in the zwitterion - close to sp^3 and sp^2 , respectively. The presence of considerable barrier connected with the reorganisation energy for a direct transformation from the $^1L_{CT}$ to 1Z_1 state cannot be excluded. Moreover, such a transformation would involve a slow adiabatic ring opening or adiabatic ring closure in the case of a reverse transition. These implications weaken the possibility of a direct equilibrium between the two emitting states. Also, population of the $^1L_{CT}$ state from the zwitterion may be excluded on the basis of the fact that in cases when the maxima of both the **L** and the **Z** fluorescence are close to each other (indicating that the $^1L_{CT}$ state lies energetically very close to the 1Z_1 state) as it is in the case of more polar solvents (e.g. propionitrile or DMF), no radiationless transitions of the 1Z_1 state are reflected either in the decay curves or in decay time of the lactone form, even when $\tau_L < \tau_Z$. Thus, the connectivity of the $^1L_{CT}$ and the 1Z_1 state could be such that it leads to either the population of the zwitterion from the $^1L_{CT}$ state or these states are linked *via* a dark (non-luminescent) state.

As mentioned above, experimental evidence regarding the question of possible $^1L_{CT} \rightarrow ^1Z_1$ transition comes from several sources:

- (i) time resolved fluorescence measurements;
- (ii) fluorescence decay curves;
- (iii) temperature dependent fluorescence measurements;
- (iv) transient absorption spectra and kinetic curves.

Time resolved fluorescence spectra reveal an astonishing property of **Z** fluorescence. This fluorescence - under conditions when double luminescence is observed - is displayed after much longer time than indicated by the main short decay time recovered from the decay analysis (see sections 3.3.1 and 3.3.2). This implies that the 1Z_1 state must be populated not

only in a very fast photodissociation process (this population is rapidly quenched, e.g. within 0.40 ns for LR101/DME) but also *via* another longer living state. In light of the above discussion, the natural explanation would be a population of the excited **Z** form from the $^1L_{CT}$ state. This explanation finds, however, an ambiguous support in fluorescence decay curves measured in **Z** band as:

- (i) in cases when the **Z** fluorescence is displayed only (more polar solvents) and where no overlap of two bands has to be assumed in the decay analysis, the decays could be fitted with a monoexponential function, which proves that when no $^1L_{CT}$ states are present, the longer living zwitterion fluorescence is not observed;
- (ii) a direct excited state equilibrium $^1L_{CT} \rightleftharpoons ^1Z_1$ would result in decaying of the 1Z_1 state commonly with the $^1L_{CT}$ state, and in a build up of the **Z** fluorescence. The build up of the **Z** fluorescence would be, however, very difficult to extract, as it would take place simultaneously with the decay of the 1Z_1 states formed in the fast process. In cases where double luminescence is displayed, decay (single curve) analysis is in addition complicated by the fact that the distinction between a simple overlap of two bands and an inherent presence of a component with the same decay time in the **Z** fluorescence is very difficult. In all cases where double fluorescence occurred, both **L** and **Z** bands strongly overlap with each other, and it was necessary to assume that decays collected in **Z** band contain significant contribution from the **L** band due to the spectral overlap of both bands. Slight increase of the ratio of intensities of the **Z** and the **L** band at longer delay times (e.g. 30 ns for LR101/DME and 40 ns for LRB/BN) in time resolved fluorescence spectra (see section 3.3.4) puts some doubt on a direct $^1L_{CT} \rightleftharpoons ^1Z_1$ equilibrium, because in the case of the equilibrium or of an unidirectional $^1L_{CT} \rightarrow ^1Z_1$ reaction, the intensity ratio (**Z/L**) should remain constant; however, the increase is roughly within the experimental error;
- (iii) conclusion drawn from the global analysis of decays measured in the **Z** band (see section 3.3.1) indicates that the presence of component with decay time of the $^1L_{CT}$ state is caused by an overlap of two bands, and not by a direct excited state $^1L_{CT} \rightleftharpoons ^1Z_1$ equilibrium;
- (iv) if one assumes that the 1Z_1 is rapidly quenched in low polar solvents then a possible $^1L_{CT} \rightarrow ^1Z_1$ transformation would represent an efficient deactivation channel of the $^1L_{CT}$ state, and the **L** fluorescence (depending on the rate of the transformation) would not be observed. On the other hand, in solvents of lower polarity, the $^1L_{CT}$ state has a much longer lifetime, which indicates that the above transformation cannot be operative;
- (v) transient absorption kinetic curves, recorded in cases where double luminescence is displayed (e.g. LRB in BN at 433 nm) show multi-exponential decay of transient absorption in the $S_1 \rightarrow S_n$ absorption band of the zwitterion. It cannot be excluded, however, that this results from an overlap of two transient absorption bands originating from two excited state species, i.e. from the 1Z_1 and the $^1L_{CT}$ state (compare transient absorption spectra of LRB in BN and in dioxane, section 5.3);

- (vi) temperature-dependent fluorescence spectra, recorded under conditions where two bands are emitted, exhibit iso-emissive points in broad temperature ranges, suggesting a connection between the two emitting states;
- (vii) furthermore, temperature and polarity dependence of the quantum yield of L fluorescence indicates a radiationless deactivation of the $^1L_{CT}$ state, which is a strong function of solvent polarity. Moreover, both quantum yield and lifetime of $^1L_{CT}$ state decrease, as positions of the maxima of L and Z fluorescence bands approach to each other (at the same time quantum yield and lifetime of the 1Z_1 state increase).

It is thus evident that the decay or the build up of both emitting states does not compel to postulate a direct transition between them. On the other hand, iso-emissive points observed in temperature-dependent fluorescence spectra prove that both states are linked. The existing coupling of the two emitting states can also be explained by involving an intermediate state (being an "excitation warehouse"), which has its own lifetime long enough and on the time scale of tens of nanoseconds does not undergo other deactivation than either a transition to the 1Z_1 or to the $^1L_{CT}$ state. Such a state may be the triplet state of the lactone form ($^3L_{CT}$) which would undergo a slow ring opening and a transition to the 1Z_1 state. This issue requires, however, detailed further investigation.

6.5. Intramolecular quenching of the singlet excited state of zwitterion

The experiments carried out in this thesis have shown that thermally activated radiationless deactivation occurs also in the excited singlet state of zwitterion form of rhodamines, which is formed in its excited state upon excitation of the lactone molecule. In contrast to the studies on this process carried out so far¹⁸ and concentrating on deactivation of zwitterions excited directly from the ground state (and by necessity limited to a narrow range of solvents where Z form can exist in the ground state), it was possible to investigate in detail the **solvent polarity effect and the temperature effect** on the kinetics of the radiationless process under conditions where no hydrogen bonding were possible. This was mainly due to a much better solubility of lactones in solvents of medium and lower polarity, which allowed us to cover a wide range of solvent polarity. Different substituents at amino nitrogen atoms in different rhodamines enabled us to study the effect **the structure of the amino group** has on the non-radiative process. An important element that must be taken into account in the case of the lactone form is a possibility of radiationless deactivation of the Z form by a **closure of the lactone ring** and a formation of the lactone molecule from the 1Z_1 state (i.e. $^1Z_1 \rightarrow L_0$ transition). Below, these three effects are discussed in a more detail.

6.5.1. Structure of the amino group

Rhodamine molecules included in the series of lactones investigated in this thesis differed mainly in the substitution pattern at the amino nitrogen atoms. There were two major reasons for such a diversification:

- (i) investigate the influence of donor-acceptor capabilities of the amino group on the initial electron transfer reaction and on the non-radiative process in zwitterions;
- (ii) investigate the effect of rigidization of the substituents at amino nitrogen atoms on the non-radiative process in zwitterions (rhodamine 101).

In contrast to earlier studies, it has been found that rigidization of alkyl substituents at the amino groups does not result in inhibition of the radiationless deactivation¹⁹ and that rhodamine 101 (with amino groups rigidly linked to the xanthene skeleton) also undergoes an efficient non-radiative process. Taking into account that the molecule has shown in this study other properties analogous to those characteristic for the remaining members of the series, this experimental evidence provides a negative structural verification for all mechanisms based on torsional or twisting motion of the amino groups as a source of radiationless deactivation of rhodamines. As a consequence, the hypothesis on population of non-emissive TICT states²⁰⁻²² has been eliminated. On the other hand, one cannot exclude that other motions of the amino group (e.g. pyramidal - umbrella like) or of other parts of the xanthene skeleton (butterfly like, see below) contribute to the non-radiative process. The quantitative differences in non-radiative process that result from structural differences at amino groups most probably relate to electron-donating properties of the group and can be stimulated by changing the polarity of the surrounding medium. Though the experimental data presented in this thesis do not cover a full range of solvents for all lactones (cf. Table 4.5), an increase of oxidation potential of amino group is accompanied by an enhanced radiationless deactivation of the 1Z_1 state:

Table 6.3

Rate constant of the non-radiative deactivation of the 1Z_1 state in butyronitrile at 295 K as a function of oxidation potential of the amino group:

	LDR10	LRMET	LRB	LR101
$E(D^{+•} / D)$ [eV] ^{a)}	b)	0.78	0.75	0.56
k_{nr} [$\times 10^{-8}s^{-1}$]	43.5	36.0 ^{c)}	11.8	0.25

^{a)} data source as in Table 6.1; ^{b)} $E(D^{+•} / D)$ not known, but definitely higher than that of LRMET; ^{c)} calculated using $k_r = 2.5 \times 10^8 s^{-1}$

6.5.2. Solvent polarity effect and temperature effect

Non-radiative process in **Z** forms of rhodamines produced upon excitation of the lactone molecule is very strongly influenced by a change of solvent polarity. The effect is so strong that, for instance, changing the solvent from MTHF ($\epsilon = 7.0$ at 295K) to propionitrile ($\epsilon = 28.9$ at 293 K) one can cover the whole range of non-radiative deactivation of the **Z** form of R101: **Z** fluorescence is totally quenched in medium polarity MTHF and there is no radiationless deactivation of the excited **Z** form in polar propionitrile (see Chapter 3). Solvents of polarity in between cause various degree of radiationless deactivation (manifested by different lifetimes of the **Z** fluorescence). In highly polar solvents the singlet state of the **Z** form is stabilised against the non-radiative process and the non-radiative rate constant, k_{nr} , decreases up to the value negligible when compared with the radiative rate constant, k_r . This

proves that solvent polarity is a crucial factor for radiationless process in rhodamines. Moreover, other properties of the solvent, e.g. the viscosity, seem to play a minor role, if any, in the radiationless deactivation. This conclusion results from experiments in different solvents (at different temperatures) under conditions where they have the same polarity in terms of dielectric constant (cf. section 4.2) and different viscosities (e.g. AN and DMSO at 293 K and 363 K have approximately the same dielectric constants and viscosities differing by about three times²³).

The effect of solvent polarity on the non-radiative process in zwitterionic forms of rhodamines excited directly from the ground state has been studied by several authors^{22, 24-27}, using mainly alcohols (or mixtures alcohol/water) as solvents. All of them have found a general tendency that an increase in solvent polarity results in an increase of k_{nr} . The changes in k_{nr} as a function of solvent polarity (expressed in terms of E_T values²⁸) were rather moderate and are shown in Table 6.4. Observed Arrhenius activation energy of the non-radiative process was reported to decrease with increasing solvent polarity²⁴.

Table 6.4

Variability range of the rate of non-radiative process in rhodamine B as a function of solvent polarity:

k_{nr} [$\times 10^{-8}s^{-1}$]	$E_T(30)$ [kcal·mol ⁻¹]	Ref.	Solvents used
0.8 ÷ 1.0	47.6 ÷ 50.7	24	alcohols from decanol to propanol
1.1 ÷ 3.6	52 ÷ 63	26, 27	water/ethanol mixtures
1.9 ÷ 4.2	49.1 ÷ 55.5	25	water/methanol mixtures
2.9 ÷ 2.1	45.0 ÷ 51.9	20	ethanol, DMSO ¹⁾
11.8 ÷ 2.0	43.1 ÷ 46.0	this work ²⁾	nitriles and DMSO

1) data for rhodamine 3B (ethyl ester of rhodamine B);

2) k_{nr} for LR101 changes from $22.7 \times 10^{-8} s^{-1}$ in 1,2-dimethoxyethane ($E_T(30) = 38.2$ kcal·mol⁻¹) to $0.25 \times 10^{-8} s^{-1}$ in butyronitrile ($E_T(30) = 43.1$ kcal·mol⁻¹).

Table 6.4 contains also results published by Vogel *et al.*²⁰ who investigated esterified rhodamines in DMSO and in ethanol, as well as the results obtained in this thesis. In contrast to the former authors, k_{nr} reported by Vogel *et al.* decreases with increase of solvent polarity. The changes are much larger along with temperature changes (e.g. k_{nr} in DMSO is equal to $2.9 \times 10^{-8}s^{-1}$ and $17.5 \times 10^{-8}s^{-1}$ at 297 K and 363 K, respectively, and the same tendency is in ethanol). The same tendency (but for a broader range of solvents) can be found in the data reported in this thesis (cf. section 4.4.1, Table 4.5), where the **rate constant of the non-radiative process decreases strongly with increasing solvent polarity**. Very good agreement of k_{nr} and E_a of the non-radiative process in rhodamine 3B (excited from the ground state) in DMSO, reported by Vogel *et al.*²⁰, and in rhodamine B (obtained upon lactone excitation $k_{nr} = 2.1 \times 10^{-8}s^{-1}$ and $E_a = 24.4$ kJ·mol⁻¹) and determined in this thesis ($k_{nr} = 2.0 \times 10^{-8}s^{-1}$ and $E_a = 24.8$ kJ·mol⁻¹, see Table 4.5) indicates that the non-radiative process may be inherently the same in both cases and cannot be the closure of the lactone ring.

An astonishing feature displayed by the data derived in present work from the temperature-dependent measurements are Arrhenius parameters determined from the dependence of k_{nr} on temperature (E_a in Table 4.5). Interpreted literally as activation energies, they would lead to the conclusion that the rate constant of the non-radiative process occurring in rhodamines is an increasing function of activation energy, i.e. the higher reaction barrier the faster the reaction proceeds! This apparent contradiction can be, however, explained using the hypothesis of reaction energy barrier height, which depends on solvent polarity.

This concept has been used by Hicks *et al.*²⁹ to explain the dynamics of isomerisation in *p*-dimethylaminobenzonitrile involving significant charge redistribution and to attribute its variations to polarity-induced changes of the barrier height. In their study on the non-radiative process in rhodamine B in alcohol/water mixtures, Chang and Cheung²² followed that idea and applied a linear dependence of barrier height on solvent polarity parameter $E_T(30)$ ²⁵ and subsequently, on the normalised E_T^N parameter³⁰. Using this model, they were able to describe satisfactorily the changes in k_{nr} with increasing solvent polarity. In addition, they assumed that the non-radiative rate can be regarded as the barrier crossing rate from the planar to the twisted configuration of the amino group. Casey *et al.*³¹ applied the same methodology to explain the dependence of k_{nr} on solvent polarity for the cation form of rhodamine B in nitriles using also a two-state model, but a different approach: assuming another mechanism of radiationless deactivation (ULM model). Though the structural assumption of twisting motion turned out to be not valid - at least in the case of zwitterions formed upon excitation of the lactone molecule - the concept of polarity-dependent barrier height may be applied to explain the non-radiative process in the **Z** form.

The barrier height (E_h) for the non-radiative process should be equal to the difference of the energy of the 1Z_1 state and the product of radiationless deactivation, being - according to the conclusions of Chapter 5 - the 3Z_x state: $E_h = E(^3Z_x) - E(^1Z_1)$ (see Fig. 6.2):

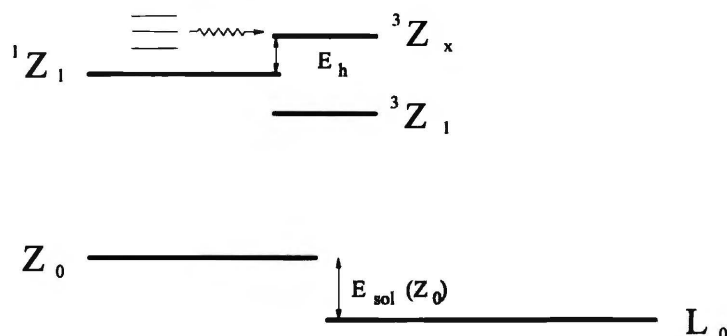


Fig. 6.2: Energy levels of states participating in radiationless deactivation. $^1Z_1 \rightarrow ^3Z_1$ transition has a very low probability due to weak coupling of these states (according to Artyukhov¹⁴, see section 6.3).

Solvent polarity can be regarded as a factor determining relative positions of individual energy levels in the lactone molecule. As concluded earlier in this Chapter (cf. section 6.3) the position of the 1Z_1 state in relation to L_0 state (measured on the energy scale as E_z) is very sensitive to solvent polarity and a more polar environment lowers E_z . The dipole moment of the zwitterion ground state (Z_0) was suggested to be very high (14.5 D³²) and solvent-

induced differences in solvation energy of that state will directly translate into the energy of the 1Z_1 state in respect to L_0 state (E_z), as the energy of ${}^1Z_1 \rightarrow Z_0$ transition exhibits rather weak solvent dependence. This transition is polarised along the long axis of the xanthene part and does not involve any significant change of the dipole moment of the molecule. Thus, the energy of the 1Z_1 state will be as sensitive to the solvent polarity as is the solvation energy of a dipole of the ground state of the **Z** form.

A second factor influencing E_h is the energy of the 3Z_x state. A necessary assumption is that the dipole moment of the 3Z_x state should be much less than that of the Z_0 - and consequently - than that of the 1Z_1 state. As the dipole moment of the Z_0 state is directed along the short axis of the xanthene molecule, its decrease must result in an intramolecular charge redistribution within the entire molecule and in approaching to each other the centre of the positive charge on the xanthene system and the centre of the negative charge localised on the oxygen atom of the carboxyl group.

Significant role of solvation in changing the energy barrier height is suggested by a linear dependence of $\ln k_{nr}$ on solvation energy of the 1Z_1 state (Fig 6.3). The stabilisation of a solute molecule with a dipole moment μ in solution can be described using the electrostatic model introduced by Kirkwood³³. According to that model, the free energy of solvation of a dipole μ in a solvent of dielectric constant ϵ can be expressed as:

$$E_{sol} = \frac{N_A \mu^2}{4\pi\epsilon_0 a^3} \frac{\epsilon - 1}{2\epsilon + 1} \quad (6.2)$$

where N_A is the Avogadro number, and a - a hydrodynamical radius of the molecule. The absolute value of the E_{sol} depends very much on the assumed radius of the molecule, a , but its changes are determined by the changes of solvent polarity function: $f = (\epsilon - 1)/(2\epsilon + 1)$. Figure 6.3 presents plots of $\ln k_{nr}$ versus f for LRB and LR101.

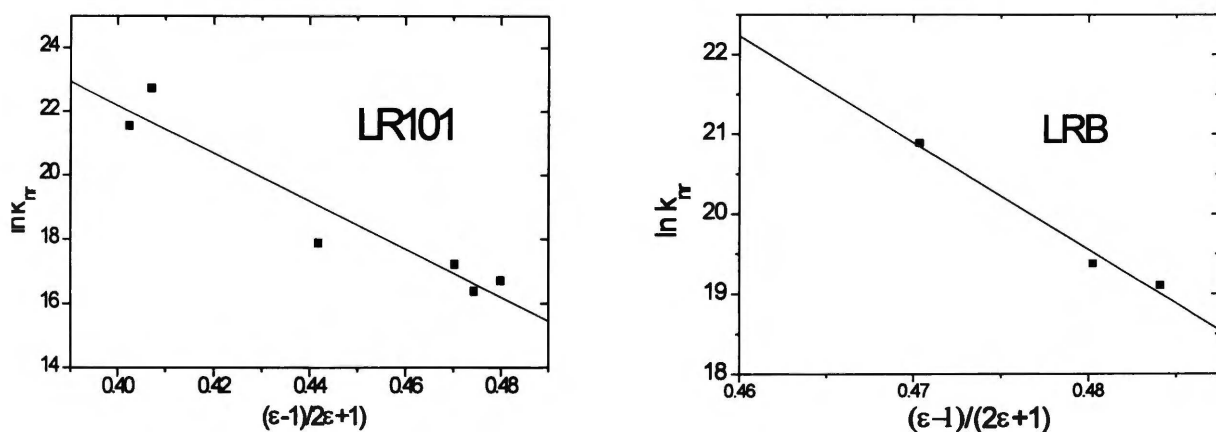


Fig. 6.3: Plots of $\ln k_{nr}$ against $(\epsilon-1)/(2\epsilon+1)$ for the non-radiative decay of the **Z** form produced upon excitation of the lactone form of rhodamine 101 (LR101) and rhodamine B (LRB). The straight lines obtained in linear regression have the following parameters: LR101- slope -74.8, intercept 53.1, correlation coefficient 0.955; LRB - slope -134.0, intercept 62.4, correlation coefficient 0.991.

Cavity radius assumed for the lactone molecule in calculations (based on solvatochromic shifts) of the excited state dipole moment by Klein and Hafner⁸ and used in

Chapter 3 of this thesis for the same purpose (but for other rhodamines) was 0.7 nm. On the other hand, in the study of pressure effects on ground-state equilibrium between the lactone and zwitterion forms of rhodamine B in alcohols, Sueishi *et al.*³² assumed much lower hydrodynamical radius value (0.3 nm) on the basis of Corey-Pauling-Coltun model. E_{sol} calculated with the formula (6.2) for rhodamine B using $a = 0.7$ nm and $\mu = 14.5$ D were, however, definitely too low (e.g. 17.9 kJ·mol⁻¹ in DMSO, 17.6 kJ·mol⁻¹ in AN and 17.0 kJ mol⁻¹ in BN), especially in view of the differences shown by k_{nr} between these solvents. On the other hand, the value 0.3 nm is much less than the real dimensions of the molecule and in addition it yields very high E_{sol} values, so the proper value of a must be in between.

As the linear correlation of $\ln k_{\text{nr}}$ with f is rather good, then - following the approach adopted by Chang and Cheung²², let's assume that the barrier height, E_{h} , is linearly dependent on $\Delta E_{\text{sol}} = E_{\text{sol}}(Z_0) - E_{\text{sol}}(^3Z_x)$ expressed as a function of solvent polarity f :

$$E_{\text{h}} = E_0 + \beta f \quad (6.3)$$

where β is an empirical parameter determining how strongly E_{h} varies with change of f , and E_0 is a constant corresponding to an energy barrier (or energy excess) under hypothetical conditions where $f = 0$. Using the formula (6.3), the non-radiative rate constant can be written as:

$$k_{\text{nr}} = k_{\text{nr}}^0 \exp\left(-\frac{E_0 + \beta f}{RT}\right) = k_{\text{nr}}^0 \exp\left(-\frac{E_0}{RT}\right) \exp\left(-\frac{\beta f}{RT}\right) \quad (6.4)$$

Assuming that k_{nr}^0 does not depend on solvent polarity, the parameter β can be calculated from the slope of a straight line describing the dependence of $\ln k_{\text{nr}}$ on f at a constant temperature. β/RT is the slope of this straight line (dimensionless) and equal 74.8 ($\beta = 18.3 \times 10^4$ J·mol⁻¹) and 134.0 ($\beta = 32.6 \times 10^4$ J·mol⁻¹) for LR101 and LRB, respectively (as measured at 293 K). To correct for the effect of solvent polarity, k_{nr} is to be modified as follows:

$$k_{\text{cor}} = k_{\text{nr}} \exp\left(\frac{\beta f}{RT}\right) \quad (6.5)$$

Table 6.5

Non-radiative rate constants for LRB and LR101 corrected according to eq. (6.5):

	Solvent	10 ⁻⁸ k_{nr}	k_{cor} [s ⁻¹] *)
LRB:	BN	11.8	2.78
	AN	2.6	2.31
	DMSO	2.0	2.98
LR101:	THF	74.4	1.26
	DME	22.8	0.27
	Pyridine	0.58	0.13
	BN	0.30	0.57
	PN	0.13	0.33
	DMF	0.18	0.71

*) Multiplied by 10⁻³⁶ in the case of LRB and by 10⁻²³ in the case of LR101.

Table 6.5 shows k_{cor} values for LRB and LR101. The values of k_{cor} are randomly distributed around the mean value. Random distribution indicates that dependence on solvent polarity is the main factor influencing the non-radiative process, and other factors (if any) are of a minor importance. It is to be noted that the dependence of the non-radiative process on solvent polarity is very strong.

Assuming that β does not change with temperature and using the values of this parameter given above for LRB and LR101, one can correct the non-radiative rate constants measured for different temperatures for the effect of solvent polarity variation with changing the temperature. The correction for solvent polarity effect can be done for non-radiative rate constants measured at different temperatures using formula (6.5) with f as a function of temperature:

$$k_{\text{cor}}(T) = k_{\text{nr}}^{\text{meas}}(T) \exp\left(\frac{\beta f(\epsilon(T))}{RT}\right) \quad (6.6)$$

where $f(\epsilon(T)) = (\epsilon(T) - 1)/(2\epsilon(T) + 1)$ and $k_{\text{nr}}^{\text{meas}}(T)$ is the non-radiative rate constant measured at temperature T . Table 6.6 shows the results of such operation together with functions describing temperature dependencies of dielectric constant for the solvents used. The functional formulae have been taken from the paper by Grampp and Jaenicke²³ (DME and DMSO) or calculated based on the data given by Jannelli *et al.*³⁴ (nitriles).

Table 6.6

Non-radiative rate constants for LRB measured at different temperatures and corrected according to eq. (6.6):

	Solvent	$\epsilon(T)$	T [K]	$\ln[k_{\text{nr}}(T)]$	$\ln[k_{\text{cor}}(T)]$ *)	
LRB	BN	-8.34 + 9724·1/T¹⁾	293	20.89	82.65	
			303	21.27	80.78	
			323	22.19	77.56	
			343	23.23	74.97	
	AN	-9.73 + 13577·1/T¹⁾	293	19.38	82.76	
			343	21.05	74.53	
	DMSO	-16.36 + 19239·1/T²⁾	293	19.11	83.40	
			323	19.95	77.93	
			343	20.52	74.90	
			353	20.85	73.58	
	LR101	DME	-2.82+2948.8·1/T²⁾	293	21.54	49.97
				313	22.14	48.00
333				23.23	46.86	
BN		-8.34 + 9724·1/T¹⁾	313	17.03	49.20	
			333	17.45	47.46	
			353	18.27	46.34	

1) formula according to the data from ref. ³⁴; formula from ref. ²³.

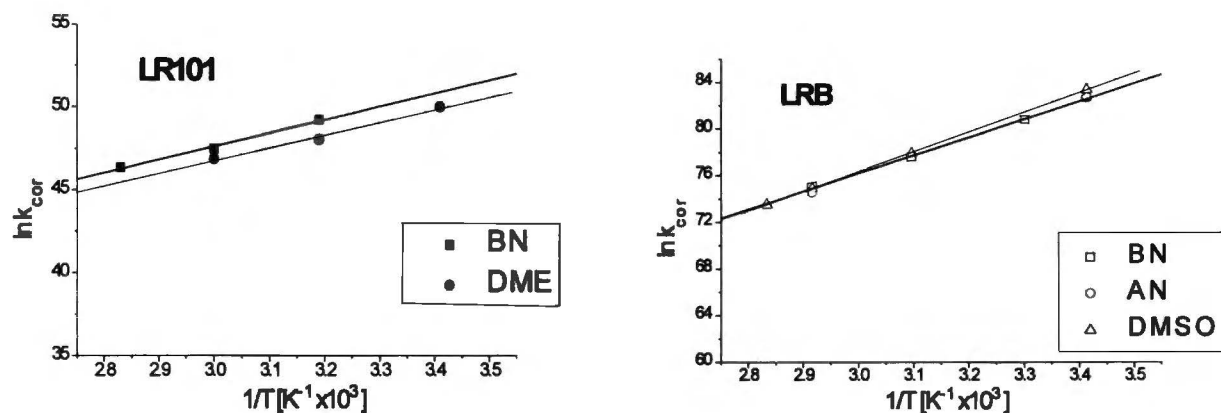


Fig. 6.4: Non-radiative rate constants for LR101 (left) and LRB (right) corrected for the effect of solvent polarity as a function of temperature. Straight lines represent best linear fits. Parameters of the straight lines obtained in linear regression are as follows: LR101/DME (thin line) - slope 7623, intercept 23.9, correlation coefficient 0.994; LR101/BN (solid line) - slope 7947, intercept 23.8, correlation coefficient 0.996; LRB/DMSO (thin line) - slope 16960, intercept 25.5, correlation coefficient 0.999; LRB/BN (solid line) - slope 15431, intercept 29.9, correlation coefficient 0.999.

Figure 6.4 shows $\ln k_{nr}(T)$ corrected for solvent polarity ($\ln k_{cor}(T)$) as a function of $1/T$. In spite of scarce data, in both cases an excellent agreement of $k_{cor}(T)$ for different solvents at the same temperature is evident. Moreover, the straight lines obtained as a result of linear regression have very similar slopes and intercepts (see caption under Fig. 6.4). The slope of the straight line obtained for $\ln k_{cor}(T)$ is equal to $-E_0/R$, with E_0 being the parameter from (6.3) equation. E_0 calculated based on the above slopes is equal $-128.2 \text{ kJ}\cdot\text{mol}^{-1}$ (BN) and $-140.9 \text{ kJ}\cdot\text{mol}^{-1}$ (DMSO) for LRB and $-60.9 \text{ kJ}\cdot\text{mol}^{-1}$ (DME) and $-66.0 \text{ kJ}\cdot\text{mol}^{-1}$ (BN) for LR101. E_0 would hypothetically be the energy difference between the 1Z_1 and the 3Z_x level after extrapolation to conditions where polarity function f would be equal 0. Negative sign of E_0 indicates that in this limit the 1Z_1 state of the **Z** form would be above the 3Z_x level. As conditions where $f = 0$ correspond to the vacuum and do not have any real condensed phase correlate, a more realistic insight into the E_0 parameter one can get considering the situation in a low polarity solvent with e.g. $\epsilon = 2$ (like cyclohexane, CH, where the non-radiative process is so fast that the 1Z_1 has no chance to emit fluorescence), and comparing it with a more polar solvent. Using the values of β and E_0 given above, the following E_h values can be obtained:

E_h [kJ·mol ⁻¹]	LRB		LR101	
	BN	CH	BN	CH
	22.19	-63.0	18.42	-29.40

As E_h was assumed to be the energy gap between the 3Z_x and the 1Z_1 state, negative values of E_h in cyclohexane suggest that in this solvent the energy of the 1Z_1 state would exceed that of the 3Z_x state by $63 \text{ kJ}\cdot\text{mol}^{-1}$ for LRB and by $29.40 \text{ kJ}\cdot\text{mol}^{-1}$ for LR101. So large variations of E_h with solvent polarity would indicate that not only the solvation of the Z_0 state (and subsequent lowering of the energy of the 1Z_1 state) contributes to these changes, but also

destabilisation of the 3Z_x state with increasing solvent polarity must be significant. The possible nature of the 3Z_x is considered in section 6.6.

In a summary, the temperature effect on k_{nr} can be related - at least in a significant part - to temperature-induced changes in solvent polarity (expressed in terms of dielectric constant, ϵ , or of a simple function of ϵ) which are responsible for variations in the energy barrier height. This has been well proven by temperature-dependent measurements of quantum yields and lifetimes of **Z** fluorescence. For a given class of solvents (e.g. nitriles or ethers) where specific solvent effects (like photochemical reaction that may occur in chlorinated solvents or interactions with aromatic system as in the case of benzonitrile) can be neglected, temperature-imposed control of solvent polarity (achieved, for instance, by cooling down the solvent) lead to similar values of k_{nr} in different solvents. The above quantitative analysis fully supports the hypothesis explaining the intramolecular quenching of the 1Z_1 state. The fact that the changes in k_{nr} with temperature can be correlated with ϵ , or with a simple function of ϵ confirms the above model postulating the shifts of energy levels induced by solvation energy changes as a principal reason of the non-radiative process.

6.5.3. Ring closure

Though the model and the arguments considered above provide - in my opinion - a convincing explanation of the non-radiative process in the excited **Z** form, a comment should be made on an additional opportunity for radiationless deactivation, namely on a lactonic ring closure reaction (and simultaneous recovery of the C-O bond). As almost no absorption from the Z_0 state could be detected in transient absorption measurements, formation of the lactone molecule in the ground state is either completed within a very short time (short on the ns time scale) or proceeds via the triplet state of the **Z** form. The experimental evidence collected in this thesis does not allow to speculate on the ground state recovery reaction. Intramolecular charge redistribution in the 3Z_x state as compared to the 1Z_1 state would suggest approaching to each other of the charge centres of the xanthene part and the carboxyl group. In other words, such a charge redistribution would facilitate the formation of the C-O bond and the closure of the lactone ring. Because of a short lifetime of the 3Z_x state, this question has to be, however, addressed on the 1Z_1 state level and requires further investigation

6.6. Intersystem crossing process in the zwitterion form

The discovery of an intense phosphorescence of the zwitterion form of rhodamines enables us to view in a new manner the question of intersystem crossing in rhodamines. Various theories attempting to explain the process of thermally activated radiationless deactivation did not pay serious attention to the possibility of the thermally activated transition to the triplet state and concentrated on the geometrical changes of the amino group. Neglecting the role of the triplet state was somewhat justified because of low quantum yield of intersystem crossing in these compounds observed in protic solvents. For instance, the quantum yield of the intersystem crossing process for rhodamine B in water was found equal

to 0.006³⁵. Rhodamine 101 exhibits in methanol or in ethanol at room temperature a fluorescence quantum yield of about 1.0 and no significant population of the triplet state is expected in these solvents. Rhodamine 101 and its ethyl ester derivative were used to prove structurally the role of torsional or twisting motion of the amino group in the thermally activated deactivation process of rhodamines. The reasons for the stabilisation of the zwitterion form against the transition to the triplet state in rhodamines in protic solvents were not investigated in more detail. The possible source of this stabilisation may be connected with a lack of significant mixing of singlet and triplet states in planar π -system of the zwitterion (low S-O coupling) and a large energy gap between the 1Z_1 and the 3Z_1 state. Especially, population of significant out-of-plane vibrations might account for this mixing. Such vibrations are known to be capable of mixing singlet and triplet states in planar hydrocarbons³⁶. The vibrations that can be taken into account in the case of rhodamines are those connected with the "pyramidal" out-of-plane motions of the nitrogen atoms or the bending vibrations of the xanthene system caused by folding this part of the molecule along the symmetry axis of the xanthene part (butterfly-like motion).

The fact that out-of-plane vibrations may influence the radiationless deactivation of the molecules finds certain support in the effect of the substituents at amino groups on the rate of intramolecular quenching and stabilisation of the excited state of the zwitterion. On the other hand, in the study of rhodamine B, rhodamine 101, and pyronine B adsorbed on the surfaces of organic crystals, Kemnitz *et al.*³⁷ have ascribed the observed radiationless deactivation in these molecules to an enhanced internal conversion resulting from the butterfly flip motion of the xanthene skeleton of the molecule.

The transition to a higher triplet state may be a natural explanation of the thermally activated radiationless deactivation in rhodamines. Very efficient quenching of the Z form in less polar solvents implies a non negligible rate constant for the intersystem crossing. Assuming that the entire non-radiative deactivation of the zwitterion is due to the transition to the triplet state we obtain, for instance, in the case of LR101 in THF ($\tau_Z = 130$ ps) $k_{ISC} \approx 7.5 \cdot 10^9$ s⁻¹. Such a value (and even larger values at more efficient deactivation) must be connected with large coupling of the 1Z_1 state and the triplet state to which the crossing occurs and is supported by the calculations made by Artyukhov and described above (see section 6.3). On the other hand, an increase of solvent polarity causes a decrease of the k_{ISC} reflecting an increase of the barrier height for the ISC process (see section 6.5.2).

This influence of the solvent polarity on the k_{ISC} can be easily explained if we assume that the strong coupling of the 1Z_1 and the triplet state participating in the radiationless transition (3Z_x) is caused by a favourable Franck-Condon factor for intersystem crossing that may result from small energy gap between these states. On the other hand, the triplet level responsible for the radiationless deactivation in more polar medium may be connected with the (n, π^*) nature of this state. Such a triplet would also explain the absence of the singlet-triplet transitions in rhodamines in protic solvents. These solvents form hydrogen bonds with rhodamine molecules stabilising in such a way their zwitterion forms. The hydrogen bonding

must considerably increase the energy of the $^3(n,\pi^*)$ state, especially in the case when the n orbital is localised on the atom directly participating in the hydrogen bonding. In rhodamines such an atom would be either the oxygen atom in the xanthene system or the oxygen atom at the carboxylphenyl group. The latter can, however, be excluded in view of the minor influence of this part of the molecule on the photophysics of the xanthene system³⁸ and analogous radiationless deactivation process observed for ester analogues of rhodamines and pyronines^{37, 39}.

The mechanism of the transition to the triplet state finds some support in the above mentioned study carried out by Kemnitz *et al.*³⁷. They have found that the fluorescence decay curves of the rhodamine 101 adsorbed at dry (water-free) surfaces of organic crystals (naphthalene, phenanthrene) were non-exponential and the main component had a short decay time (0.2 ns, contribution 61%). The decay curves changed completely upon adsorbing water at the crystal surface, and the main decay time became much longer (3.14 ns, contribution 67%). The authors have ascribed the observed radiationless deactivation to an enhanced internal conversion resulting from a folding of the xanthene skeleton in non-ideally flat sites of the crystal surface. The effect of water was interpreted in such a way that the water weakens the bond to the surface (partial solvation) thus enabling the rhodamine molecule to accommodate more planar conformation of the xanthene system. In the light of our results we reinterpret these observations in this manner that the folding of the xanthene skeleton (butterfly motion) would contribute to the enhanced spin orbit coupling and would facilitate the transition to the 3Z_x state. Water forms a hydrogen bond to the R101 molecules and thus stabilises the zwitterion form both in the excited and in the ground states. This hydrogen bonding causes rising up of the triplet level, which results in disabling of the $^1Z_1 \rightarrow ^3Z_x$ transition and - indirectly - confirms the (n,π^*) nature of the 3Z_x triplet state.

References and notes

- ¹ F. Barigelletti, *Chem. Phys. Lett.* **140** (1987) 603
- ² D. A. Hinckley and P. G. Seybold, *Spectrochim. Acta* **44A** (1988) 1053
- ³ D. Rehm and A. Weller, *Isr. J. Chem.* **8** (1970) 259
- ⁴ A. Kapturkiewicz, *Chem. Phys.* **166** (1992) 259
- ⁵ D. W. Leedy and D. L. Muck, *J. Am. Chem. Soc.* **93** (1971) 4264
- ⁶ A. Kapturkiewicz, *J. Electroanal. Chem.* **372** (1994) 101
- ⁷ S. Efrima and M. Bixon, *Chem. Phys.* **13** (1976) 447
- ⁸ U. K. A. Klein and F. W. Hafner, *Chem. Phys. Lett.* **43** (1976) 141
- ⁹ T. M. Grigoryeva, V. L. Ivanov and M. G. Kuzmin, *Dokl. Akad. Nauk SSSR* **238** (1978) 603
- ¹⁰ J. Karpiuk, Z. R. Grabowski and F. C. De Schryver, *Proc. Indian Acad. Sci. (Chem. Sci.)* **104** (1992) 133

-
- ¹ V. I. Vlaskin, A. J. Gorolenko, S. V. Melnitchuk, N. Nizamov, S. A. Tichomirov and G. B. Tolstorozev, *Dokl. Akad. Nauk* **302** (1988) 1141
 - ² V. V. Rylkov and E. A. Cheshev, *Opt. Spekt.* **63** (1987) 1030
 - ³ V. Ya. Artyukhov, *Izv. VUZ, Fizika*, **1986** 39, 50
 - ⁴ V. Ya. Artyukhov, *Elektronnye spektry i fotoprocesy v molekulach ksantenovykh krasiteley* (Electronic spectra and photoprocesses in molecules of xanthene dyes), autopresentation of the PhD thesis, Tomsk University, Soviet Union, 1987
 - ⁵ M. Siegmund and J. Bendig, *Ber. Bunsenges. Phys. Chem.* **82** (1978) 1061
 - ⁶ U. Mayer, V. Gutmann and W. Gerger, *Monatsh. Chemie* **106** (1975) 1235
 - ⁷ V. Ya. Artyukhov, *Izv. VUZ, Fizika*, **1986** 96
 - ⁸ see section 1.4 for review of the previous work on this subject
 - ⁹ J. Karpiuk, Z. R. Grabowski and F. C. De Schryver, *J. Phys. Chem.* **98** (1994) 3247
 - ¹⁰ M. Vogel, W. Rettig, R. Sens and K. H. Drexhage *Chem. Phys. Lett.* **147** (1988) 452
 - ¹¹ K. G. Casey and E. L. Quitevis, *J. Phys. Chem.* **92** (1988) 6590
 - ¹² T. L. Chang and H. C. Cheung, *Chem. Phys. Lett.* **173** (1990) 343;
 - ¹³ G. Grampp and W. Jaenicke, *J. Chem. Soc. Faraday Trans.* **81** (1985) 1035. Table 1 in this paper contains some errors and the formula for the viscosity of DMSO given in that table could be used only after making the following correction: $\ln \eta = -4.47 + 1550/T$.
 - ¹⁴ T.-L. Chang and W. L. Borst, *J. Phys. Chem.* **93** (1990) 4724
 - ¹⁵ T.-L. Chang and H. C. Cheung, *J. Phys. Chem.* **96** (1992) 4874
 - ¹⁶ F. López Arbeloa, T. López Arbeloa, M. J. Tapia Estevéz and I. López Arbeloa, *J. Phys. Chem.* **95** (1991) 2203
 - ¹⁷ T. López Arbeloa, F. López Arbeloa, P. Hernández Bartolomé and I. López Arbeloa, *Chem. Phys.* **160** (1992) 123
 - ¹⁸ K. Dimroth, C Reichardt, T. Siepmann and F. Bohlmann, *Liebigs Ann. Chem.* **661** (1963) 1
 - ¹⁹ J. Hicks, M. Vandersall, Z. Babarogic and K. B. Eisenthal, *Chem. Phys. Lett.* **116** (1985) 18
 - ²⁰ C. Reichardt and E. Harbusch-Görnert, *Liebigs Ann. Chem.* **1983** 721
 - ²¹ K. G. Casey, Y. Onganer and E. L. Quitevis, *J. Photochem. Photobiol. A.* **64** (1992) 307
 - ²² Y. Sueishi, Y. Sugiyama, S. Yamamoto and N. Nishimura, *Bull. Chem. Soc. Jap.* **67** (1994) 572
 - ²³ J. Kirkwood, *J. Chem. Phys.* **2** (1934) 351
 - ²⁴ L. Janelli, A. Lopez and L. Silvestri, *J. Chem. Eng. Data* **28** (1983) 166, 169
 - ²⁵ V. E. Korobov, U. V. Shubin and A. K. Chibisov, *Chem. Phys. Lett.* **45** (1977) 498
 - ²⁶ S. L. Madej, S. Okajima and E. C. Lim, *J. Chem. Phys.* **65** (1976) 1219
 - ²⁷ K. Kemnitz, N. Tamai, I. Yamazaki, N. Nakashima and K. Yoshihara, *J. Phys. Chem.* **91** (1987) 1423
 - ²⁸ R. Sens, *Thesis*, University of Siegen, 1984
 - ²⁹ M. Vogel, W. Rettig, R. Sens and K.-H. Drexhage, *Chem. Phys. Lett.* **147** (1988) 461

CHAPTER 7

CONCLUSIONS

The main objective of this thesis was to investigate excited state processes occurring in the lactone forms of selected rhodamines in low and in highly polar aprotic solvents. It has been found that spiro-structure of lactones with orthogonal π -electron systems seems to be especially favourable for stabilisation of charge separation. In all lactones studied, occurrence of the reaction leading to generation of the excited charge-transfer state, ${}^1L_{CT}$, and the excited state of the zwitterion form 1Z_1 , formed after a cleavage of the C-O bond in the lactone ring, has been found. Investigations of the mechanism of this process have been carried out as well as the investigations of formation and deactivation of intermediates occurring upon excitation of the lactone molecule. Both excited states are products of relaxation of a higher, primary excited ion radical pair which is produced upon excitation due to an electron transfer reaction: the ${}^1L_{CT}$ state after vibrational excitation and the 1Z_1 state after the back electron transfer reaction. In contrast to the results published so far, it has been found that both forms are produced always, and under conditions where one of them (**Z**) is not observed - it undergoes a fast radiationless deactivation. In addition to this ultrafast C-O bond dissociation, a slow process of 1Z_1 formation has been found. Though its mechanism remains unknown, it has to be connected with presence of the ${}^1L_{CT}$ state. The quantum efficiency of **Z** form population is independent of the solvent, which suggests a purely intramolecular mechanism of its generation. Occurrence of the triplet state of the **Z** form and the charge-transfer triplet state of the lactone have been found. Intramolecular quenching of the **Z** form has been investigated more thoroughly and it has been concluded that its mechanism consists of a thermally activated transition to a higher triplet state (e.g. 3Z_2). The mechanism has been confirmed by transient absorption measurements for LRB. Solvent polarity was found to play a crucial role in the mechanism of ${}^1L_{CT}$ and 1Z_1 excited state deactivation by shifting the relative positions of energy levels of the states participating in the process and modifying the energy barrier heights for individual transitions. Special attention was devoted to the solvent-induced non-radiative process in the 1Z_1 state and a detailed model of this process, together with a quantitative formulation of the rate constant dependence on solvent polarity, has been proposed. The intense phosphorescence observed in perfectly glassed solvents (with quantum yield more than 0.7) was ascribed to the triplet state of the **Z** form, which is populated either directly, together with the 1Z_1 state, or via the 3Z_2 state, the latter being accessible due to an increase of the energy of the 1Z_1 state in the glass matrix. In conclusion, a consistent energy level diagram has been proposed for the lactone molecule.

Apart from gaining new insights into the photophysics of rhodamine dyes, this thesis implies also some questions, which could not have been answered by the work covered by this thesis and which might be a subject of a future research. These issues include first of all:

- very early stages of the excited state process (subpicosecond and picosecond time domain), and in particular the primary (hot) photodissociation reaction leading to formation of the zwitterion,
- coexistence of the excited **L** and **Z** forms (iso-emissive points, branching into **L** and **Z**),
- nature of the upper triplet 3Z_x state, participating in the deactivation of the 1Z_1 state,
- nature and properties of triplet state of the lactone form ($^3L_{CT}$).

In closing it is to be pointed out that the results presented in this thesis force us to verify the existing views on the photophysics of rhodamines, and in particular, on the role played by the solvent (medium) in photophysics of these compounds. The picture existing so far was based on the investigation of zwitterion forms of rhodamines in protic media. These conditions, however, are very specific ones and hide the whole plethora of the processes taking place in rhodamines that could be discovered while investigating the lactone forms.

Part of the results of this thesis has been already published and presented on numerous conferences. Reference to relevant papers was given in Chapter 1.

B. 319/96



Biblioteka Instytutu Chemii Fizycznej PAN

B.319/1996



00000000278409